SEL-64-012

The Opposite-Stream Plasma Diode

/l/ASA CuS-8200

N 67-17764

by

Peter Burger

April 1964

Technical Report No. 0254-1

D D C

JUL 1 5 1964

DDC-IRA B

ELECTRON DEVICES LABORATORY

STANFORD ELECTRONICS LABORATORIES

STANFORD UNIVERSITY · STANFORD, CALIFORNIA

CASE FILE COPY

THE OPPOSITE-STREAM PLASMA DIODE

by

Peter Burger

"Available to U.S. Government Agencies and U.S. Government Contractors Only."

April 1964

Technical Report No. 0254-1

Prepared under

Electron Devices Laboratory
Stanford Electronics Laboratories
Stanford University   Stanford, California

ABSTRACT

The possible dc states of a one-dimensional plasma diode are analyzed. This diode consists of opposing thermionic ion and electron emitters in parallel-plane geometry. The emitters can have different temperatures. The assumptions of nonreflecting boundaries and complete lack of collisions are made. Electrons and ions are assumed to be generated with half-Maxwellian velocity distributions corresponding to their respective temperatures.

For the case of nonnegative potential of the ion emitter with respect to the electron emitter all possible dc states are found. It is shown that if the continuity of the spatial derivative of the space-charge function is required in the diode space, then only one self-consistent dc state is possible for a diode with a given applied potential across it. This dc state is called the "basic solution."

Neither Maxwell's equations nor the collisionless, steady-state Boltzmann equation require the continuity of the derivative of the space-charge function. If discontinuities in this derivative are permitted, spatially periodic dc states also become possible solutions for some diodes. Curves are given for the determination of the possible presence of periodic solutions in an arbitrary opposite-stream diode. The characteristics of periodic dc states are computed with similar numerical methods as used for basic states.

The derivative of the space-charge function does not enter into the strict dc problem; however, if it is discontinuous then a small amount of collisions would give rise to large diffusion currents, thus destroying this discontinuity. Even in a strictly collisionless model a small rf perturbation would affect the periodic dc solution in a similar manner through the process of phase mixing. Thus, dc solutions with discontinuous derivatives of their space-charge functions are expected (and found) to be unstable.

The stability of the dc states is examined by simulating the motions of the electrons and ions on a computer. The computer model showed that under time-varying conditions the basic solution is formed and that it is in qualitative and quantitative agreement with the

results of the forementioned dc calculations. The fluctuations present in the model are due only to shot-noise effects. When the periodic solution is set up in the diode model initially, it changes rapidly into the basic solution, showing that the discontinuous derivative of the space-charge function makes this dc solution highly unstable. Characteristics of this computer diode and the step-by-step transformation of the periodic state are shown.

An experimental model of the opposite-stream diode is constructed with a solid-state, thermionic, lithium-ion emitter and a barium-oxide-coated electron emitter. The current vs voltage characteristics of this diode agree with the theoretical values predicted for the basic solution, if the contact potential of the emitters is taken into account. The contact potential is determined by comparing the experimental data with the predicted current values that should flow theoretically in the diode when the applied potential is zero.

CONTENTS

TABLES

ILLUSTRATIONS

ACKNOWLEDGMENT

I. INTRODUCTION

Direct-current theories for charged particle flow between two plane electrodes have been developing for over 60 years. The development began with the formulation of Child's law, which was the direct consequence of the law of the electrons' motion in a steady electric field and of Poisson's equation. This simple law of single-velocity electrons was the starting point of extensive analysis of more complicated situations.

The addition of ions to the simple electron diode was made, retaining the assumption of single-velocity particles. Langmuir [Ref. 1] and later Müller-Lübeck [Ref. 2] made extensive calculations of the characteristics of a parallel-plane diode consisting of cold, opposed electron and ion emitters. In their analysis both kinds of particles were emitted with zero velocity while assuming unlimited current densities of the emitters (space-charge-limited operation). The Langmuir and Müller-Lübeck analyses showed a 3/2-power law between voltage and current such as that of Child's law. However, the factor of proportionality (i.e., perveance) of this electron-ion diode was found to be 1.86 times larger than the perveance factor of the simple electron diode.

Temperature effects must be taken into consideration for physically realizable diodes. The theory of a thermionic electron diode has been worked out by many authors. An excellent summary of this work can be found in Langmuir and Compton's paper [Ref. 3], and highly accurate numerical results for their work were calculated by Kleynen [Ref. 4].

In the development of the theory of the double sheath, Langmuir went a step further when he considered hot electrons and cold ions emitted from the same plane in a parallel-plane diode. He gave a detailed discussion of this system, including periodic types of solutions [Ref. 5].

In the last few years several papers have dealt with one or more aspects of plasma diodes; most of them have included temperature effects of the particles. A theory of dc states with thermionic emitters was presented by Auer [Ref. 6], and later by McIntyre [Ref. 7]. This theory

SEL-64-012

dealt with hot-ion and hot-electron emission from the same plane and considered most of the possible dc cases--though McIntyre did not include the possibility of periodic solutions shown by Auer.

A paper by McIntyre [Ref. 8] deals with the hot three-stream diode which has electron and ion emission from the cathode and electron emission from the anode. The two emitting planes have different temperatures. He considers ten important dc cases, shows transitions between these, and discusses periodic types of solutions. Some of these dc states would coincide with the ones presented in this paper if electron emission from the cathode of his model could be neglected. Aside from the fact that there is no simple way of neglecting this electron emission, McIntyre's aims were different from ours. Consequently, we arrived at different conclusions.

Further studies aimed at specialized applications may be mentioned, e.g., the work of Auer and Hurwitz [Ref. 9] or the paper by Eichenbaum and Hernquist [Ref. 10].

The most general case of a parallel-plane plate, thermionic diode is the "four-stream" diode, which allows for both ion and electron emission from both planes and for different emission temperatures at these planes. The number of independent parameters for this problem is six. To work out a complete theory, which includes all possible dc solutions for this general case, would be too laborious and of doubtful value.

Since our first aim was to find a complete theory, the simpler model of the opposite-stream diode was selected and is shown schematically on Fig. 1. This model has the advantage that it could be approximated fairly well by an experimental device and yet it is simple enough for a tractable theoretical analysis. If allowance is made for different temperatures of the emitters, we find that four independent parameters are sufficient to determine the problem (see Sec. IIIB). The two-stream diode is a good approximation to a real diode only for positive voltages on the ion emitter. At decelerating potentials, electron emission from the ion emitter and ion emission from a possible ion surface layer at the electron emitter could become important, hence the general four-stream diode has to be studied.
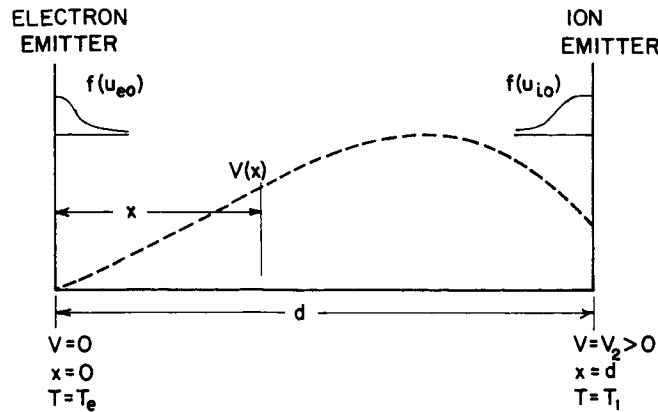
FIG. 1. MODEL OF THE OPPOSITE-STREAM
DIODE. The symbols $f(u_{eo})$ and $f(u_{io})$
represent the velocity-distribution
functions of the emitted electrons and
ions respectively. Both functions are
of half-Maxwellian types, with electron
temperature T_e and ion temperature T_i.

Once the dc states are known, their stability can be determined by
simulating on a computer the model of our one-dimensional plasma diode.
We have developed a complete dc theory for the opposite-stream diode,
therefore we can determine the stability of all the possible dc states
of this device by using the forementioned computer model. To do this,
we need to calculate the self-consistent dc states of our model by
numerical integrations. A procedure for these calculations is presented
in Chapters III and IV.

There is a further advantage in determining the exact dc charac-
teristics of our diode. The obtained theoretical data can be compared
with measurements made on an experimental opposite-stream diode. The
construction of this diode became possible when a thermionic, lithium-ion
emitter was developed in our laboratory. The experiment is described
in Chapter VII.

The following representative case of an opposite-stream diode was
chosen to demonstrate the theoretical results. (This example will be
used throughout the dc theory whenever it becomes necessary to demonstrate
results or procedures for a typical diode.) This representative diode
has the following construction:

Electron emitter: Temperature: 1200 °K
                           Saturation current density: 0.1 amp/cm^2

Ion emitter: Temperature: 1400 °K
                           Saturation current density: 1 ma/cm^2

Ions: Lithium

Separation of emitters: 0.2 cm

In Fig. 2 the predicted voltage-current characteristic of this particular diode is compared to that of other diode models. The "cold electron diode" exhibits Child's law. The "cold electron + ion diode" also has a 3/2-power law between current and voltage.

We also show the V-I characteristic of the temperature-corrected pure electron diode. Although the characteristics of this diode can be determined from Kleynen's tables [Ref. 4], the numerical procedure described in this report was used to determine both this curve and the V-I characteristics of the opposite-stream temperature-corrected diode. The curves are shown on a "perveance diagram" with 3/2-power scale for voltage, so that the curves representing the two diodes with single-velocity particles appear as straight lines.

We will also examine the stability of the found dc states by simulating this diode on a computer, and finally compare the results to the characteristics of an experimental opposite-stream diode which has the operating parameters listed above.
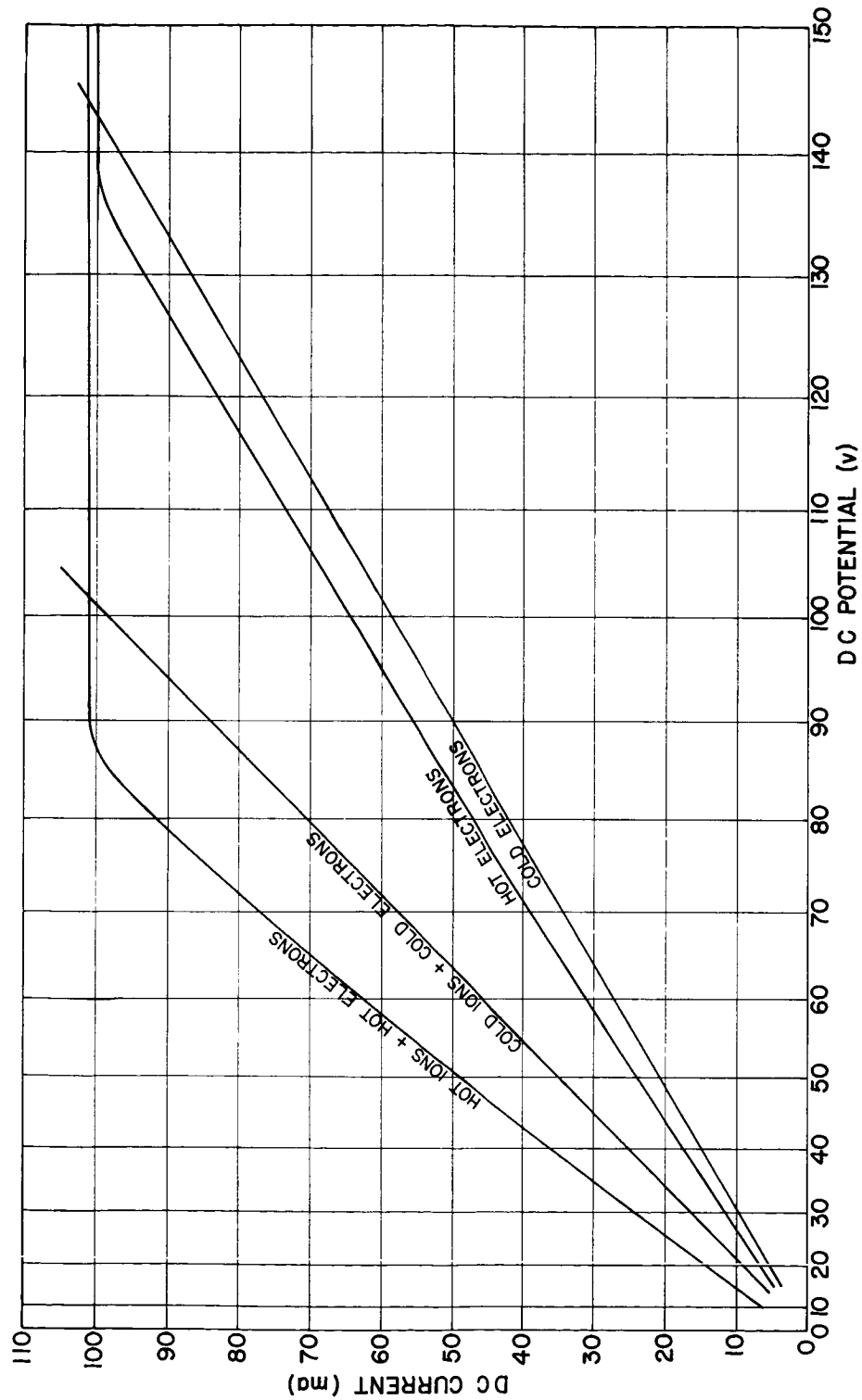
FIG. 2. COMPARISON OF VOLTAGE-CURRENT CURVES OF DIFFERENT DIODE MODELS. The voltage scale is proportional to $V^{3/2}$, therefore the curves of the space-charge-limited models appear as straight lines on the diagram. The difference between the curves of the thermionic electron diode and the thermionic opposite-stream diode shows the space-charge neutralization effect of the ions.

II. CHARGED PARTICLES THERMIONICALLY EMITTED
INTO A DC POTENTIAL FIELD

A. FORMULATION OF THE PROBLEM

As a first step we want to calculate the space-charge contribution of one kind of charged particle to the total space charge when these particles are emitted thermionically into an evacuated space. This contribution is given by an integral of the particles' velocity-distribution function; therefore we solve an equivalent problem by finding the velocity distribution of the emitted particles as a function of potential. We use parallel-plane geometry and assume that some dc potential as some function of distance is set up between the two end-planes.

For convenience, the emission of these particles is taken to occur at the left plane with a given velocity distribution (see Fig. 3). Both planes absorb incoming particles. Since we neglect any type of collision in the diodes, it is clear that once the dc state is set up the velocity-distribution function of the emitted stream has to satisfy the collisionless, static Boltzmann's equation with boundary conditions

d = separation distance
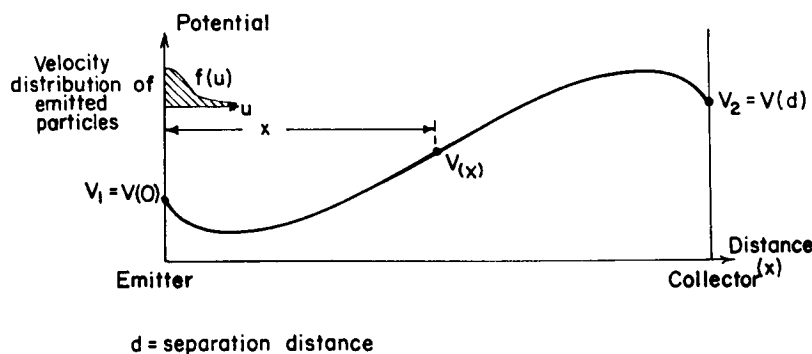
FIG. 3. THE SYSTEM FOR CALCULATING THE SPACE-CHARGE
CONTRIBUTIONS OF ONE KIND OF PARTICLE. The parti-
cles are emitted at the left plane with a velocity-
distribution function $f(u)$. The potential
distribution in the diode is arbitrary.

given at the two planes. As stated before, no reflection occurs at the boundaries, therefore the distribution function of the particles must be asymmetrical: there will be velocity classes which do not appear in the distribution function.

The form of the velocity-distribution function of the emitted particles will be determined in a general manner. In the next chapter we will use the results of the following analysis for solving our opposite-stream diode problem.

B. THE INTRODUCTION OF SYMBOLIC FUNCTIONS

There are several ways to arrive at the expressions of the contributions to the space charge of the particles, which are necessary to the numerical calculation of the problem. The commonly used method is to follow velocity classes of the particles and separate them into those which return to their respective emitting planes and those which escape at the opposite side (see for example Ref. 5). This procedure could be quite laborious for the general four-stream diode with a complicated potential function, and not much general information could be extracted from it before solving the problem with Poisson's equation simultaneously. Also, it is not clear that the solutions arrived at by this method are solutions to the collisionless Boltzmann equation. A different approach will be used here.

The emitted particles have a velocity-distribution function $f(u)[0 \leq u \leq +\infty]$, a charge "q," and a mass "m." (See Fig. 3.) Our first observation is that conservation of energy sets up a restriction on the velocity-distribution function of the particles. At every point in the diode where returned particles are present, the equality $f(u) = f(-u)$ must hold under our assumptions. On the other hand, as mentioned earlier, one cannot exclude the possibility of missing velocity classes. In order to account for this possibility, the general form of the distribution function of the particles inside the diode could be represented by an even function of velocity multiplied by some kind of "cutoff" function. The latter has the property that it is "one" in some intervals and "zero" elsewhere (Fig. 4). It is quite evident that we are able to use here the powerful mathematical

- 7 -
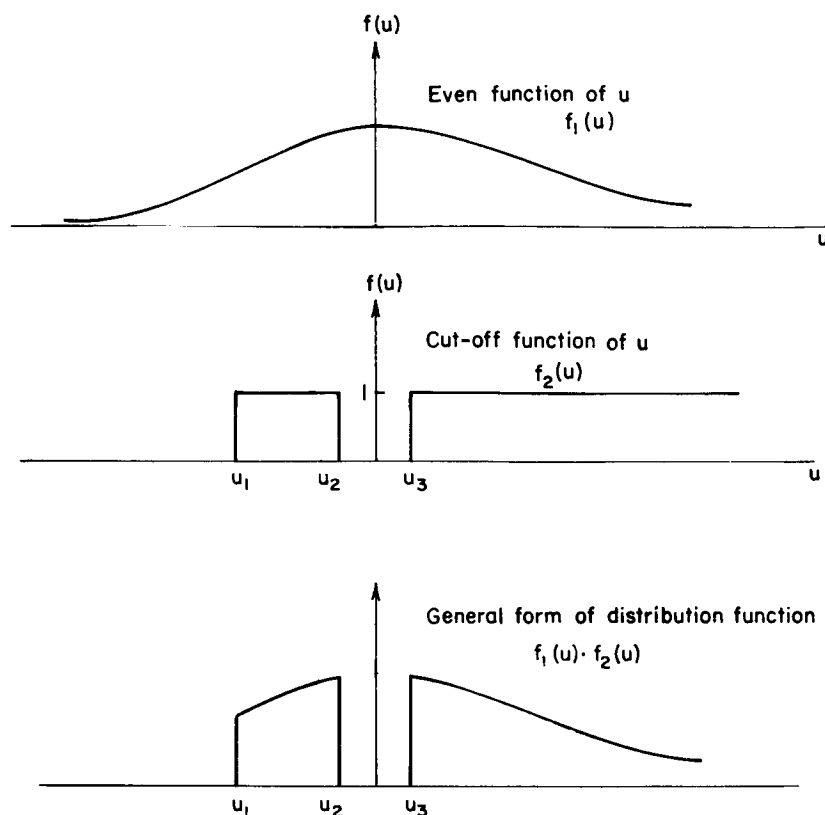
FIG. 4. THE FORM OF THE VELOCITY-DISTRIBUTION FUNCTION
OF THE EMITTED PARTICLES UNDER COLLISIONLESS, DC
CONDITIONS FOR A COMPLICATED DIODE. The parameters
u_1, u_2 and u_3 are functions of the position. For
the opposite-stream diode, $u_2 = u_3 = 0$; but u_1 can
be positive or negative depending on x.

tool of symbolic functions: the Dirac delta function $\delta(x)$ and its
integral--the Heaviside unit function [Ref. 11]. The latter is
denoted by $h(u)$, with the known property:

$$\left. \begin{array}{ll} h(u) = 0 & \text{for } u < 0 \\ h(u) = 1 & \text{for } u > 0 \end{array} \right\}. \qquad (1)$$

These symbolic functions are defined only through an integral over
the range $-\infty \leq u \leq +\infty$. This definition agrees with the physics of

the problem since all physical quantities (space charge, electric field, etc.) are defined by integrals of the distribution functions.

C. THE VELOCITY-DISTRIBUTION FUNCTION OF THE EMITTED PARTICLES

Now that we know the general form of the distribution function in its dependence on velocity, we are ready to substitute it into the time-independent, collisionless Boltzmann equation, which has the form

$$u \frac{\partial f(u,x)}{\partial x} + \frac{q}{m} E(x) \frac{\partial f(u,x)}{\partial u} = 0 \qquad (2)$$

where $E(x)$ is the dc electric field defined by $E(x) = -dV(x)/dx$.

The diode space can be divided into a finite number of regions, in each of which the potential $V(x)$ is a monotonic function of distance. For any one of these regions $V(x)$ is a unique function; therefore one can write the velocity-distribution function as a function of u and V instead of u and x. To do this, the following relation is used:

$$\frac{\partial f(u,x)}{\partial x} = \frac{\partial f(u,V)}{\partial V} \frac{dV}{dx} = -E(x) \frac{\partial f(u,V)}{\partial V} \qquad (3)$$

Let us introduce two normalized quantities. We define a normalized potential:

$$\eta_n(x) \stackrel{\triangle}{=} \frac{q_n}{kT_n} (V(x) - V_n) \qquad (4)$$

where T_n and V_n are the temperature and the potential of the emitter respectively, k is Boltzmann's constant, and q_n is the charge of species n. The subscript "n" distinguishes between species. Note that $\eta_n(x)$ has the sign of potential energy of the particles regardless of whether they are ions or electrons.

This normalization procedure refers to one stream only. The subscript n is used here to show this fact. In Chapter III we will refer to the different normalizations used for ions and electrons by

η_i, η_e; and later on will introduce a uniform normalization procedure for both streams [see Eq. (26)]. We normalize velocity also:

$$v_n \overset{\triangle}{=} \sqrt{\frac{m_n}{2kT_n}} \ u_n \tag{5}$$

There will be a corresponding change in the scale of $f(v_n, \eta_n)$ because of the condition $q_n \int_{-\infty}^{\infty} f(v_n, \eta_n) \ dv_n = \rho_n(\eta_n)$ where $\rho_n(\eta_n)$ is the space-charge density of the particles. This condition will be satisfied by the choice of the constant of proportionality of $f(v_n, \eta_n)$ [see Eq. (14)]. Substituting Eqs. (3), (4), and (5) into Eq. (2) gives

$$2v_n \frac{\partial f(v_n, \eta_n)}{\partial \eta_n} - \frac{\partial f(v_n, \eta_n)}{\partial v_n} = 0 \tag{6}$$

The solution of this first-order, partial-differential equation is $F(v_n^2 + \eta_n)$, which represents an arbitrary continuous function of its argument. This result gives the even-function part of the solution which we were looking for. We still have to incorporate our cutoff function into the solution. We take the functional form of $f(v_n, \eta_n)$ to be the product of an even function of v_n: $F(v_n^2 + \eta_n)$ multiplied by the cutoff function $h[v_n + v_{no}(\eta_n)]$ [see Eq. (7)].

$$f(v_n, \eta_n) = h[v_n + v_{no}(\eta_n)] \ F(v_n^2 + \eta_n) \tag{7}$$

We proceed to find the unknown function $v_{no}(\eta_n)$ that satisfies the differential equation. By substituting Eq. (7) into Eq. (6), the terms containing $F(v_n^2 + \eta_n)$ cancel and the following expression remains:

$$\delta[v_n + v_{no}(\eta_n)] \left[2v_n \frac{dv_{no}(\eta_n)}{d\eta_n} - 1 \right] = 0 \tag{8}$$

In symbolic representation $\delta(u - u_o) \; f(u) = f(u_o)$. By using this relation, the differential equation for $v_{no}(\eta_n)$ is determined from Eq. (8).

$$2v_{no} \frac{d}{d\eta_n} v_{no}(\eta_n) = -1 \tag{9}$$

After integrating Eq. (9), the form of $v_{no}(\eta_n)$ becomes:

$$v_{no}(\eta_n) = \pm\sqrt{\eta_{no} - \eta_n} \tag{10}$$

where η_{no} is a constant.

Looking for other forms of the velocity-distribution function of the particles, one can prove that the function $F(v_n^2 + \eta_n)$ itself does not have to be continuous. It can contain a step function of the form $h[v_n^2 - (\eta_{nr} - \eta_n)]$, where $\eta_{nr} < \eta_{no}$, and η_{nr} is a local extremum in the diode. In the opposite-stream diode this form never appears, but for the sake of generality, this function is included here. With the forms mentioned, all the possible forms of velocity-distribution functions have been exhausted for any one of the streams in a one-dimensional plasma diode. We have assumed nonreflecting boundaries, collisionless flow, and particle emission at one of the boundary planes only. For these conditions, any one stream can have only three basic forms of the velocity-distribution function. These are:

1. $f(v_n, \eta_n) = h[v_n - \sqrt{\eta_{no} - \eta_n}] \; F(v_n^2 + \eta_n)$

2. $f(v_n, \eta_n) = h[v_n + \sqrt{\eta_{no} - \eta_n}] \; F(v_n^2 + \eta_n)$

3. $f(v_n, \eta_n) = h[v_n^2 + \eta_n - \eta_{nr}] \; h[v_n + \sqrt{\eta_{no} - \eta_n}] \; F(v_n^2 + \eta_n)$

$$\tag{11}$$

The constant η_{no} is the same throughout the diode space, but η_{nr} is a constant only in an interval. At both ends of this interval η_n must be equal to η_{nr} in order to insure continuity of the space charge in the diode.

SEL-64-012

We can observe that in any one of the monotonic regions the distribution function $f(v_n, \eta_n)$ depends only on the particles' total energy $(v^2 + \eta)$ and on the direction of the velocity of the particles (in the sense that one must know the direction of their motion in order to tell about the cutoff of their distribution function).

D. CHOICE OF DISTRIBUTION-FUNCTION FORMS

It can be seen already that it was an advantage to approach the problem with the help of symbolic functions. Even in the most general case one could narrow the number of possible forms of the velocity-distribution functions to three. Unfortunately, the number of possible combinations of four streams with three different forms of distribution functions is 81, still too large a number to handle without finding conditions to rule out some combinations of these forms. Our problem is simplified since the two-stream diode does not allow the third form in Eq. (11).

Note that the first two forms appearing in Eq. (11) differ only by a sign. Since it is necessary to use only these two forms of the distribution function, we will distinguish between them by the superscripts (+) and (-). Using this notation we can write:

$$f^{\pm}(v_n, \eta_n) = h[v_n \pm \sqrt{\eta_{no} - \eta_n}\,] \; F(v_n^2 + \eta_n) \qquad (12)$$

Our task is to determine the signs applicable for the streams for all the regions in the diode. We know that $\rho(x)$, the space-charge density function of the stream, has to be continuous in space. This condition requires that the velocity-distribution function cannot be changed from one form to another at an arbitrary point in the diode. We can change form 1 of Eq. (11) to form 2 only at the point where $\eta_n = \eta_{no}$; and form 2 to form 3 only where $\eta_n = \eta_{nr}$. In our case when we do not have to make the latter change, the points where $\eta_n = \eta_{no}$ will always be at the end points of the monotonic regions of $\eta_n(x)$. If a change in the form of $f(v_n, \eta_n)$ is not made, then $\rho(x)$ will be automatically continuous.

To choose between the two forms, one observes that η_n is always less than or equal to η_{no} (see Fig. 5). The immediate consequence is that returning particles can be present only between the emitting plane and the plane where $\eta_n = \eta_{no}$. In this region, therefore, one has to use the form with the (+) before the square root. Everywhere else the first form is applicable (see Fig. 5a). This assignment of the forms of the distribution functions has to be made separately for each stream. One must remember that the normalization factor in Eq. (11) contains
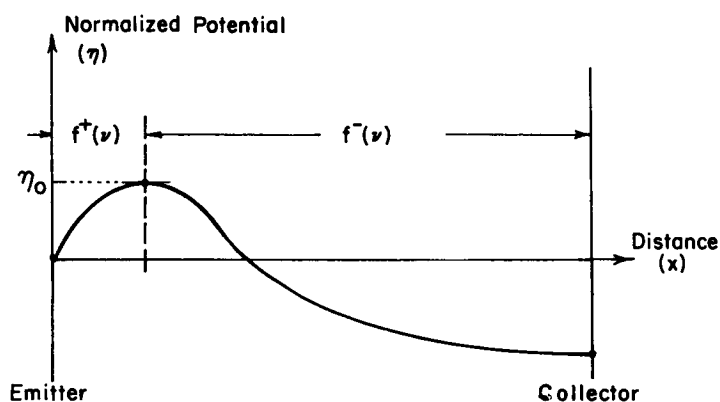
a. The basic solution
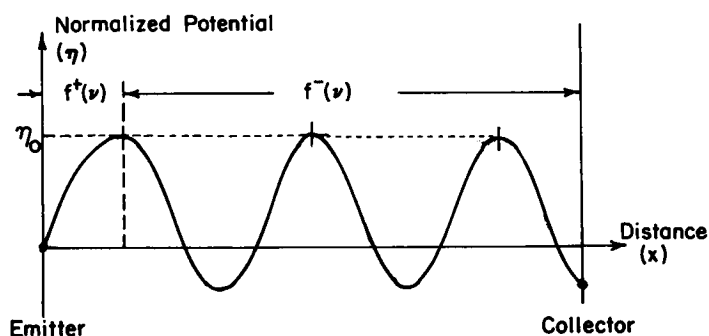
b. The periodic solution

FIG. 5. THE CHOICE OF THE FORM OF THE VELOCITY-DISTRIBUTION FUNCTION OF ONE KIND OF EMITTED PARTICLE IN THE OPPOSITE-STREAM DIODE. The potential and the velocity are normalized with respect to the kind of particles emitted. The choice of the form is shown for the basic and the periodic solutions.

SEL-64-012

the sign of the charge of the particles and therefore η_{no} will represent the most negative potential in the diode for the electrons, and the most positive potential for the ions.

It has been assumed until now that the normalized potential function $\eta_n(x)$ takes up the value η_{no} only once in the diode. If this is true for both ions and electrons, we call the solution "basic." Let us assume that the dc potential function takes the value η_{no} more than once in the diode, or to be more specific, that it is periodic in space (see Fig. 5b). The first extremum will still act as a potential barrier, but the other points where $\eta_n = \eta_{no}$ will have no such role because there could be no returning particles of this stream where these extrema are. Following this argument with the choice of the form of the distribution function, it is seen that $f(v_n, \eta_n)$ will change from $f^+(\ )$ to $f^-(\ )$ at the first extremum but will not change afterward. This difference between the first extremum and succeeding ones implies directly the important difference between basic and periodic types of solutions. Boltzmann's equation can be satisfied by requiring the continuity of the space charge as a function of distance. Since Eq. (6) is a first-order differential equation, we cannot set an arbitrary value for $d\rho/dx$, and we cannot even enforce continuity of $d\rho/dx$ if the boundary values of the equation are given. This derivative is determined by the equation and the boundary conditions. The following analysis will show that the continuity of $d\rho/dx$ depends directly on this change of the form of the distribution function at the extremum point.

Now that we know the form of the velocity distribution of the particles in the diode, we can calculate their contribution to the space charge with a simple integration $\rho_n(\eta_n) = q_n \int_{-\infty}^{\infty} f(v_n, \eta_n) dv_n$. This final step is postponed to the next chapter, which deals with the opposite-stream diode explicity.

III. THE BASIC SOLUTION

Now that we are equipped with the expressions for the velocity distributions of the emitted streams, these results can be applied to the two-stream diode. It has already been mentioned that the opposite two-stream diode has physical meaning only when there is an accelerating voltage applied on the diode or when the temperature difference of the two emitting planes is very large. We arrived at this conclusion from the Second Law of Thermodynamics since we know that when there is no potential difference across the diode and no temperature difference between the planes, no current can flow. This condition could be satisfied only with the general four-stream diode.

A. THE FORMAL SOLUTION

As shown in the preceding chapter, the distribution functions of the streams can be expressed conveniently with symbolic functions. Since thermionic emission is assumed, the emitted particles will have half-Maxwellian velocity distributions at the plane $\eta_n = 0$. So the general form of the distribution function will be:

$$f^{\pm}(\nu_n, \eta_n) = C_n h[\nu_n \pm \sqrt{\eta_{no} - \eta_n}\,]\, \exp\,(-\nu_n^2 - \eta_n) \qquad (13)$$

where C_n is a constant. The normalization for the two streams will be different, but the functional form of their distribution functions will be given by Eq. (13). The Constant C_n is related to the saturation current of the emitter, but instead of using current density it is more convenient to define equivalent number densities for both streams by

$$C_n \overset{\triangle}{=} \frac{N_n}{\sqrt{\pi}} \qquad (14)$$

where N_n is the number density of the full-Maxwellian distribution at the source. With this choice the ratio of electron-to-ion masses in the equations is eliminated. The relation between the experimentally measured, saturation-current densities and the number densities defined above is given by

- 15 -

$$J_n = N_n q_n \sqrt{\frac{kT_n}{2\pi m_n}} \tag{15}$$

where the subscript denotes either ions or electrons. One can go still further in this general manner (applicable for more than two streams) by calculating the space-charge contribution of one such stream as a function of the normalized potential:

$$\rho_n(\eta_n) = q_n \int_{-\infty}^{\infty} f(\nu_n, \eta_n) d\nu_n$$

$$= \frac{N_n q_n}{\sqrt{\pi}} \int_{-\infty}^{\infty} h[\nu_n \pm \sqrt{\eta_{no} - \eta_n}] \, \exp\left(-\nu_n^2 - \eta_n\right) d\nu_n \tag{16}$$

Equation (16) can be integrated by introducing the following functions:

$$F^{\pm}(\eta) = \exp(\eta)(1.0 \pm \operatorname{erf} \sqrt{\eta}) \tag{17}$$

where

$$\operatorname{erf}(x) = \frac{2}{\sqrt{\pi}} \int_0^x e^{-t^2} dt \tag{18}$$

Using Eq. (17) in Eq. (16), the space charge due to the two streams is found to be:

$$\rho_e(\eta_e) = q_e \frac{N_e}{2} \exp(-\eta_{eo}) F^{\pm}(\eta_{eo} - \eta_e) \tag{19}$$

$$\rho_i(\eta_i) = q_i \frac{N_i}{2} \exp(-\eta_{io}) F^{\pm}(\eta_{io} - \eta_i) \tag{20}$$

In our case the total space charge will be just the algebraic sum of Eq. (19) and Eq. (20).

Using Poisson's equation, $d^2V/dx^2 = -\rho/\epsilon_0$, one can integrate once to obtain

$$E^2(V) = -\frac{2}{\epsilon_0} \int \rho_i(\eta_i)dV - \frac{2}{\epsilon_0} \int \rho_e(\eta_e) \, dV \qquad (21)$$

where $E(V)$ is the electric field.

The stress balance for our model is expressed by Eq. (21). The functions $F^{\pm}(\eta)$ are integrable:

$$\int F^{\pm}(\eta)d\eta = G^{\pm}(\eta) = F^{\pm}(\eta) \mp \frac{2\sqrt{\eta}}{\sqrt{\pi}} \qquad (22)$$

The normalization for the two streams, given by Eq. (4), is

$$\eta_{i,e} = \frac{q_{i,e}}{kT_{i,e}} \, (V_{i,e} - V) \qquad (23)$$

where $V_{i,e}$ is the potential of the ion and electron emitters respectively. This reduces Eq. (21) to

$$E^2(V) = \frac{k}{\epsilon_0} \left[N_i T_i \exp(-\eta_{io}) \, G^{\pm}(\eta_{io} - \eta_i) \right.$$

$$\left. + N_e T_e \exp(-\eta_{eo}) \, G^{\pm}(\eta_{eo} - \eta_e) + \text{constant} \right] \qquad (24)$$

where the subscripts refer to the different normalization factors of the two streams.

The problem has now been reduced to a quadrature which gives the separation distance as the function of potential:

$$x(V) = \int_{V_1}^{V} \frac{dV}{[E^2(v)]^{1/2}} \qquad (25)$$

Equation (25) is a formal solution only, since we have to decide where to use $G^+(\eta)$ or $G^-(\eta)$. For this we would have to know the form of the potential function in the diode (η_{io}, η_{eo} are not given). But how could we ensure that for an assumed potential function we could adjust the arbitrary constants in Eq. (24) in such a way that the total integral will give the separation distance of the diode? The constants are not completely arbitrary since $E^2(V)$ cannot be negative in the diode space.

Fortunately, the choice of the form of the potential function for the two-stream diode is simplified. We will show shortly that only four basic forms could be present.

B. NORMALIZATION FOR THE TWO-STREAM DIODE

At this point it is convenient to introduce a general normalization procedure that takes both streams into account. When one of the saturation-current densities becomes zero, the normalization should be the same as in Eq. (4). This suggests the definition of the following quantities:

$$\text{Number density:} \quad \overline{N} \triangleq N_i + N_e$$

$$\text{Temperature:} \quad \overline{T} \triangleq \frac{N_e T_e + N_i T_i}{N_e + N_i} \tag{26}$$

$$\text{Debye length:} \quad \overline{\lambda} \triangleq \sqrt{\frac{\epsilon_0 k \overline{T}}{e^2 \overline{N}}}$$

For convenience we take the potential to be zero at the electron emitter and define the normalized potential as: $\eta = (e/k\overline{T})V$. If we call the most positive potential in the diode η_M and the most negative η_m, these will be related to η_{eo}, η_{io} which were defined in the preceding section as follows:

$$\eta_{eo} = \frac{\overline{T}}{T_e} \eta_m; \quad \eta_{io} = \frac{\overline{T}}{T_i} (\eta_M - \eta_2) \tag{27}$$

where $\eta_2 = (e/k\overline{T})V_2$ and V_2 is the true potential difference across the diode in volts. The distance measured from the electron emitter can be normalized by the defined Debye length of the diode:

$$\xi \triangleq \frac{x}{\overline{\lambda}} \tag{28}$$

Even though they are not independent, four characteristic constants for the problem are defined as follows:

$$\alpha_e \triangleq \frac{N_e T_e}{\overline{N}\,\overline{T}} \; ; \qquad \alpha_i \triangleq \frac{N_i T_i}{\overline{N}\,\overline{T}} \; ; \left.\vphantom{\frac{\overline{T}}{T_e}}\right\} \tag{29}$$

$$\beta_e \triangleq \frac{\overline{T}}{T_e} \; ; \qquad \beta_i \triangleq \frac{\overline{T}}{T_i}$$

There are two identities between these four quantities:

$$\alpha_e + \alpha_i = 1 \; ; \qquad \alpha_e \beta_e + \alpha_i \beta_i = 1 \tag{30}$$

Therefore only two of the four are independent, and all four can be calculated from two independent ratios of the physical data of the diode. These ratios are

$$\alpha = \frac{J_{se}}{J_{si}} \sqrt{\frac{m_e}{m_i}} \; ; \qquad \beta = \frac{T_e}{T_i} \tag{31}$$

The relations between $\alpha_e, \beta_e, \alpha_i, \beta_i$ and α, β are:

$$\left. \alpha_e = \frac{\alpha\sqrt{\beta}}{1 + \alpha\sqrt{\beta}} \atop \alpha_i = \frac{1}{1 + \alpha\sqrt{\beta}} \right\} \qquad\qquad \left. \beta_e = \frac{1 + \alpha\sqrt{\beta}}{\beta + \alpha\sqrt{\beta}} \atop \beta_i = \frac{1 + \alpha\sqrt{\beta}}{1 + \dfrac{\alpha}{\sqrt{\beta}}} \right\} \tag{32}$$

For easier identification γ is used for the arbitrary constant of $E^2(\eta)$. If the quantities defined in Eq. (32) are used, the normalized electric field will have the form

$$\mathcal{E}^2(\eta) = \left(\frac{d\eta}{d\xi}\right)^2 = \alpha_i \exp\left[-\beta_i(\eta_M - \eta_2)\right] G^{\pm}\left[\beta_i(\eta_M - \eta)\right]$$

$$+ \alpha_e \exp\left(\beta_e \eta_m\right) G^{\pm}\left[\beta_e(\eta - \eta_m)\right] + \gamma \tag{33}$$

In the normalized form the space-charge function is expressed by the relation

$$\rho(\eta) = \frac{\alpha_i \beta_i}{2} \exp\left[-\beta_i(\eta_M - \eta_2)\right] F^{\pm}\left[\beta_i(\eta_M - \eta)\right]$$

$$- \frac{\alpha_e \beta_e}{2} \exp\left(\beta_e \eta_m\right) F^{\pm}\left[\beta_e(\eta - \eta_m)\right] \tag{34}$$

And then the formal solution of the problem is

$$\xi(\eta) = \int_0^{\eta} \frac{d\eta}{[\mathcal{E}^2(\eta)]^{1/2}} \tag{35}$$

C. FOUR TYPES OF THE BASIC SOLUTION

Our next task is to prove that only four different types of the potential function can exist in our diode.

1. Type D Solution

First, we assume that an arbitrary dc potential function of the basic type is present in the diode. Let us take the case when $\eta_M > \eta_2$, $\eta_m < 0$ (see Fig. 6). It was shown earlier that returning particles can be present only between the current-limiting extremum and the emitter. This is true for both streams separately. If the potential minimum is near the electron emitter and the maximum near the ion emitter (see Fig. 6), there will be no returning particles of either kind in the region $\eta_m < \eta < \eta_M$ (region II). In the regions near the emitters, returning particles of only one kind are present. Consequently, there are no regions in the diode where both kinds of particles are traveling

in both directions. This means that the third type of the velocity-
distribution functions [Eq. (11)] cannot apply for either stream when
the assumed potential function is present. The other two types, $f^+(v)$
and $f^-(v)$, can be assigned to the streams by following the discussion
in the preceding chapter. This assignment will result in a monotonically
increasing, space-charge function in the whole diode space. Since space
charge is a monotonic function of distance in the diode, the potential
function has to be monotonic in the three separate regions, and we have
determined the shape of the potential function. This potential is
denoted as the type D solution.
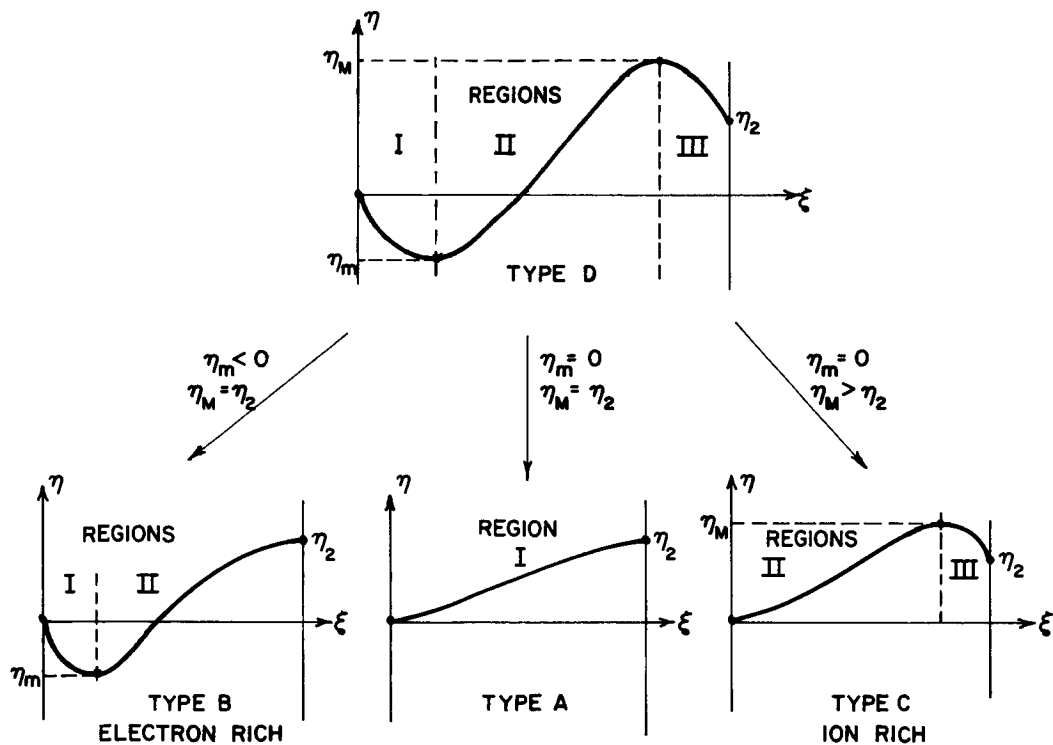
FIG. 6. THE FOUR BASIC TYPES OF POTENTIAL FUNCTION IN THE
OPPOSITE-STREAM DIODE. The space-charge function, as a
function, of potential, is expressed differently in the
three different regions, but it is continuous in the diode.

The foregoing analysis assumes that the potential maximum is near the ion emitter and the minimum is near the electron emitter. This is the only possible form of the potential function when $\eta_m < 0$, $\eta_M > \eta_2$. If the positions of these extrema are interchanged, returning particles of both kinds will be in the middle of the diode. This interchange, however, is not possible. Looking at the second derivative of the potential function after interchanging the extrema, we get the condition that $\rho(\eta_M) < \rho(\eta_m)$. Substituting the values $\eta = \eta_M$, $\eta = \eta_m$ into the space-charge functions for such a potential distribution, we get $\rho(\eta_M) > \rho(\eta_m)$ if $\eta_M > \eta_m$. Since the last statement is always true, this gives a contradiction.

2. Type B and Type C Solutions

When only one of the extremum points is inside the diode, only one kind of particle is returned in the whole diode space. This happens when either $\eta_m = 0$ (type C) or $\eta_M = \eta_2$ (type B). Using a similar argument for these potential functions as was used for the type D case, we can show that the potential functions will be monotonic in the two regions for both type B and type C solutions (see Fig. 6).

3. Type A Solution

It is also possible that both extremum points are at the boundaries. This means that $\eta_m = 0$ and $\eta_M = \eta_2$ and that there are no returning particles of either kind in the diode. The function $F^-(\eta)$ has to be used for both streams in their respective space-charge formula [see Eqs. (19) and (20)] and since there is only one region, the potential is monotonic in the whole diode space.

D. THE COMPLETE SOLUTION

With the four types of potential functions, all possible basic-solution types have been covered. It is still necessary to show how one can find the type of potential function that is applicable for a diode with given boundary values, and how one can calculate the characteristics of the device.

The four basic types of the potential function are shown on Fig. 6. Three regions can be distinguished on these diagrams. Region I is between the electron emitter plane and the plane where $\eta = \eta_m$. Region II extends for the potential values $\eta_m \leq \eta \leq \eta_M$. Region III is near the ion emitter where $\eta_M \geq \eta \geq \eta_2$. Looking at our diode from this point of view, we can consider all four types as type D (see Fig. 6). Types A, B, and C are only degenerate cases of type D. Degeneracy occurs when the lengths of region I or region III, or both, become zero. Mathematically this yields to a formula valid for all possible basic solutions. Equation (35) now becomes:

$$\xi_2 = -\int_0^{\eta_m} \frac{d\eta}{\sqrt{\mathcal{E}_I^2(\eta)}} + \int_{\eta_m}^{\eta_M} \frac{d\eta}{\sqrt{\mathcal{E}_{II}^2(\eta)}} - \int_{\eta_M}^{\eta_2} \frac{d\eta}{\sqrt{\mathcal{E}_{III}^2(\eta)}} \qquad (36)$$

where $\eta_m \leq 0$, $\eta_M \geq \eta_2$. Using the procedure outlined in the preceding section, $\mathcal{E}_I^2(\eta)$, $\mathcal{E}_{II}^2(\eta)$, $\mathcal{E}_{III}^2(\eta)$ can be given explicitly as

$$\left.\begin{array}{l}
\mathcal{E}_I^2(\eta) = \alpha_i \exp\left[-\beta_i\left(\eta_M - \eta_2\right)\right] G^-\left[\beta_i\left(\eta_M - \eta\right)\right] \\[2em]
\qquad + \alpha_e \exp\left(\beta_e \eta_m\right) G^+\left[\beta_e\left(\eta - \eta_m\right)\right] + \gamma \\[2em]
\mathcal{E}_{II}^2(\eta) = \alpha_i \exp\left[-\beta_i\left(\eta_M - \eta_2\right)\right] G^-\left[\beta_i\left(\eta_M - \eta\right)\right] \\[2em]
\qquad + \alpha_e \exp\left(\beta_e \eta_m\right) G^-\left[\beta_e\left(\eta - \eta_m\right)\right] + \gamma \\[2em]
\mathcal{E}_{III}^2(\eta) = \alpha_i \exp\left[-\beta_i\left(\eta_M - \eta_2\right)\right] G^+\left[\beta_i\left(\eta_M - \eta\right)\right] \\[2em]
\qquad + \alpha_e \exp\left(\beta_e \eta_m\right) G^-\left[\beta_e\left(\eta - \eta_m\right)\right] + \gamma
\end{array}\right\} \qquad (37)$$

Equation (36) gives the total separation distance ξ_2. To evaluate the integrals, one must know the boundary values α, β, η_2 of the problem and the three parameters η_M, η_m, γ. For convenience, we will call the total potential drop in the diode, $\eta_T = \eta_M - \eta_m$. Ordinarily ξ_2 is also a given quantity; therefore our task is to set the values of the three parameters η_M, η_m, and γ such that the total separation distance given by Eq. (36) be the desired diode separation. Fortunately this task is simplified by the following relations:

1. For the type A case, $\eta_m = 0$, $\eta_M = \eta_2$, and only γ is a parameter. The constant γ could be any large positive number, and as $\gamma \to +\infty$, ξ_2 approaches zero. On the other hand, we cannot set γ arbitrarily large when negative, because at some point $\mathcal{E}_{II}^2(\eta)$ would become negative. Hence for a given set of α, β, η_2, if we change γ, ξ_2 will cover some range $0 \le \xi_2 \le \xi_{A_{max}}$. This $\xi_{A_{max}}$ will be the separation length of a potential function for which the electric field becomes zero at one of the emitter planes. We call this case a transition case.

2. Types B and C are mutually exclusive. Depending on the values of α, β, and η_2, either type B (electron-rich case) or type C (ion-rich case) can exist in the diode. The conditions are:

$$\left. \frac{\alpha_i \, [G^-(\beta_i \, \eta_2) - 1]}{\alpha_e \, [G^-(\beta_e \, \eta_2) - 1]} \right| \begin{array}{l} < 1.0 \quad \text{(electron-rich case)} \\[2ex] > 1.0 \quad \text{(ion-rich case)} \end{array} \qquad (38)$$

When the expression is equal to one, we have a unique situation. In this case type B or C cannot be present in the diode since type A changes to type D directly; the electric field becomes zero at both emitters at the same time. For B or C types, $\eta_T \ge \eta_2$. Once η_T is set, all three parameters can be calculated because of the condition that the electric field has to be

zero at the extremum. The case where $\eta_T = \eta_2$ corresponds to the transition case mentioned, and hence the separation distance for this case is $\xi_{A_{max}}$, which would be a transition from A to B (ξ_{AB}) or from A to C (ξ_{AC}) depending on whether it is an electron-rich or an ion-rich case. (See Table 1 for transition cases.) Upon increasing η_T, ξ_2 will increase monotonically. Another transition case will occur if we increase η_T when neither electron nor ion emission is zero. In this case the electric field becomes zero at the boundary plane where the extremum has not been formed yet. Transition thus occurs from type B or C to type D. The length associated with this transition is ξ_{BD} or ξ_{CD}. For both cases, this length is called $\xi_{D_{min}}$ because it is the minimum separation length for the D case when α, β, and η_2 are given.

3. For type D, $\eta_T = \eta_M - \eta_m$ and $\eta_M > \eta_2$, $\eta_m < 0$. If η_T increases, ξ_2 increases monotonically so that with increasing η_T we could set ξ_2 as large as we please.

From the above observations we can construct the complete basic solution. Experimentally α, β, η_2, and ξ_2 are given. First we have to decide which type of solution is applicable for this set of boundary values. To do this, we calculate the transition lengths $\xi_{A_{max}}$ and $\xi_{D_{min}}$. We set $\xi_{D_{min}} > \xi_2$ corresponding to the emission of one kind of particle only.

The term $\xi_{A_{max}}$ can be calculated by finding γ for the transition case A-B or A-C from the formulas:
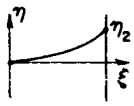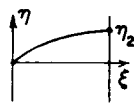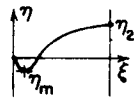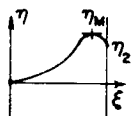
Electron-Rich Case (A-B)

$$\gamma = -\alpha_e - \alpha_i \ G^-(\beta_i \ \eta_2) \tag{39}$$

Ion-Rich Case (A-C)

$$\gamma = -\alpha_e \ G^-(\beta_e \ \eta_2) - \alpha_i \tag{40}$$

Transition Type	Potential Form	Required Condition	Equations Determining the Three Parameters
A-B		Electron-rich	$\eta_m = 0$ $\eta_M = \eta_2$ $\gamma = -a_e - a_i G^-(\beta_i \eta_2)$
A-C		Ion-rich	$\eta_m = 0$ $\eta_M = \eta_2$ $\gamma = -a_e G^-(\beta_e \eta_2) - a_i$
B-D		Electron-rich	$\eta_T = \eta_2 + \dfrac{1}{\beta_e} \log\left(\dfrac{a_e}{a_i} \dfrac{G^-(\beta_e \eta_T)-1}{G^-(\beta_i \eta_T)-1}\right)$ (Solved by Iteration) $\eta_m = \eta_2 - \eta_T$ $\eta_M = \eta_2$ $\gamma = -a_e \exp\{\beta_e \eta_m\} G^-(\beta_e \eta_T) - a_i$
C-D		Ion-rich	$\eta_T = \eta_2 + \dfrac{1}{\beta_i} \log\left(\dfrac{a_i}{a_e} \dfrac{G^-(\beta_i \eta_T)-1}{G^-(\beta_e \eta_T)-1}\right)$ (Solved by Iteration) $\eta_m = 0$ $\eta_M = \eta_T$ $\gamma = -a_i \exp\{\beta_i(\eta_2-\eta_M)\} G^-(\beta_i \eta_T) - a_e$

Setting $\eta_M = \eta_2$, $\eta_m = 0$, and knowing the calculated value of γ from Eq. (36), we get $\xi_{A_{max}}$. Now if $\xi_2 < \xi_{A_{max}}$, we know that the type A potential function is applicable.

The term $\xi_{D_{min}}$ can be calculated by the conditions that the electric field has to be zero at two points--one of which is at a boundary plane. Again we have to distinguish between electron-rich and ion-rich cases:

Electron-Rich Case (B-D)

By iteration η_T can be found from the following equation:

$$\eta_T = \eta_2 + \frac{1}{\beta_e} \log \left[\frac{\alpha_e}{\alpha_i} \frac{G^-(\beta_e \, \eta_T) - 1}{G(\beta_i \, \eta_T) - 1} \right] \tag{41}$$

then

$$\eta_m = \eta_2 - \eta_T$$

$$\eta_M = \eta_2 \tag{42}$$

$$\gamma = -\alpha_e \exp(\beta_e \, \eta_m) \, G^-(\beta_e \, \eta_T) - \alpha_i$$

Ion-Rich Case (C-D)

Similarly, the following equation is solved by iteration:

$$\eta_T = \eta_2 + \frac{1}{\beta_i} \log \left[\frac{\alpha_i}{\alpha_e} \frac{G^-(\beta_i \, \eta_T) - 1}{G(\beta_e \, \eta_T) - 1} \right] \tag{43}$$

then

$$\eta_m = 0$$

$$\eta_M = \eta_T \tag{44}$$

$$\gamma = -\alpha_i \exp[\beta_i (\eta_2 - \eta_M)] \, G^-(\beta_i \, \eta_T) - \alpha_i$$

Knowing the set of parameters η_M, η_m, and γ and the constants α, β, and η_2, Eq. (36) again can be evaluated, resulting in $\xi_{D_{min}}$. If $\xi_2 > \xi_{D_{min}}$, we know that the type D potential function is applicable for

our diode. If $\xi_{A_{max}} < \xi_2 < \xi_{D_{min}}$, then depending on whether we have an electron-rich or an ion-rich case, type B or type C potential has to be used respectively.

With the described procedure we can determine for any given set of boundary values, i.e., α, β, η_2, and ξ_2, which potential form is applicable. We now must determine the values of the three parameters such that if they are substituted into Eq. (36), the resulting integral expression gives the desired separation distance.

For the type A case we have to change only γ and hence can get a correspondence between the parameter γ and the separation distance calculated by Eq. (36). Some kind of interpolating method then could give γ, which corresponds to the given separation length.

For the others cases, η_T is changing, and the correspondence is set up between η_T and the separation length calculated by Eq. (36). The only slight complication is that we have to calculate the three parameters from η_T and from conditions on the electric field at the extremum points. Table 2 presents these relations for all four cases in a tabulated form.

In all cases it was found that the separation distance was a unique function of the chosen parameter $(\gamma$ or $\eta_T)$ and that by changing these parameters this distance can be varied continuously from zero to any desired value.
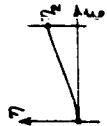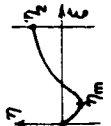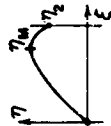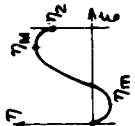
We have written a BALGOL[*] program which performs all numerical and logical procedures automatically. A detailed analysis of this program can be found in Appendixes A and B.

For demonstrations, we have calculated the separation distance as a function of the parameters η_T, γ for the diode presented in Chapter I. For example, if we apply 20 v across the diode, the normalized constants are: $\alpha = 1.12$, $\beta = 0.857$, $\eta_2 = 390$. The result is shown in Fig. 7.

Now that we have shown that a self-consistent dc solution of the basic type always exists and can be determined uniquely from an arbitrary set of boundary values, we will examine the spatial derivative of the space-charge function of this basic solution.

---

[*]Stanford version of Burroughs algorithmic language.

TABLE 2. RELATIONS GOVERNING THE FOUR BASIC TYPES OF SOLUTIONS OF THE OPPOSITE-STREAM DIODE

Potential Type	Potential Form	Conditions on α, β, η_2	Independent Parameter	Values of Other Parameters
A		No condition	γ	$\eta_m = 0$ $\eta_M = \eta_2$ $\gamma \geqq -\min\begin{Bmatrix} \alpha_i[G^-(\beta_i\eta_2)-1.0] \\ \alpha_e[G^-(\beta_e\eta_2)-1.0] \end{Bmatrix}$
B		$\alpha_i[G^-(\beta_i\eta_2)-1.0] <$ $\alpha_e[G^-(\beta_e\eta_2)-1.0]$ (Electron-rich)	$\eta_T = \eta_2-\eta_m$	$\eta_M = \eta_2$ $\eta_m = \eta_2-\eta_T$ $\gamma = -\alpha_e \exp\{\beta_e\eta_m\} - \alpha_i G^-(\beta_i\eta_T)$
C		$\alpha_i[G^-(\beta_i\eta_2)-1.0] >$ $\alpha_e[G^-(\beta_e\eta_2)-1.0]$ (Ion-rich)	$\eta_T = \eta_M$	$\eta_m = 0$ $\eta_M = \eta_T$ $\gamma = -\alpha_e G^-(\beta_e\eta_T) - \alpha_i \exp\{\beta_i(\eta_2-\eta_T)\}$
D		Nonzero emission of both species	$\eta_T = (\eta_M-\eta_m)$	$\eta_M = \dfrac{\beta_e\eta_T+\beta_i\eta_2}{\beta_e+\beta_i} - \dfrac{1}{\beta_e+\beta_i} \log \dfrac{\alpha_e[G^-(\beta_e\eta_T)-1.0]}{\alpha_i[G^-(\beta_i\eta_T)-1.0]}$ $\eta_m = \eta_M-\eta_T$ $\gamma = -\alpha_e \exp\{\beta_e\eta_m\} - \alpha_i \exp\{\beta_i(\eta_2-\eta_M)\}G^-(\beta_i\eta_T)$
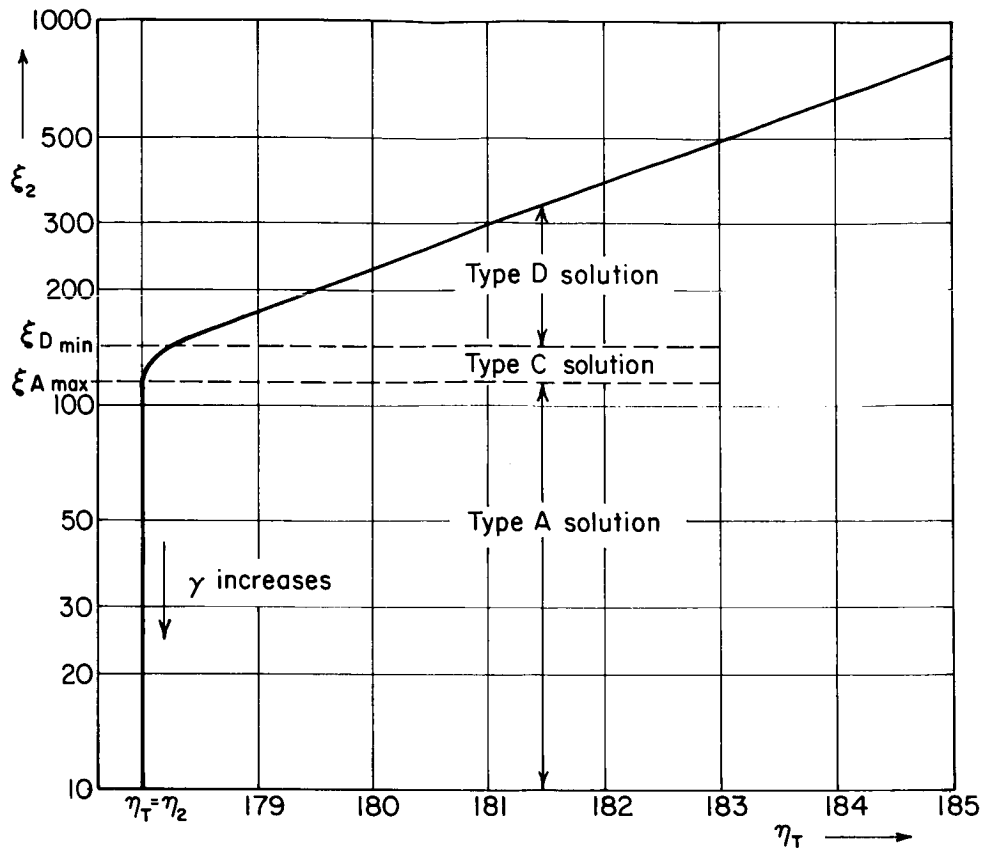
FIG. 7. THE RELATION BETWEEN THE CALCULATED SEPARATION LENGTH AND $\eta_T = \eta_M - \eta_m$ FOR AN OPPOSITE-STREAM DIODE.

E. THE CONTINUITY OF $d\rho/d\xi$ OF THE BASIC SOLUTION

We have to examine the continuity of $d\rho/d\xi$ at the points $\eta = \eta_m$ and $\eta = \eta_M$ only. Elsewhere $d\rho/d\xi$ is well-behaved.

Physical intuition suggests that the spatial derivative of the space-charge function should be continuous everywhere inside the diode; therefore we take the case when $\eta_m < 0$, $\eta_M > \eta_2$, so both points are located inside. If $d\rho/d\xi$ were discontinuous or infinite in the diode, it would be necessary to reexamine our model. First of all, collisions are always present. Even if the number of collisions can be neglected under ordinary circumstances, their effect will certainly be pronounced in a situation where the collisionless model predicts discontinuity of the space-charge function. Diffusion currents caused by such discontinuities could hardly be considered negligible, for they would destroy

such discontinuity. In the case when collisions are totally absent, a small rf perturbation of the dc state would have the same effect through the process of phase mixing. Consequently, whenever discontinuities of such a kind appear, collisionless dc analysis is not adequate.

To calculate $d\rho/d\xi$ we use the equality:

$$\frac{d\rho}{d\xi} = -\mathscr{E}(\eta) \frac{d\rho}{d\eta} \tag{45}$$

Let us make our calculation at the point $\eta = \eta_m$. Here the space-charge contribution of the ions is a regular function of η, so $d\rho_i/d\eta$ is finite. The electric field, on the other hand, approaches zero like $\pm C_1 \sqrt{\eta - \eta_m}$. (See Eq. (37) for the expression of the electric field.) The major contribution of $d\rho/d\eta$ comes from the electrons because $d\rho_e/d\eta$ approaches infinity like $C_2/\pm \sqrt{\eta - \eta_m}$ when η approaches η_m. Neither C_1 nor C_2 is zero, therefore $d\rho/d\xi$ will be finite and non-zero. The continuity of $d\rho/d\xi$ will now depend on the sign of $d\rho_e/d\eta$ and of $\mathscr{E}(\eta)$ at both sides of the point $\eta = \eta_m$. The potential has a true minimum at $\eta = \eta_m$ (as opposed to the case where $\eta_m = 0$), therefore $\mathscr{E}(\eta)$ will change sign when η is passing through η_m. Whether $d\rho_e/d\eta$ will also change sign depends on the functional form of $\rho_e(\eta)$. If we have to change $F^+(\eta)$ to $F^-(\eta)$ at the point $\eta = \eta_m$ in the expression given for $\rho_e(\eta)$ in Eq. (19), the sign of the derivative of $\rho_e(\eta)$ will also change. In this case $d\rho/d\xi$ will be continuous. As shown in this section for the basic solution, this condition is always satisfied for both the electron space-charge function at the potential minimum and the ion space-charge function at the potential maximum. Consequently, we can conclude that $d\rho/d\xi$ will always be continuous for the basic solution inside the diode.

As mentioned earlier, the potential function can become periodic in space under some circumstances, in which case it will be seen that $d\rho/d\xi$ is discontinuous. This case is discussed in the following chapter.

IV. THE PERIODIC DC SOLUTION

The preceding chapter showed that a basic solution of the dc potential function always exists in the opposite-stream diode and it is single valued. The term "basic solution" is used for the case when the potential in the diode reaches its maximum and minimum values only once. When both maximum and minimum appear inside the diode it is easy to extend the basic solution to the periodic type of solution shown on Fig. 8.
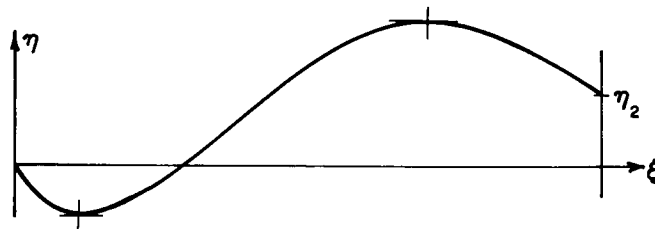
a. The basic solution
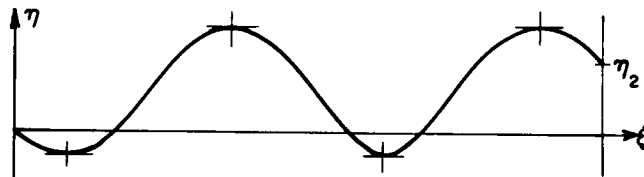
b. Periodic solution with three half periods
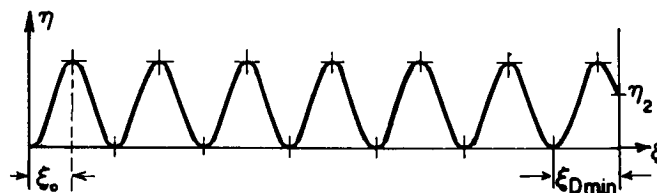
c. Periodic solution with the largest number of half periods possible for this diode

FIG. 8. THE CONSTRUCTION OF THE PERIODIC SOLUTION FOR A DIODE.

A. THE CONSTRUCTION OF THE PERIODIC SOLUTION

In Chapter II it was seen that the differential equation of our problem was satisfied with both signs of the square root in the velocity-distribution functions [see Eq. (11)]. The choice of these signs has to meet the boundary conditions of the physical diode. Let us start at the electron emitter of a diode inside of which there is a basic dc potential function of type D. Before the electrons reach the minimum, their space-charge function contains $F^+(\eta)$ which changes to $F^-(\eta)$ after the minimum. On the other side of η_m, both streams have $F^-(\eta)$ in their respective space-charge functions. Going toward the ion emitter, we arrive at the point of maximum potential. For the basic solution, $F^-(\eta)$ would change to $F^+(\eta)$ in the space-charge function of the ions. However, let us keep $F^-(\eta)$ for both streams, in which case the solution becomes periodic. Since we have an ion emitter at the far right, we have to change $F^-(\eta)$ to $F^+(\eta)$ in the space-charge function of the ions at the maximum point after a finite odd number of half periods. The potential on the other side of η_M is continued to the ion emitter. Hence, we have constructed a periodic solution for our differential equation which satisfies the boundary conditions also.

B. THE SPACE-CHARGE FUNCTION OF THE PERIODIC SOLUTION

As mentioned before, there is a difference between the two extrema that are near the respective emitter planes (which actually limit the currents) and the remaining extrema which appear periodically between the first two. The form of the space-charge function does not change at the latter points; however, there is a change at the current-limiting extrema. The physical difference in these cases is apparent from the determination of the spatial derivative of the space-charge function in Sec. IIIE. For the periodic extrema the derivative $d\rho/d\xi$ will be finite and it will have different signs if we approach the periodic extrema from different sides (see Fig. 9). This discontinuity makes our dc analysis of questionable value. It requires some rf analyses to determine how long, if at all, these periodic types of solutions could be supported in a diode of given dimensions.

THE PERIODIC SOLUTION
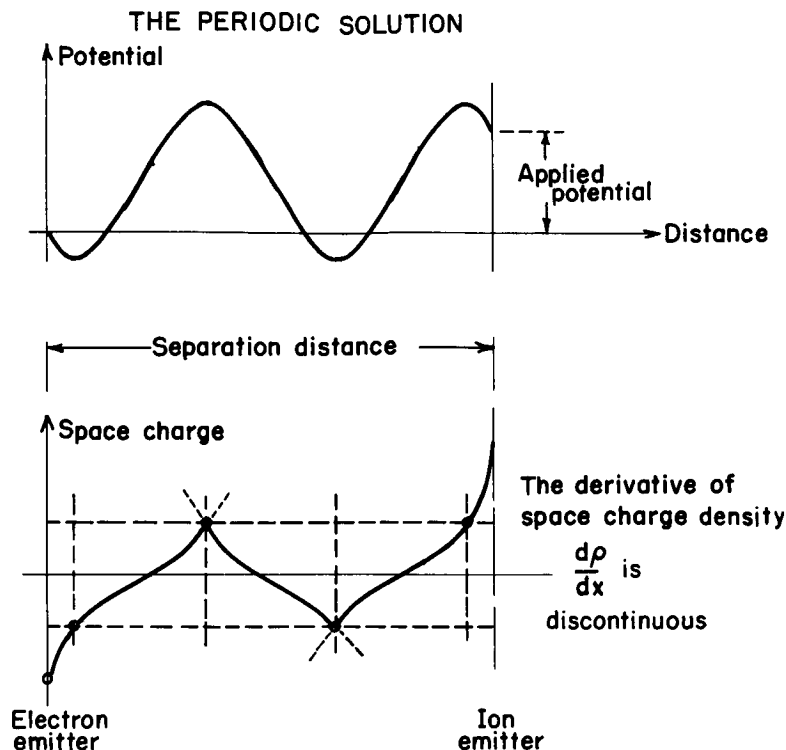
FIG. 9.   THE SPACE-CHARGE FUNCTION OF A PERIODIC SOLUTION.
The derivative of the space-charge function is continuous
at the first minimum and at the last maximum, but it is
discontinuous at the other extrema.

C.   DETERMINATION OF THE POSSIBILITY OF PERIODIC SOLUTIONS FOR A
     GIVEN OPPOSITE-STREAM DIODE

    For a given separation distance between the emitters, periodic
solutions would allow more current to flow in the diode than the basic
solution, and hence could be detected by simple dc measurements.
Consequently it would be desirable to be able to predict from theory
whether, in a given diode, periodic types of potential functions could
exist or not.   A simple procedure is presented which could establish
this fact for any given opposite-stream diode.

    If we follow the procedure of generating periodic solutions explained
in Sec. IVA, we can construct any odd number of half periods by increas-
ing the separation distance between the emitters.   In an experimental
diode, the separation distance is usually fixed; therefore, in order to
fit more than one period into the space, we have to decrease η_M and

increase η_m. We can thus increase the number of periods in the diode until one of the extrema is shifted to the boundary plane (see Fig. 8c). When this occurs, no more periods can be fitted in the diode space for the given conditions.

This procedure offers a convenient way to determine the maximum number of half-periods which could be present in the diode. In Fig. 8 it is seen that the length of one half-period of the highest order solution, ξ_0, is slightly less than the separation length of the transition case D-B or D-C. We called this length $\xi_{D_{min}}$. The difference between ξ_0 and $\xi_{D_{min}}$ is the region between the unsaturated emitter and the current-limiting extremum, which is usually small. Even for small η_2 the length of this region is no larger than 10 percent of ξ_0.

Since we are presenting a graphical procedure for designing purposes, the use of $\xi_{D_{min}}$ in the place of ξ_0 gives no noticeable error. If we divide the normalized separation distance ξ_2 by this length ξ_0, then the largest odd integer still less than this ratio ξ_2/ξ_0 will give the maximum number of half-periods that could exist in the diode.

We have calculated and presented here curves which give ξ_0, for most practical cases, as a function of the values of α, β, and η_2. We can calculate these values from the known construction and operation of the diode, by Eq. (31), and by the aforementioned normalization procedure. Given the values of α, β, and η_2, one can determine ξ_0 by the aid of the curves presented in Appendix C. The curves are given only for $\beta > 1$ because by simultaneously taking $1/\beta$ instead of β, and $1/\alpha$ instead of α, ξ_0 will remain unchanged. Since ξ_2 is also given, we can form the ratio ξ_2/ξ_0 and determine the maximum number of half-periods possible in the diode.

We can show the work involved in this procedure by using the diode example which was presented in Chapter I. Let us assume that we operate this diode with 30 v across it and would like to determine whether periodic types of solution could be present. Summarizing, the boundary values of this diode are:

$$J_{se} = 0.1 \text{ amp/cm}^2, \qquad J_{si} = 10^{-3} \text{ amp/cm}^2,$$

$$T_e = 1200^\circ \text{ K}, \qquad T_i = 1400^\circ \text{ K},$$

$$V_2 = 30 \text{ v},$$

$$d = 0.2 \text{ cm},$$

$$\sqrt{m_i/m_e} = 112$$

From these values and Eq. (15), we obtain

$$N_e = J_{se} \sqrt{\frac{2\pi m_e}{e^2 kT_e}} = 4.02 \times 10^{13} \frac{J_{se}}{\sqrt{T_e}} = 1.16 \times 10^{11} \text{ electrons/cm}^3$$

$$N_i = J_{si} \sqrt{\frac{2\pi m_i}{e^2 kT_i}} = 4.02 \times 10^{13} \sqrt{\frac{m_i}{m_e}} \frac{J_{si}}{\sqrt{T_i}} = 1.2 \times 10^{11} \text{ ions/cm}^3$$

so that, from Eq. (26), we have

$$\overline{N} = N_i + N_e = 2.36 \times 10^{11} \text{ particles/cm}^3$$

$$\overline{T} = \frac{N_i T_i + N_e T_e}{N_i + N_e} = 1302 \ ^\circ\text{K}$$

$$\overline{\lambda} = \sqrt{\frac{\epsilon_0 k \overline{T}}{e^2 \overline{N}}} = 6.9 \sqrt{\frac{\overline{T}}{\overline{N}}} = 5.13 \times 10^{-4} \text{ cm}$$

Then,

$$\xi_2 = \frac{d}{\overline{\lambda}} = 390$$

$$\eta_2 = \frac{e}{k\overline{T}} V_2 = \frac{11600}{\overline{T}} V_2 = 178$$

$$\alpha = \frac{J_{se}}{J_{si}} \sqrt{\frac{m_e}{m_i}} = 0.893$$

$$\beta = \frac{T_e}{T_i} \cong 1$$

For $\beta = 1$, $\alpha = 0.89$, $\eta_2 = 178$, the first diagram of Appendix C gives $\xi_0 = 140$. The ratio $\xi_2/\xi_0 = 390/140 \cong 2.8 < 3$, so that no periodic solution is possible.

If the diode separation were 1 cm, ξ_2/ξ_0 would be 14 and thus the maximum number of half-periods possible would be 13.

D. DETERMINATION OF CURRENT FLOWING THROUGH THE DIODE WHEN ONE EMITTER IS SATURATED

As we have seen, the potential function with the largest number of half-periods that can exist in the diode causes saturation of one of the emitters. The same effect happens if periodic solutions are not possible; but we apply such a large potential across the diode that the corresponding $\xi_{D_{min}}$ becomes equal to ξ_2, the separation distance. In both cases we have to determine whether the diode is ion- or electron-rich in order to tell which emitter will saturate first and what value of current is flowing through the diode for this voltage. We can do this by the function $G^-(x) - 1.0$ (see Table 2 for conditions for the diode to be ion- or electron-rich). This function is shown graphically on Fig. 10. With the aid of this graph, we determine two quantities:

$$Q_e = \alpha_e [G^-(\beta_e \eta_2) - 1.0] \tag{46}$$

$$Q_i = \alpha_i [G^-(\beta_i \eta_2) - 1.0] \tag{47}$$

where η_2 is the normalized potential difference of the emitters when saturation of one emitter occurs.
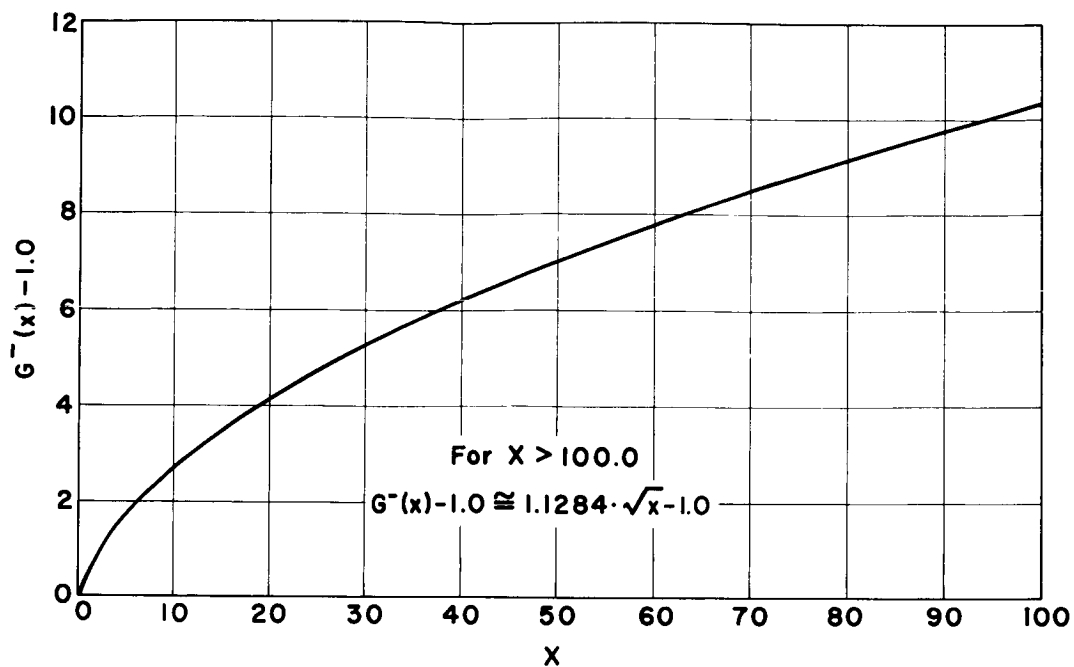
FIG. 10. THE FUNCTION $G^-(x) - 1.0$, WHICH IS USED FOR DETERMINING
WHETHER THE DIODE IS ELECTRON- OR ION-RICH.

When $Q_e > Q_i$, the diode is electron-rich and the ion emitter saturates first. The total current density in the diode at this saturation point is given by

$$J_{s_{total}} = J_{si} + \frac{Q_i}{Q_e} J_{se} \qquad (48)$$

When $Q_i > Q_e$, the diode is ion-rich and the electron emitter saturates first. The current density will be

$$J_{s_{total}} = J_{se} + \frac{Q_e}{Q_i} J_{si} \qquad (49)$$

For the diode example used, no periodic solution was possible; therefore, at $V_2 = 20$ v neither emitter can saturate. If we look for the potential which saturates one of the emitters of the diode that causes D-B or D-C transition of the basic type, we can simply set ξ_0 (or $\xi_{D_{min}}$) equal to ξ_2, and look up in the given curves the corresponding potential value. Since $\alpha = 0.89$ and $\beta \cong 1$, we find that the saturating potential η_s is equal to 780 (see diagram (a) in Appendix C). This is equivalent to 88 v. Working out values for Q_e and Q_i, we obtain

$$Q_e = \frac{\alpha \sqrt{\beta}}{1 + \alpha \sqrt{\beta}} [G^-(\beta_e \, \eta_s) - 1.0] \cong 14.6$$

$$Q_i = \frac{1}{1 + \alpha \sqrt{\beta}} [G^-(\beta_i \, \eta_s) - 1.0] \cong 16.3$$

Hence the diode is ion-rich, and the total current density at saturation is:

$$J_{s_{total}} = J_{se} + \frac{Q_e}{Q_i} J_{si} = 0.109 \text{ amp}/\text{cm}^2$$

It does not seem practical to give tables of data of diode characteristics since four boundary values are involved and even limited ranges of these values would require numerous tables. The computer program we have written does this job efficiently for any desired set of boundary values. Therefore, we are using the program as the final means of calculating diode characteristics. Information on this numerical program can be found in Appendixes A and B.

V. COMPUTER SIMULATION OF THE OPPOSITE-STREAM PLASMA DIODE

In the earlier chapters a complete dc theory of the opposite-stream plasma diode was presented. The results of this theory were calculated after making three basic assumptions. These were: motions of particles are confined in one dimension, collisionless conditions are present, and the state of the diode is time independent. To determine how closely these results can predict the behavior of an actual device, it is necessary to examine these assumptions as to their realizability under laboratory conditions.

The first two assumptions can be well approximated experimentally. The assumption of time-independent behavior, however, is not realistic and is necessary only in order to make the mathematical analysis feasible. Nevertheless, if the dc states are stable under time-varying conditions, then the time-average behavior of an experimental device will approximate its theoretical dc operation. But the question of stability can be . decided only by a time-dependent analysis. This question becomes more complex when, as happened in our analysis, more than one self-consistent dc state is possible for a set of boundary conditions. In this case, not only the stability of these dc states is of importance but also the knowledge of the conditions under which a particular dc state can develop in the diode.

The usual technique of linearizing the time-dependent, collisionless Boltzmann equation by assuming small-amplitude perturbations could not be applied to our problem. The nonlinear effects of particle trapping in potential wells would be lost in a linearized theory, and these effects play a major roll in the operation of our diode, since a potential maximum is formed near the ion emitter and a minimum near the electron emitter. On the other hand, if we try to follow the same procedure for the time-varying case as was used for the dc theory, we find a hopelessly complicated set of integrodifferential equations. This set includes the time-varying collisionless Boltzmann equation, Maxwell's equations, and the boundary conditions of our diode. Even if there were hope of obtaining an analytical solution to this set of equations, the extensive use of a computer would be unavoidable.

Fortunately, our efforts and computer time could be used much more efficiently by applying the well-known computer model of a one-dimensional plasma to our problem.

A. HISTORICAL DEVELOPMENT OF THE COMPUTER MODEL OF ONE-DIMENSIONAL PLASMAS

As early as 1943, D. R. Hartree and P. Nicolson [Ref. 12] used the computer simulation of the motion of charged particles in one dimension. In their paper, as in all subsequent papers written on computer models of one-dimensional plasmas, charges are represented as infinitely thin charged sheets that are moving perpendicular to their plane and carrying a set number of coulombs per area surface charge. Advance of time occurs in steps. During one time step the positions of the charged sheets are changed according to their velocities, and their velocities are changed according to their accelerations. The acceleration of a charged sheet is determined by the electric field that is acting on it, while the electric field is calculated from the positions of the charged sheets. If the duration of one time step is taken short enough, the electric field can be considered constant during this time interval. This means that the motion of sheets can be calculated independently for this time interval, since they experience constant acceleration. After the positions of all the sheets are changed, the electric field is recalculated and time advances by one time step. The calculation of the trajectories of the sheets involves only elementary arithmetic operations and a record of the positions and velocities of all the sheets employed. Hence the facilities of a digital computer are sufficient to perform these calculations.

Many authors since Hartree and Nicolson used the described procedure of computation for their various applications of one-dimensional plasmas. These works differ mainly by their methods of introducing the charged sheets into the plasma and by the boundary conditions of their models. The model of an infinite plasma (periodic boundary conditions) with equal number of electron and ion sheets was used by Buneman [Ref. 13] to show the randomization process of the motions of electrons and ions that had directed energies initially in a plasma. Dawson [Ref. 14] gave

an extensive study of the statistical behavior of the computer model of a one-dimensional plasma considering the motions of electron sheets in a neutralizing background of infinitely heavy ions.

The same computer model with minor alterations was applied also to finite or semifinite models of diodes, electron beams, or electron-ion systems. Analysis of the limiting perveance of electron beams and the investigation of transient effects in electron diodes were carried out by Birdsall and Bridges [Ref. 15], Twombly and Lauer [Ref. 16], and by Lomax [Ref. 17]. In these works electron sheets were injected at a plane with a given entrance velocity into a diode of finite size. Dunn and Ho [Ref. 18] considered a semi-infinite space that started at a plane where ion and electron sheets were injected. Assigning the electron sheets and ion sheets different masses and entrance velocities, they observed the neutralization effects of cold electrons in ion beams. The same problem with randomly emitted electron sheets was analyzed by Buneman and Kooyers [Ref. 19]. The random emission of electron sheets simulated a thermionic electron emitter in their model.

A paper by Tien and Moshman [Ref. 20] is different from those described above because they considered thermionically emitted electrons at a fixed position in a finite diode. For this reason this paper is more closely related to our approach than the papers already mentioned. They considered a finite space with a thermionic electron emitter as one of the boundary planes. The other plane was a collector of electrons. A constant potential was applied across the two planes. They were interested in the noise figure of an electron diode that is influenced by the fluctuations of the potential minimum near the thermionic electron emitter. Having an average of 363 electron sheets in the diode that were injected at the plane of the electron emitter in a random manner, they were able to determine this minimum noise figure.

For the computer simulation of the opposite-stream plasma diode, the model of Tien and Moshman has to be used with the addition of a thermionic ion emitter at the second boundary plane. This addition posed no difficulty. The major problem arose from the fact that we were interested in the formation of stable dc states in the diode and that only a very large number of ion and electron sheets could reveal

that the diode has a quiescent state. It is impossible to handle
several thousand sheets in accordance with the strict rules of the
computer models described above; even on a modern, high-speed computer
these calculations would take a long time. Consequently, we had to
alter the computer models in many ways. These alterations will be
discussed in the next section.

B. COMPUTER MODEL OF THE OPPOSITE-STREAM DIODE

Our aim was to construct a computer model of a one-dimensional
plasma diode with thermionic electron and ion emitters and with the
capability of handling thousands of sheets at every time step. Theoreti-
cally, the computer models described above would be sufficient for this
aim, but, because of their slowness of operation, they do not suffice.
In these programs the major part of the time is spent on the calcula-
tion of the electric field. In order to assign the right acceleration
to the sheets, the electric field has to be determined at each point
where a sheet is located. This can be done only if the sheets are
arranged, i.e., sorted according to their positions in the diode. For
several thousand sheets this sorting procedure is so slow that it makes
the whole program uneconomical. Fortunately, the calculation of the
exact field in the diode is not necessary; an approximating procedure
that uses coarse graining in space can avoid the complete sorting of the
sheets and produce results in a much shorter time.

1. Coarse Graining in Space

In the computer diode a charged sheet represents a certain amount
of surface charge; therefore, the electric field is discontinuous across
it. Let us assume that the value of the electric field is given at the
left boundary plane, and for convenience, that it is zero. (The calcula-
tion of the true field at the left plane will be discussed in a later
section.) The calculation of the field in the diode, or of the accelera-
tions of the sheets according to the exact field, is as follows. (See
Fig. 11a.) The field is unchanged until a sheet is reached, i.e., the
one nearest to the left plane. At the position of this sheet the

ION
SHEET

ELECTRON
SHEETS

ION
SHEET

ELECTRON
EMITTER

SHEET
NUMBER → 1   2   3   4 5

EXACT
ELECTRIC
FIELD

E_1 E_2

E_3

E_4 E_5

POSITION

a.   Exact field

APPROXIMATE
FIELD

MIDPOINTS

E_1

$E_2 = E_3$

$E_4 = E_5$

POSITION

LENGTH
OF
SEGMENT

0   1   2

SEGMENT NUMBERS
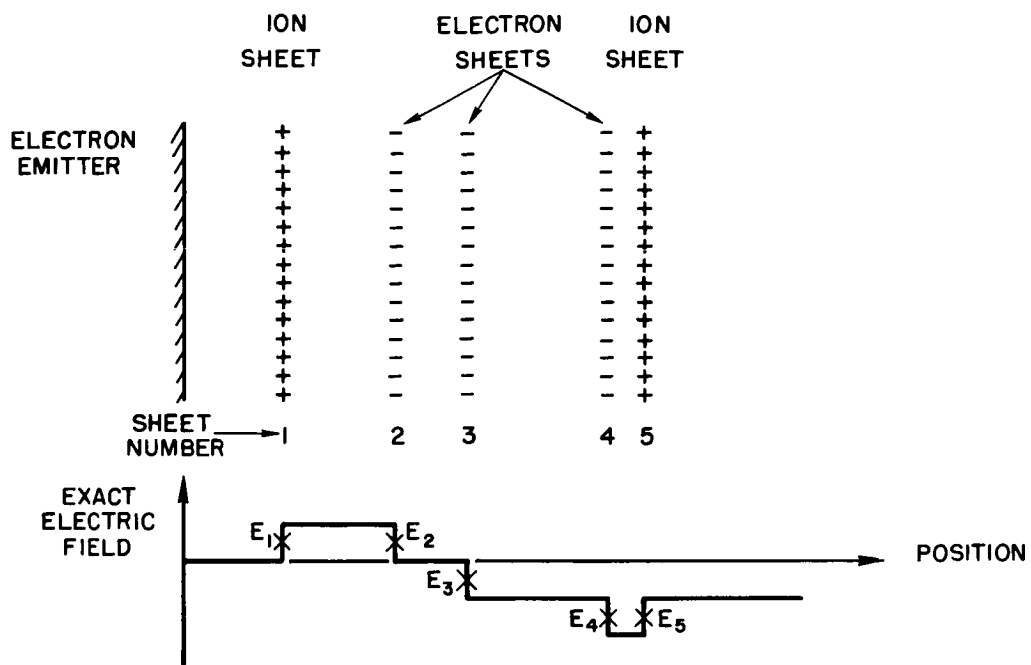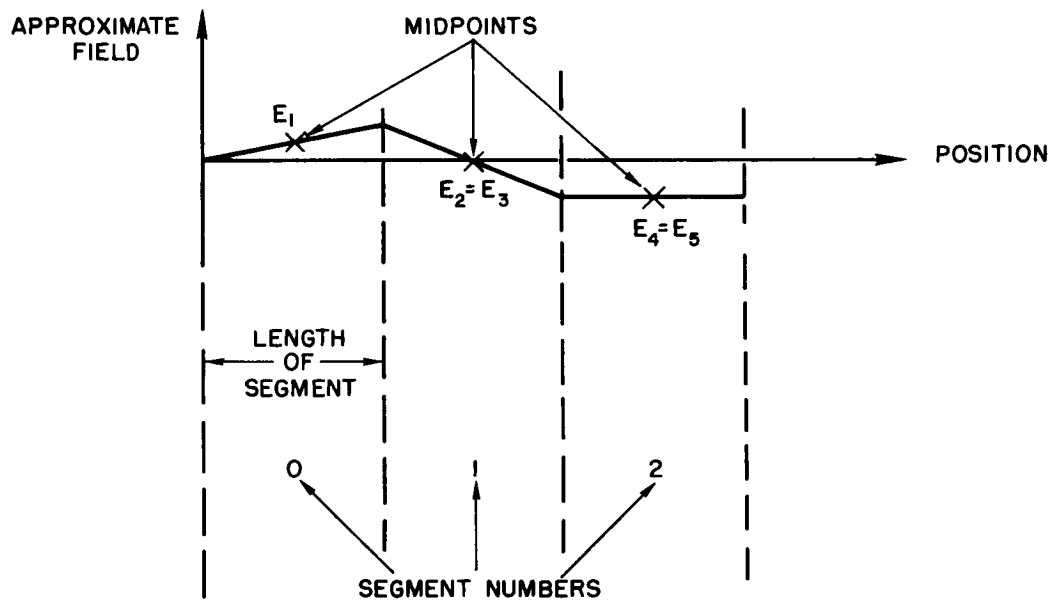
b.   The field calculated by a spatial coarse-graining procedure

FIG. 11.   THE FORM OF THE ELECTRIC FIELD IN A ONE-DIMENSIONAL
DIODE DETERMINED BY CHARGED SHEETS IN THE DIODE SPACE.

electric field jumps to a new value. The amount of the jump is pro-
portional to the surface charge that the sheet represents. The accelera-
tion of this sheet is determined from the field at the middle of the
jump, E_1, on Fig. 11a. On the other side of the sheet the field is again
constant until the next sheet is reached, where it changes its value by
the same amount as before. The direction of the change is determined by
the sign of the charge on the sheet. The accelerating field acting on
this new sheet, E_2, is taken again at the middle of the jump. Since the
order in which the sheets are following each other in space is known,
this procedure can be continued from sheet to sheet.

In the coarse-grained model (coarse graining in space was first used
by Dunn and Ho in Ref. 18 and it was also applied by Hockney for the
computer model of a two-dimensional plasma [Ref. 21] p. I-102), the diode
space is divided into a number of small segments that have equal lengths.
The position of a sheet is recorded exactly as in the earlier models,
but its charge is assumed to be uniformly distributed in the segment in
which it is located. If there is more than one sheet in a segment, the
algebraic sum of their charges is taken and distributed uniformly.
Consequently, in each segment the field is a linear function of distance
and its total change across a segment is determined by all the sheets
that are located in it (Fig. 11b). All these sheets are given the same
acceleration that is determined from the value of the electric field at
the middle of the segment.

When we use this coarse-graining procedure we are allowing for an
error both in the calculation of the electric field and in giving the
same acceleration to all the sheets that lie in one segment. The error
in the evaluation of the electric field is small if there are a large
number of sheets in the diode and if the length of a segment is a frac-
tion of the characteristic Debye length, $\overline{\lambda}$. The error in giving
neighboring sheets exactly the same acceleration cannot cause a false
collective phenomenon in our model because even initially the velocities
of the sheets are in disorder. We have made trial calculations with
both the exact and the coarse-grained methods having an average of 1000
sheets in the diode. We have divided the diode that was 40 Debye lengths
long into 1024 segments. The results obtained by the coarse-grained

method did not differ noticeably from that of the exact calculations; furthermore, there was a considerable saving in computer time. In later calculations we used nearly 10,000 sheets and could expect that the approximations used did not affect our results at all.

The sorting of the sheets is eliminated because the electric field is now calculated at fixed points in the diode and not at the changing positions of these sheets. A detailed description of these calculations, as well as other parts of this computer program, is given in Appendix D.

2. Moving the Sheets During a Time Step

On Fig. 12 the schematic diagram of the computer model is shown. The first major function that the program executes is the advancing of sheets according to their velocities, accelerations, and equation of motion. The equation of motion of the sheets can be represented by a vector equation in the space of N dimensions where N is the number of sheets.

$$\ddot{\vec{x}} = \vec{f}(\vec{x}) \tag{50}$$

The two dots signify the second derivative with respect to time. The components of the position vector $\vec{x}$ are the x positions of the N sheets, and the components of the vector $\ddot{\vec{x}}$ are the accelerations of the sheets, respectively. The solution of this highly complicated, nonlinear differential equation is carried out by increasing time in small steps and making some assumptions about the behavior of the diode during one time step. The state of the diode can be calculated from its known state at the previous time step. The assumption is usually made that during a time step (Δt) the accelerations of the sheets are constant. Then, if the positions and velocities of the sheets at time t_n are $\vec{x}(t_n)$ and $\dot{\vec{x}}(t_n)$, their new positions and velocities are calculated from the following expressions:

$$\vec{x}(t_{n+1}) = \vec{x}(t_n) + \dot{\vec{x}}(t_n) \, \Delta t + \frac{1}{2} \ddot{\vec{x}}(t_n) \, (\Delta t)^2$$

$$\dot{\vec{x}}(t_{n+1}) = \dot{\vec{x}}(t_n) + \ddot{\vec{x}}(t_n) \, \Delta t \tag{51}$$
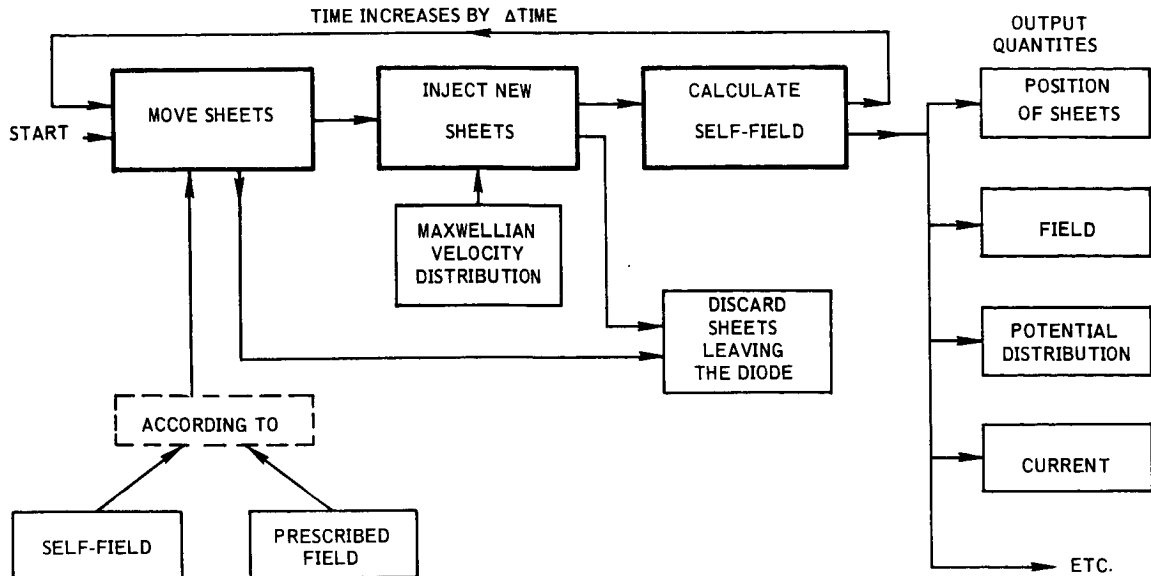
FIG. 12. FLOW CHART OF THE COMPUTER PROGRAM THAT
SIMULATES THE MOTIONS OF CHARGED SHEETS IN A
ONE-DIMENSIONAL DIODE.

where $\dot{\vec{x}}(t_n)$ is given by Eq. (50) from $\vec{x}(t_n)$. This procedure is
correct when Δt approaches zero, but it could cause a considerable
error in the calculations for a finite Δt if there are regions in
the diode that are greatly influenced by the distribution of charges.
In this case a small change in the position vector could cause a large
change in the acceleration of the sheets during a time step. Naturally,
this is the case for a nearly neutral plasma, in which the assumption
of constant acceleration even for a small time step cannot be made.
Dunn [Ref. 21] has demonstrated that when using the above procedure in
a nearly neutral plasma the amplitudes of oscillations were increasing,
though rigorous analysis showed that only sinusoidal oscillations could
be present.

The assumption of constant acceleration of the sheets during a
time step is not necessary. Any model that gives the exact results for
the case of constant field in the diode is acceptable. This means
that if the field in the diode is a constant both in space and in time,

the results of the computer calculations cannot be functions of the size of the time step and they have to agree with those calculated by Eq. (51). If this condition is satisfied, then we are certain that the calculations give the right results when Δt approaches zero. Furthermore, if we do not assume that sheets have constant accelerations during a time step, our solution is a good approximation to the exact solution when a small but finite Δt is used for any physical problem.

Let us observe first that the acceleration of the sheets $\ddot{\vec{x}}$, given by Eq. (50), is determined at times when the position of the sheets are known. Hence, $\ddot{\vec{x}}$ is known only at times separated by certain time intervals. Let us assume that our calculation was exact up to time t_n, and from the past motion of the sheets and their accelerations at time t_n, we would like to calculate their positions at a future time t_{n+1}. (See Fig. 13.) Since we know the positions of the sheets at time t_{n-1}, we know the change in their positions that occurred in the time interval $t_{n-1} \leq t_n \leq t_{n+1}$. We call this change $(\Delta\vec{x})_{t_{n-1}}$. Our aim is to calculate $(\Delta\vec{x})_{t_n}$, which determines the positions of the sheets at time t_{n+1}. We know the value of the second derivative of $\vec{x}$ at time t_n; we make the assumption that this derivative does not differ much from the second difference of $\vec{x}$ divided by the square of the time step. The second difference of $\vec{x}$ can be calculated from the first differences $(\Delta\vec{x})_{t_n}$ and $(\Delta\vec{x})_{t_{n-1}}$, giving

$$\ddot{\vec{x}}(t_n) \cong \frac{(\Delta\vec{x})_{t_n} - (\Delta\vec{x})_{t_{n-1}}}{(\Delta t)^2} \tag{52}$$

From Eq. (52), $(\Delta\vec{x})_{t_n}$ can be expressed and the new positions of the sheets are given by the expression:

$$\vec{x}(t_{n+1}) = \vec{x}(t_n) + (\Delta\vec{x})_{t_n} = \vec{x}(t_n) + (\Delta\vec{x})_{t_{n-1}} + \ddot{\vec{x}}(t_n)\,(\Delta t)^2 \tag{53}$$
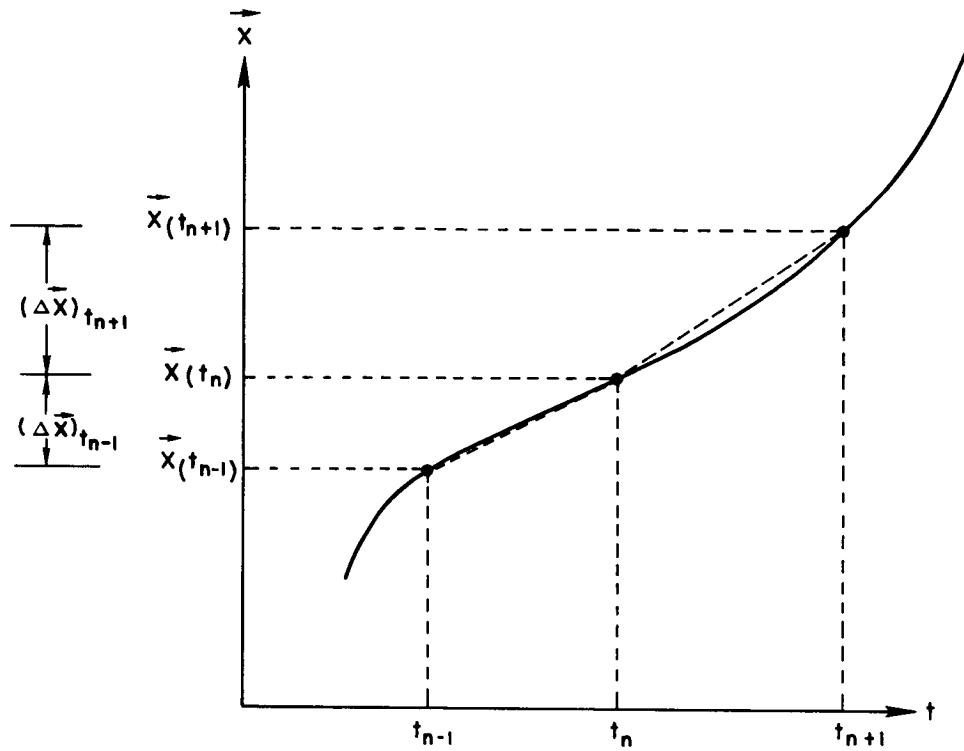
FIG. 13. TRAJECTORIES OF CHARGED SHEETS AS APPROXIMATED BY A STEP-BY-STEP ADVANCE OF TIME. The acceleration $\overset{\cdot\cdot}{\vec{x}}(t)$ is given at time t_n.

If the acceleration of a sheet is constant, the trajectory of the sheet becomes a second-order parabola and the described method gives this trajectory independently of the size of Δt used. Let us consider a sheet that has a position $x(t_{n-1})$, and velocity $v(t_{n-1})$ at time $t = t_{n-1}$, and that it is in a constant field region. If the acceleration of the sheet is "a" (a constant), then the change in the position of the sheet during the time interval $t_{n-1} \leq t_n \leq t_{n+1}$ is

$$(\Delta x)_{t_{n-1}} = v(t_{n-1})\,\Delta t + \frac{1}{2}\,a(\Delta t)^2 \tag{54}$$

The position of the sheet at time $t = t_n$ is $x(t_n)$, and

$$x(t_n) = x(t_{n-1}) + v(t_{n-1})\,\Delta t + \frac{1}{2}\,a(\Delta t)^2 \tag{55}$$

Equation (53) gives the value of $x(t_{n+1})$ since the acceleration of the sheet is "a" at time $t = t_n$ also. The resulting relation is

$$x(t_{n+1}) = x(t_n) + v(t_{n-1})\,\Delta t + \frac{1}{2}\,a\,(\Delta t)^2 + a\,(\Delta t)^2 \tag{56}$$

$$= x(t_{n-1}) + v(t_{n-1})\,(2\Delta t) + \frac{1}{2}\,a\,(2\Delta t)^2$$

which is the exact position of the sheet at time $t = t_{n+1}$ calculated by its equation of motion. This result shows that our model approaches the true physical diode if $\Delta t \to 0$. By treating Δt as a parameter of the computer model, we can examine the results of computer runs that were made with different Δt but which apply to the same physical situation. If we decrease Δt and do not observe any change in the results, then it is certain that the error in using finite differences instead of differentials is not significant. Since we deal with a physical device, we are certain that this limit can always be reached with a small but finite Δt.

We have shown how our computer program advances the sheets during a time step. A record is kept of the position and the previous change of the position of each sheet as long as the sheet stays in the diode space. The accelerations of the sheets can be calculated from their self-field, in which case the natural behavior of the diode is reproduced; or it can be calculated from a prescribed dc field distribution, in which case a desired state is forced on the diode. The actual procedures of the computer program that execute the advancing of the sheets are discussed in Appendix D.

3. Injecting New Sheets in the Diode

The electron and ion emitters of our model are simulated by the injection of electron and ion sheets at their respective emitter planes. Before discussing the assignment of the initial velocities to these sheets, it is necessary to show the relation between the initial velocity of an injected sheet and its equation of motion for the first time step it spends in the diode space. The successive motion of the sheet is then calculated by the procedure of the previous section.

Let us assume that a sheet is injected into the diode during the time interval $t_{n-1} < t < t_n$ (Fig. 14) at one of the boundary planes, and with an initial velocity v_0. Since we do not know the exact time of injection, we assume that it was injected at time $t = t_n - R \Delta t$, where R is a number between zero and one. At time $t = t_n$ a position $x(t_n)$ and a previous change of position $(\Delta x)_{t_{n-1}}$ has to be assigned to this sheet so that it can be moved during the next time step.
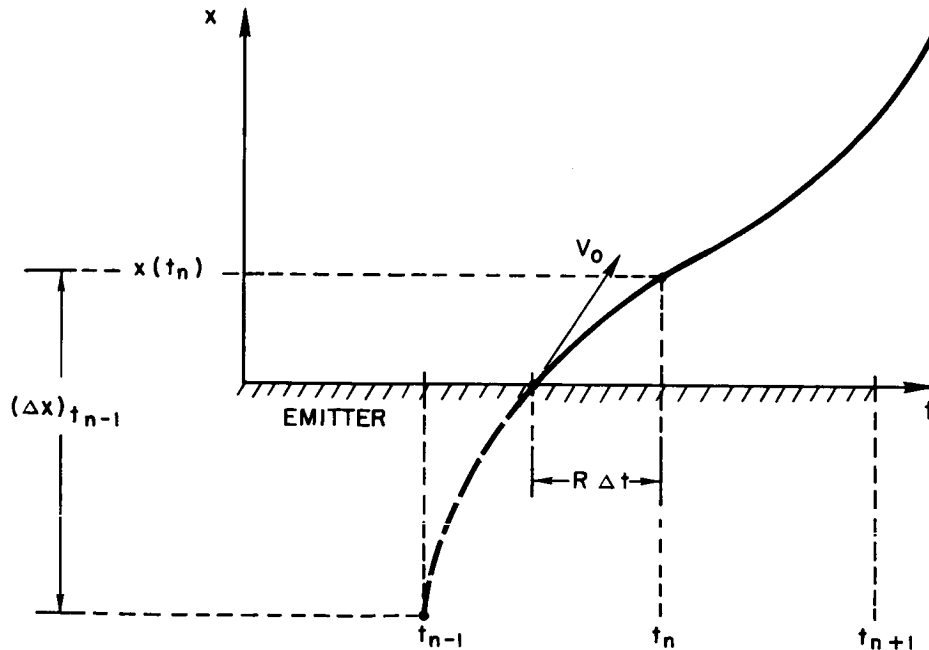
FIG. 14. TRAJECTORY OF AN INJECTED SHEET DURING THE FIRST TIME STEP IT SPENDS IN THE DIODE SPACE.

In order to determine the values of these two quantities as functions of v_0 and R, we use the condition that our model has to be exact when the field is uniform in the diode. Consequently, the simplest assumption is that the acceleration of the injected sheet is a constant during the time interval $t_{n-1} \leq t \leq t_n$. This acceleration is calculated from the field in the segment nearest to the emitter plane, and at time $t = t_{n-1}$. Let us call this acceleration $a_0(t_{n-1})$ for the sheet injected, then the position of the sheet at time $t = t_n$ can be expressed as

$$x(t_n) = v_0 \, R \, \triangle t + \frac{1}{2} a_0(t_{n-1}) \, (R \, \triangle t)^2 \qquad (57)$$

assuming that the injection plane is located at $x = 0$. When calculating the previous change in the position of the injected sheet, we extrapolate its trajectory to time $t = t_{n-1}$. (See Fig. 14.) Assuming constant acceleration for this trajectory, this change can be calculated by the following expression:

$$(\triangle x)_{t_{n-1}} = v_0 \, \triangle t + a_0(t_{n-1}) \, (R - \frac{1}{2}) \, (\triangle t)^2 \qquad (58)$$

The injection of sheets occurs at a constant mean rate, i.e., a set average number per time step. In Eqs. (57) and (58), R could be represented as a random number uniformly distributed between 0 and 1. This arrangement would simulate the continuous operation of the emitter. In our case, however, such an arrangement would be an unnecessary complication, since the initial velocities of the sheets are already randomized. We can eliminate R by considering it as a random number and calculate the average values of the above expressions. The averaging yields to the following values of the initial conditions of an injected sheet:

$$x(t_n) = \frac{1}{2} v_0 \, \triangle t + \frac{1}{6} a_0(t_{n-1}) \, (\triangle t)^2$$

$$\qquad (59)$$

$$(\triangle x)_{t_{n-1}} = v_0 \, \triangle t$$

This rigorous derivation of the initial conditions for the injected sheets has not been used in earlier works, though an error in assigning x and $\triangle$x to the injected sheets could cause large deviations (10-20 percent) in the values of the current limiting extrema near the emitters. The random velocity v_0 and the instant of injection indicated by R are uncorrelated.

We used the method of Tien and Moshman [Ref. 20] to simulate the thermionic emitters of the opposite-stream diode. A sequence of numbers R', called pseudo random numbers, is generated in the IBM 7090 computer with the Power Residue Method [Ref. 22]. These numbers are uniformly distributed in the unit interval, so $0 < R' < 1$, where R' signifies a member of the sequence. Whenever a sheet is injected, a successive member of the sequence is calculated. If the sheet is an electron sheet, it will be assigned the initial velocity:

$$v_{0e} = \sqrt{\frac{2kT_e}{m_e}} \sqrt{- \log R'} \qquad (60)$$

If it is an ion sheet, its initial velocity will be given by

$$v_{0i} = \sqrt{\frac{2kT_i}{m_i}} \sqrt{- \log R'} \qquad (61)$$

The symbols mean the same as before: T is temperature, m is mass, and k is Boltzmann's constant. The symbol R' stands for a particular member of the sequence of pseudo random numbers uniformly distributed in the unit interval and uncorrelated with R.

4. Calculation of the Electric Field, and Current Density in the Diode

The electric field is determined by the combined effect of the distribution of charges in the diode (ρ) and the applied potential across the emitters, (V_2). We have considered only the former (Sec. 1) until now. When the applied potential is constant in time, as was the case in all the aforementioned papers on computer models, the separation of these two effects is immediate. This method can also be used

when the applied potential is a function of time, but we have to show that it is compatible with the physics of our problem.

The electric field in the diode, $E(x,t)$, satisfies the following equations:

$$\int_0^d E(x,t) \, dx = - V_2(t) \tag{62}$$

and

$$\frac{\partial E(x,t)}{\partial x} = \frac{\rho(x,t)}{\epsilon_0} \tag{63}$$

The field is separated into two parts as in the case when V_2 was constant, so one part will not be a function of space:

$$E(x,t) = E_1(x,t) + E_2(t) \tag{64}$$

We can force a condition on the other part:

$$\int_0^d E_1(x,t) \, dx = 0 \tag{65}$$

From Eqs. (62), (64), and (65), E_2 can be determined, giving

$$E_2(t) = - \frac{V_2(t)}{d} \tag{66}$$

The substitution of Eq. (64) into Eq. (63) yields the result

$$\frac{\partial E_1(x,t)}{\partial x} = \frac{1}{\epsilon_0} \rho(x,t) \tag{67}$$

The separation is completed, since E_1 depends only on the space-charge distribution in the diode and E_2 is a function only of the applied potential. In order to calculate the total field that is acting on the sheets, E_1 and E_2 are determined separately and then their sum is taken.

In Sec. B1 of this chapter we showed the construction of the field in the diode with the assumption that it is zero at the left boundary plane $(x = 0)$. These calculations involved only E_1; the applied potential was ignored. With the assumption of zero field at the position $x = 0$, Eq. (67) can be integrated. Let us call this field E_1'. The difference between E_1 and E_1' is not a function of distance and can be determined by using Eq. (65). The relation is:

$$E_1(x,t) = E_1'(x,t) - \frac{1}{d} \int_0^d E_1'(x,t)\, dx \tag{68}$$

With the help of Eq. (67), E_1 can be expressed as a function of $\rho(x,t)$ only. The result is given by Eq. (69).

$$E_1(x,t) = \frac{1}{\epsilon_0} \left[\int_0^x \rho(x,t)\, dx - \frac{1}{d} \int_0^d \left(\int_0^x \rho(x,t)\, dx \right) dx \right] \tag{69}$$

For the coarse-grained model of our diode (see Fig. 11b) the integrals of the above expressions become sums of integrals. The integral of the coarse-grained field is calculated in each segment and then the results summed over all segments. In Eq. (68) for example, the expression $\frac{1}{d} \int_0^d E_1'(x,t)\, dx$ becomes

$$\frac{1}{d} \sum_{n=0}^{N_s - 1} \int_{(n/N_s)\, d}^{(n+1/N_s)\, d} \overline{E}_1'(x,t)\, dx \tag{70}$$

where N_s is the number of segments in the diode, $\overline{E}_1'$ is the coarse-grained field, and d is the length of the diode. Since the field varies linearly in each segment, the area under it is given by the product of the length of the segment (d/N_s) and the value of the field at the middle of the segment, which we will call $\overline{E}_1'(n,t)$. Here "n" signifies the segment number. Hence,

$$\int_{(n/N_s)\,d}^{(n+1/N_s)\,d} \overline{E}_1'(x,t)\,dx = \frac{d}{N_s}\,\overline{E}_1'(n,t) \tag{71}$$

and the total integral becomes the summation:

$$\frac{1}{N_s} \sum_{n=0}^{N_s-1} \overline{E}_1'(n,t) \tag{72}$$

Since the coarse-grained field is determined at the midpoint of each segment, the above expression is used in the place of the integral in Eq. (68).

Current is continuous in space; therefore, the current density of our model cannot be a function of position. Maxwell's equations show that current has a conductive and a displacement part; similarly, the current density ($J(t)$) of a one-dimensional plasma breaks up into two parts: a conductive part that is carried by the charged sheets of the model, and a displacement part that is determined from the time derivative of the electric field. We can represent this by the following equation:

$$J(t) = j_c(x,t) + \epsilon_0 \frac{\partial E(x,t)}{\partial t} \tag{73}$$

The electric field is separated into two parts (see Eq. (64)). Substituting Eq. (64) into Eq. (73), we arrive at the following form of the current density:

$$J(t) = j_c(x,t) + \epsilon_0 \frac{\partial E_1(x,t)}{\partial t} + \epsilon_0 \frac{dE_2(t)}{dt} \tag{74}$$

The first two terms on the right-hand side of Eq. (74) depend only on the distribution of charged sheets in the diode. The sum of these two terms can be a function of time only, for the other terms of the equation are both independent of distance. This sum, the convection current density in our diode, will be represented by the symbol $J_{conv}(t)$

and calculated by the following expression:

$$J_{conv}(t) = j_c(x,t) + \epsilon_0 \frac{\partial E_1(x,t)}{\partial t} \qquad (75)$$

The last term in Eq. (74) signifies a current that is due only to the applied potential across the diode. This current is zero if the applied potential is constant. Consequently, this term represents the displacement current density in the capacitance of the empty diode. The symbol $J_{disp}(t)$ is used for this part of the current density. If Eq. (66) is substituted into Eq. (74), the last term of the equation becomes

$$J_{disp}(t) = - \left(\frac{\epsilon_0}{d}\right) \frac{dV_2(t)}{dt} \qquad (76)$$

We constructed an equivalent circuit diagram of the computer model on the basis of Eqs. (75) and (76). The application of this circuit diagram becomes important for the case when an external impedance is connected to the diode. With the help of the circuit equivalent, one can determine conveniently the relations between voltages and currents in the circuit and calculate these quantities at every time step by the computer. We will show a simple application of the equivalent-circuit model in the next chapter.

Since the current density of the diode is the sum of two terms, the circuit equivalent is represented by a parallel circuit (Fig. 15). One branch represents the capacitance of the empty diode, the other shows a current generator that can be influenced by the voltage that is applied across it. The current of this generator at each time step is influenced also by the momentary distribution and motions of the sheets in the diode. We showed this dependence simply by writing the current as a function of both V_2 and time. The equivalent-circuit diagram of the computer diode is shown on Fig. 15. The symbol "A" is the cross-sectional area of the diode.

It is still necessary to describe the method by which $J_{conv}(t)$ is calculated in our diode model. Since this convective term is the sum of two expressions that are both functions of distance, a reference
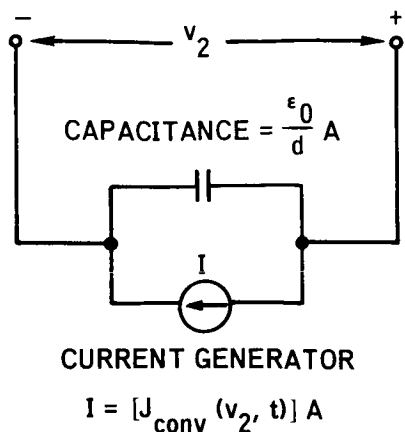
FIG. 15.   EQUIVALENT-CIRCUIT DIAGRAM
OF THE COMPUTER-SIMULATED DIODE.

position has to be given at which these expressions are calculated.
For convenience, we take the plane of the electron emitter as reference.

The first term on the right-hand side of Eq. (75) gives the value
of the current density that the charged sheets carry. Each charged
sheet represents a set amount of surface charge, σ . During a time
step, Δt, a certain number of sheets cross the reference plane, or what
is equivalent, some amount of charge per area crosses the electron
emitter. All sheets carry the same absolute amount of charge, only the
sign of σ is different for the ion and electron sheets. We can deter-
mine the total amount of charge that crosses the reference plane during
a time step in the following manner. We add the number of electron
sheets that are injected in this time interval to the number of ion
sheets that leave the diode space at the electron emitter during the
same time interval. We subtract from this sum the number of electron
sheets that return to their emitter during Δt and call the resulting
number ΔN. The product $\sigma \Delta N$ is the amount of positive charge per
area that crossed the plane of the electron emitter from right to left
during the time interval Δt, hence the contribution of this charge to
the current density is $\sigma \Delta N/\Delta t$. The direction of this current is in
the direction of decreasing position, therefore it is substituted into
Eq. (75) with a minus sign. The time step Δt is a constant, but the

SEL-64-012   - 58 -

number of the crossing sheets is a function of time, for the sheets are arriving at the electron emitter in a random manner.

With the known value of $j_c(x,t)$ and with the substitution of differences in the place of the derivative, Eq. (75) can now be calculated. At time $t = t_{n-1}$ the value of $E_1(x,t)$ at the electron emitter is $E_1(0,t_{n-1})$. During the time interval $\triangle t$, sheets are advanced and new sheets are injected; also $\triangle N$ is calculated. The moving sheets change the electric field; E_1 also changes and is recalculated at time $t = t_{n-1} + \triangle t$, i.e., at time $t = t_n$. This new value is $E_1(0,t_n)$. The convective current density is given by Eq. (75); or with the substitution of the above quantities, it becomes:

$$J_{conv}(t_n) = - \frac{\sigma \triangle N}{\triangle t} + \epsilon_0 \frac{E_1(0,t_n) - E_1(0,t_{n-1})}{\triangle t} \qquad (77)$$

Current is continuous in the computer model, since the value of Eq. (77) is independent of the reference plane used.

We have described the sheet model of the opposite-stream plasma diode. This model is made suitable for computer calculations by a normalization procedure and several numerical methods. The success of our computer model depends greatly on these methods, for they determine the accuracy and speed of the calculations. These methods are described in Appendix D.

VI. CHARACTERISTICS OF THE COMPUTER-SIMULATED, OPPOSITE-STREAM PLASMA DIODE

In the preceding chapter and in Appendix D the construction of the computer program was described. We proceed to use this program to find the behavior of the opposite-stream plasma diode, i.e., conduct a large number of computer experiments from whose results we are able to predict the diode's behavior with certainty in all circumstances. The use of a high-speed computer has to be limited to time intervals of the order of minutes to make the computer calculations economically feasible; on the other hand, a computer experiment has to refer to a real-time interval that is meaningful for a real experiment. Consequently, the relation between computer time and its equivalent in real time has to be discussed first.

In a finite diode, such as the opposite-stream diode, the shortest "meaningful" time interval for an experiment can be derived from the average transit time of the slowest particles. The transient behavior of the diode must depend on this transit time, for an equilibrium state can develop only in the order of a few average transit times of the slowest particles. It can be shown easily that the average transit time of the ions for very low applied voltages is directly proportional to the length of the diode and to the square root of the ratio of ion-to-electron mass.

Time in the computer model (τ) is measured in a normalized form (see Appendix D). The relation between normalized time and real time is given by the following expression:

$$\tau = \frac{\bar{v}}{\bar{\lambda}} t \tag{78}$$

(Note that τ is a measure of time in a physical sense, not a measure of the actual time the calculations take. The relation between τ and the time of computations will be discussed later.) In the above expression, t is real time; $\bar{v}$ is a characteristic thermal velocity for the diode $\sqrt{2k\bar{T}/m_e}$; and the quantities $\bar{N}$, $\bar{\lambda}$, and $\bar{T}$ have all been defined in Chapter III. The average transit time of the ions, expressed

in terms of normalized time, is of the order of $\xi_2 \sqrt{m_i/m_e}$, where ξ_2 is the length of the diode measured in Debye lengths (ξ_2 was also defined in Chapter III). For insuring the possible existence of a periodic solution in the diode, the value of ξ_2 must be at least 40. Using this separation distance for a diode, a normalized time interval of $150 \sqrt{m_i/m_e}$ should be a meaningful experiment on the computer.

We still have to determine the actual time spent by the computer calculations for such an experiment. This time naturally depends upon how many times the positions of the sheets are recalculated during a complete computer run. The longer the time that elapses between time steps ($\Delta \tau$), the less time is spent by the computer for a particular experiment. The duration of a time step cannot be increased without limit, however, for the accuracy of the computer model depends upon the fact that this quantity is kept small. In order to determine how small $\Delta \tau$ should be, we have to find a time interval that characterizes the fastest particles in the diode. We take the average plasma period of the electrons as this characteristic time interval, and make certain that the positions of the sheets are recalculated at least a few times within one electron plasma period. The average plasma period can be estimated by the characteristic electron plasma frequency $\bar{\omega}_{pe} = \sqrt{\bar{N} e^2 / \epsilon_0 m_e}$. Using this $\bar{\omega}_{pe}$, the average electron plasma period in a normalized form is

$$\tau_{pe} = 2\sqrt{2}\, \pi \cong 9$$

Hence a normalized time interval of unity means that the positions of the sheets are recalculated nine times during τ_{pe}, which should be sufficient for our model. We have also found that if we choose $\Delta \tau$ smaller than unity, it does not influence the results of the computer calculations.

We have already mentioned that when the full capacity of the IBM 7090 is used (an average of 10,000 sheets within the diode space), the computations for a time step take less than 2 sec. Hence, $2 \cdot 150 \sqrt{m_i/m_e}$ sec, or approximately $5 \sqrt{m_i/m_e}$ min, are sufficient for a

complete computer experiment. It is evident that the value of the ion-to-electron mass ratio in the computer model must be chosen much smaller than it is in reality; however, we will show later that the hypothetical values of 1, 4, 16 for m_i/m_e clearly demonstrate the effect of this mass ratio on the results. Hence, by calculating computer runs for these values, one can predict the behavior of the diode for larger mass ratios also. Consequently, the longest computer runs take 20 min computer time, a short enough time to prove the computer model highly practical and economical.

A. PARAMETERS OF THE COMPUTER DIODE

The parameters of an opposite-stream diode were selected such that it could support both the basic and some periodic solutions. We had to keep the length of the diode as short as possible in order to save computer time, for the relaxation time of the diode depends on the transit time of the ions. Choosing the diode to be 40 Debye lengths long satisfied all the required conditions, and we did not have to choose different diodes for the various computer experiments performed.

For simplicity's sake, the temperatures of the emitters were set equal $(\beta = 1)$. This choice did not introduce a symmetry into the computer calculations because the saturation current densities of the electron and ion emitters were different, even for equal masses of ions and electrons. The dc parameter α that determines this ratio was chosen to be 1.5.

The applied potential across the diode determines whether periodic solutions could exist in principle in the diode. The diagrams presented in Appendix C answer this question for an arbitrary potential value. We used a normalized potential value $\eta_2 = 1.6$ for our diode. The transition length associated with our diode is 10. (This was determined from Appendix C.) The separation length of the diode is 40, and the value of the ratio is 4. This shows that a periodic solution with three half-periods could be present in our diode.

The mass ratio m_i/m_e is not an important parameter of the normalized dc problem, because the dc potential distribution, given in a normalized form, is independent of this ratio. The normalized

dc current, however, depends on the mass of the ions because of the way it is normalized. Transient phenomena also depend on the mass ratio. In particular, computations showed that the mass of the ions determines the time interval within which the diode establishes its equilibrium state. This time interval is approximately proportional to the square root of the ratio m_i/m_e. In order to keep the computation time as short as possible, we used the hypothetical mass ratios 1, 4, and 16.

There are two other parameters of the computer model that have to be determined. One is the length of the time step $\Delta\tau$, the other is the number of electron sheets injected per normalized time Γ_e. We used for $\Delta\tau$ the value 1 throughout our calculations. We have showed that in this case the electric field and the state of the diode are recalculated about nine times in every electron plasma period. Trial calculations with smaller values of $\Delta\tau$ gave the same results as those calculated with $\Delta\tau = 1$. This showed that the exchange of differences for differentials introduced only a very small error in the calculation of the trajectories of the sheets in the diode.

For each computer calculation the electron injection rate, Γ_e, was chosen as large as possible. The memory-core storage capacity of the IBM 7090 limits the choice of Γ_e, for the maximum number of sheets present in the diode space during a computer run is proportional to Γ_e. The choice of this parameter is discussed in the next section.

The parameters of the diode are summarized in Table 3, together with the corresponding dc currents. The values of these dc currents

TABLE 3. PARAMETERS AND CORRESPONDING DC CURRENTS

Parameter					Calculated dc Current	
α	β	ξ_2	η_2	m_i/m_e	J_{basic}/J_{sat}	J_{per}/J_{sat}
1.5	1.0	40	1.6	1	0.239	0.700
				4	0.225	0.656
				16	0.214	0.625

were computed by the numerical procedure for the dc states of the diode described earlier (see Appendixes B and C).

B. FORMATION OF THE BASIC SOLUTION

We want to find the equilibrium state of the computer-simulated diode and compare it to the dc states. The computer calculations start with an empty diode and with the normalized potential value, $\eta_2 = 1.6$, applied across the emitters. During each time step a constant number of electron and ion sheets are injected into the diode space at their respective emitter planes. These sheets are moved under the influence of the electric field that is determined from the combined effect of the charges in the diode and the applied potential. The number of sheets in the diode is increasing until there are as many sheets leaving on an average as are injected. When this happens, the diode has reached its equilibrium state.

No matter what diode parameters we chose for the above calculations, the diode always settled down to, and its equilibrium state agreed with, the basic dc solution. During these calculations the current through the diode was recorded at each time step. The value of the current vs normalized time is shown on Fig. 16 for the diode parameters of Table 3, and with $m_i/m_e = 16$. When a smaller mass ratio is used, the diode reaches its equilibrium state in a shorter time, but otherwise there is no difference in its behavior.
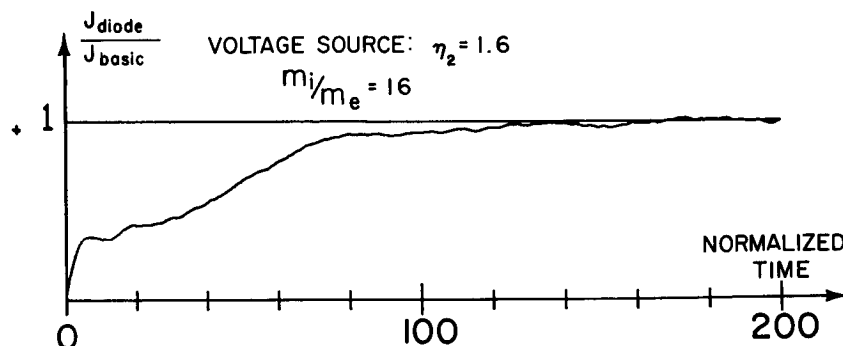
FIG. 16. FORMATION OF THE BASIC SOLUTION IN
THE COMPUTER-SIMULATED DIODE WHEN AN IDEAL
VOLTAGE SOURCE IS CONNECTED ACROSS IT.

There are naturally fluctuations in the value of the current, for the velocities of the sheets are randomly distributed. The fluctuations in the potential of the diode show up most prominently in the values or positions of the potential extrema. It is well known that these points (the potential minimum and maximum) are the most sensitive for any disturbance in the diode. In order to show that these fluctuations are only shot-noise effects, the values of the potential minimum were recorded at each time step for computer calculations with different numbers of sheets. The number of sheets in the equilibrium state of the diode is determined by Γ_e, the injection rate of the electron sheets. For three different values of Γ_e, the variations in the potential minimum as functions of time are shown on Fig. 17. The mass ratio of 1 was used for these computations. The standard deviations (STDE) of the potential minimum were calculated for the three cases after they reached equilibrium. (See Fig. 17.) The results show that the standard deviation of these fluctuations decreases when Γ_e is increased, and it is approximately proportional to $1/\sqrt{\Gamma_e}$. Since Γ_e is proportional to the average number of sheets in the diode, this result agrees with the statistical law that holds for the standard deviation of fluctuations about the mean of uncorrelated events. In our case, the events are the positions of the charged sheets. These are randomly distributed in the diode and uncorrelated because of their random injection. Consequently, the fluctuations of the computer-simulated diode are only shot-noise effects, and the average behavior of the diode agrees with the basic solution that was calculated by a dc theory.

With the circuit equivalent of the computer diode, it is possible to observe the diode's behavior when an external circuit, different from an ideal voltage source, is connected to the diode. Let us assume that an ideal current source, with the current value of 0.3 times the saturation current of the diode, is connected to the terminals of the circuit shown on Fig. 15. The calculations start with an empty diode and with no potential difference across the emitters. During the first time steps, because there are only a few sheets present, the convection current through the diode is only a very small fraction of the saturation

SEL-64-012

THE VARIATION OF THE POTENTIAL MINIMUM
THEORETICAL DC VALUE $\eta_m = -1.61$
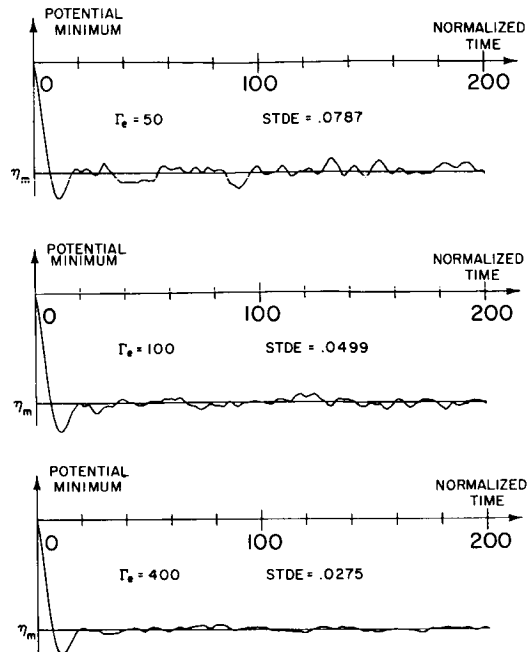
FIG. 17. FLUCTUATION OF THE POTENTIAL
MINIMUM IN TIME FOR THE BASIC SOLUTION.
Increasing Γ_e means increasing sheet
concentration in the diode.

current; therefore, the major part of the total current has to flow

through the cold capacitance of the diode (see Fig. 15). The voltage

across this capacitance changes at each time step by the amount

$J_{disp} \Delta\tau/C_d$, where J_{disp} is the current density in the capacitance,

and C_d is the capacitance per unit area between the two emitters.

The direction of this current is such that the ion emitter becomes

positive with respect to the electron emitter, thus giving a forward

bias to the diode and causing the convective current to increase.

Since the current through the diode is constant, the increase of the

convective current causes the displacement current to decrease until

equilibrium is reached. The voltage vs time characteristic of this

circuit is shown on Fig. 18. The parameters of the diode are the same as the ones used before. The equilibrium state agrees again with the dc calculated basic state.
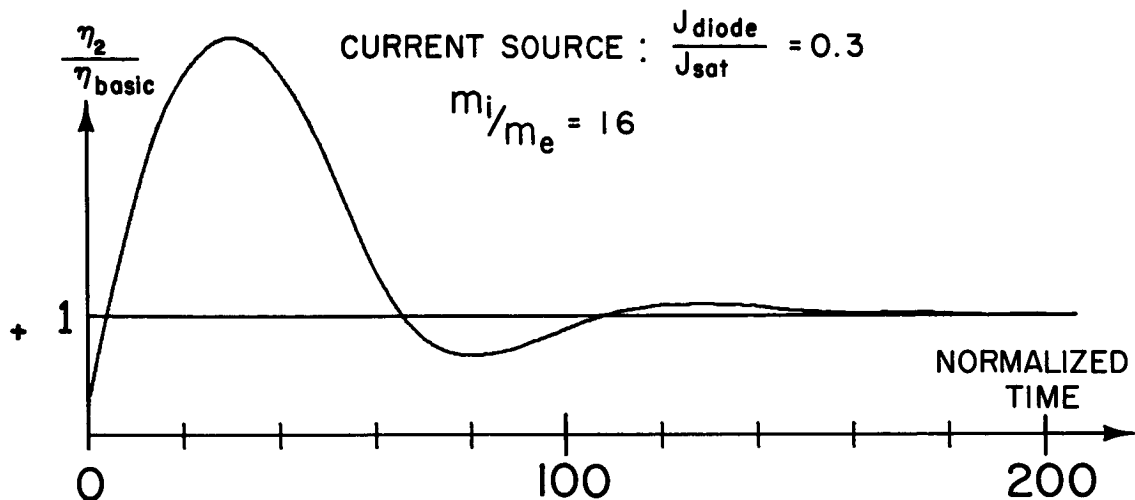
FIG. 18. THE RESULTS OF THE COMPUTER-
SIMULATED DIODE: The formation of the
basic solution with an ideal current
source connected to the diode.

We can conclude that the basic solution is a stable solution under time-varying conditions, when either a voltage source or a current source is connected to the diode. From the quantitative agreement between the time-dependent and the dc states of the diode, it is apparent that the computer model is a very good statistical approximation to the theoretical model of the opposite-stream plasma diode.

C. THE BREAKDOWN OF THE PERIODIC SOLUTION

We know from dc theory that the periodic solution is a self-consistent dc solution of the opposite-stream diode. It is true that

in the already described computer calculations only the basic solution was present; still, we have to examine the stability of the periodic solution in order to tell whether it could exist in the diode for a considerable length of time. Using the dc theory and the computer program of the dc states, we can accurately calculate the electric field of the periodic solution as a function of position in the diode. If this dc field is used to move the sheets in the diode, then these sheets will be forced to follow the trajectories that the dc theory predicts. Consequently, after the equilibrium state of the diode has developed under these circumstances, the self-field of the sheets must agree also with the predicted dc field. By this procedure the self-consistent periodic state is set up in the diode. This procedure was carried out on the computer model utilizing the fact that the sheets could be moved by a prescribed field (see Fig. 12). The prescribed field, i.e., the field of the periodic dc state, was calculated by numerical integrations (see Chapter IV) and its values at the midpoints of the segments fed into the computer program. These values were then used to move the sheets in the diode instead of the calculated self-field of the sheets.

After the self-consistent state has been achieved, the diode may now be allowed to arrange its state by its normal operation, i.e., the sheets may be allowed to move under the influence of their self-field. We are interested in the behavior of the diode after its normal operation has begun; therefore, we count time from the instant when the sheets start to move under the influence of their self-field.

It seemed possible that an external circuit could influence the stability of the periodic solution; therefore, both an ideal voltage source and an ideal current source were used for these calculations. The voltage source was simulated, as before, by the application of a constant potential value ($\eta_2 = 1.6$) across the emitters. The periodic dc solution was set up for this potential difference, and then the sheets were allowed to move under the influence of their self-field. We could observe that the periodic solution changed rapidly into the basic solution under these circumstances.

Since the diode current of the periodic solution is higher than that of the basic solution for the same potential difference, the current vs time diagrams on Fig. 19 show this change clearly. These curves are shown for three different mass ratios. The heavier the mass of the ions, the longer it takes for the current to reach its basic dc value. This long time effect is connected to the normal transient behavior of the diode that is determined by the average transit time of the slower particles. We have already shown that the average normalized transit time of the ions is of the order of $40 \sqrt{m_i/m_e}$. This indicates (see Fig. 19) that the current reaches its basic value within a time interval not larger than three times the average transit time of the ions.
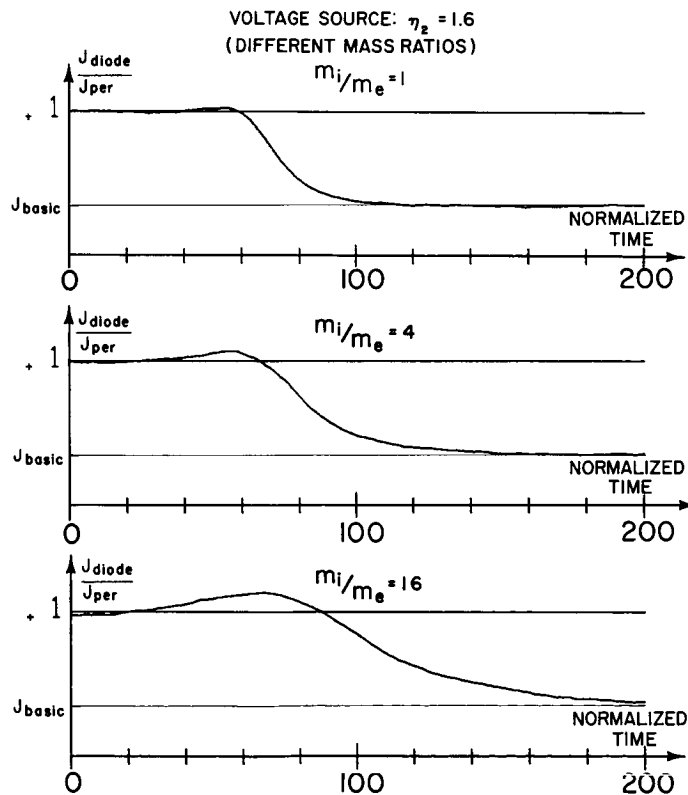
FIG. 19. THE BREAKING UP OF THE INITIALLY
SET UP PERIODIC SOLUTION AS SHOWN BY THE
DECREASE IN THE CURRENT VALUE THROUGH THE
DIODE. Three different mass ratios are used.

- 69 -

The disappearance of the periodic type of solution, i.e., the disappearance of the two periodic extrema, occurs in a much shorter time than the diagrams on Fig. 19 indicate. This fact is demonstrated on Fig. 20, where the potential distribution of the diode is shown at different times during the transformation of the periodic solution.

POTENTIAL PROFILES IN THE DIODE
τ=NORMALIZED TIME
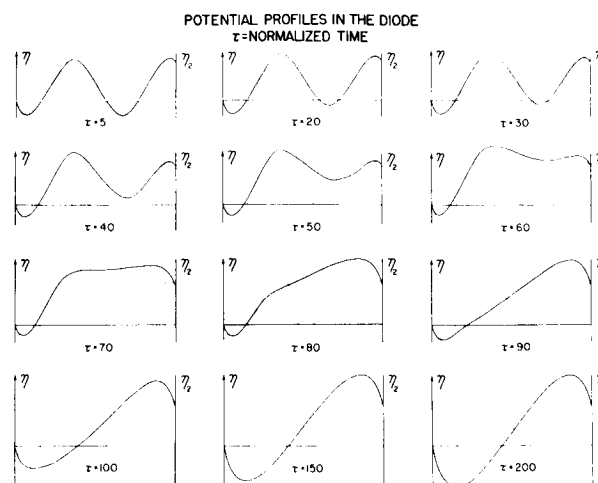
FIG. 20.   THE BREAKING UP OF THE INITIALLY SET UP
PERIODIC SOLUTION AS SHOWN BY THE POTENTIAL PROFILES
IN THE DIODE AT DIFFERENT TIMES.

These curves are shown for the mass ratio $m_i/m_e = 16$. After 70 time steps the periodic extrema have disappeared. This short time interval depends on the electrons and is not influenced by the mass of the ions, for it is the same for the lower values of the mass ratio.

We pointed out in our dc analysis that at these two extrema the spatial derivative of the space-charge function is discontinuous. Consequently, the discontinuities cause instabilities at these points and the distribution of the electrons is rapidly rearranged. During this small time interval, the distribution of the heavy ions has not changed much, and the electron current-limiting minimum is still at its periodic value. The current even increases initially, because the excess amount of electrons that has been depressing the potential at

the periodic minimum then leaves the diode space rapidly at the plane of the ion emitter. After this initial rearrangement of the electron sheets, the nonperiodic profile changes its shape as the minimum and maximum become more prominent. The consequence of this change is the decreasing of current through the diode. This slow time effect occurs similarly in the change of the current when the voltage is changed across a diode that is already in equilibrium. In this case, the basic type of profile remains in the diode at all times; only the potential minimum and maximum are taking up different values. This is the reason why we called the long time effect in the diode its natural transient behavior.

When a current source is used, it is the voltage across the emitters that shows whether the periodic or basic solution is present in the diode. For the same value of current, the applied potential of the basic solution is larger than that of the periodic solution. The potential across the diode as a function of time is shown on Fig. 21. At time $\tau = 0$, the periodic solution has already been set up as in the earlier cases. From this time on, the current is held constant and the potential across the emitters is allowed to change. The change in the potential at each time step is determined by the displacement current in the diode with the assumption that this displacement current is zero initially.
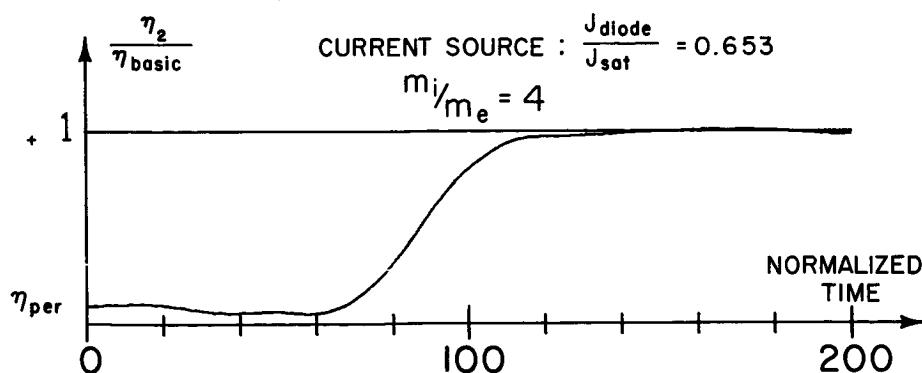
FIG. 21. THE BREAKING UP OF THE PERIODIC
SOLUTION (WHEN AN IDEAL CURRENT SOURCE IS
CONNECTED TO THE DIODE) AS SHOWN BY THE
INCREASE IN THE DEVELOPED POTENTIAL ACROSS
THE DIODE.

The diagram on Fig. 21 shows that the periodic solution changes again into the basic solution. The disappearance of the periodic extrema is not influenced by the external circuit, for it again takes approximately 70 time steps. This result is consistent with our earlier explanation of the transformation of the periodic solution, since this transformation is not connected to the normal transient effects of the diode but to internal instabilities which cannot be influenced by an external circuit.

VII. THE EXPERIMENTAL OPPOSITE-STREAM PLASMA DIODE

Experimental data supply the most conclusive proof of a theoretical analysis that predicts the behavior of a physical device. The "experimental" results of the computer-simulated diode have already given us proof that the theoretically calculated, basic dc solutions are stable under time-varying conditions, hence their existence in a physical device can be expected. The agreement between theory and experiment depends on how well an ideal theoretical situation can be materialized in the laboratory. The theoretical model of the opposite-stream diode was well suited for our experiment inasmuch as a thermionic ion emitter was available to the Electron Device Laboratory (a thermionic electron emitter is the most commonly used component of laboratory experiments).

A. CONSTRUCTION OF THE DIODE

The two major assumptions of our theory are one-dimensional flow and collisionless conditions. A parallel-plane construction of the diode is a good approximation to a one-dimensional model only if the separation of the emitters is smaller than their area, so that the effect of the fringe fields can be neglected. The collisionless conditions are realized by a low background pressure of neutral atoms and by keeping the separation distance of the diode much smaller than the mean free path of the particles. Consequently, our aim is to keep the distance between the emitters as short as possible.

The design of the diode is determined by the available form of the ion emitter. The construction and the properties of the lithium-ion emitter, called the "spodumene button," are described in great detail in reports of the Stanford Electronics Laboratories. (See pp. I-33 and I-41 in Ref. 21; and Ref. 23). The basic material of the ion emitter, spodumene, is a glasslike material that emits lithium ions when heated above 900 °C. The maximum safe operating temperature of this emitter is 1200 °C. The emitter is cylindrically shaped, with the emitting surface ground flat. Heating is provided by a zigzag platinum wire that is imbedded in the spodumene. The heater wire is running back and forth in a plane that is parallel to the emitting surface and placed at

the middle of the cylindrical button (see Fig. 22). The diameter of a button is typically 0.3 in.; its length is approximately the same.

In the spodumene buttons used in our experiments a second zigzag wire was also imbedded in the material near the emitting surface. The exposed ends of this second wire were welded to a cylindrical heat shield which surrounded the button. The inside diameter of the heat shield was 0.375 in. Electrical contact to the emitter was made by the imbedded second wire through the heat shield.

Since the diode has a parallel-plane construction, the surface areas of the electron and ion emitters have to be equal. In order to insure a uniform field distribution in the diode, the emitters were similarly constructed (a cylindrical emitter surrounded by a heat shield). The separation between the emitters was 0.1 in. This gave a ratio of 3:1 between the diameter and the length of the diode, which is a reasonably good approximation to the one-dimensional model.

At this small distance from the spodumene button, a pure metallic electron emitter could not be used because the radiation heat from it would have melted the face of the button. Hence, it was necessary to use an oxide-coated cathode. This cathode, a cylindrical cup, was pressed out of a 0.005-in.-thick, pure nickel sheet. It was 0.5 in. long and had a diameter of 0.27 in. The bottom of this cup was sandblasted and sprayed evenly with barium-oxide cathode coating. The cup was heated from inside by a heavy tungsten heater that was insulated from the emitter by high-purity alumina parts (see photograph of the heater assembly in Fig. 23). The emitter was supported at the back by a stainless steel band to which the heat shield was also welded. Electrical contact to the emitter and to the heat shield was made through this steel band.

The use of an oxide-coated cathode for the electron emitter created two difficulties. First, the cathode had to be activated, and during the activating procedure the ion emitter had to be shielded from it. Secondly, the applied voltage across the diode had to be limited, since oxide cathodes are poisoned easily by ion bombardment. It was found by earlier experiments that noticeable poisoning sets in when 20 v is
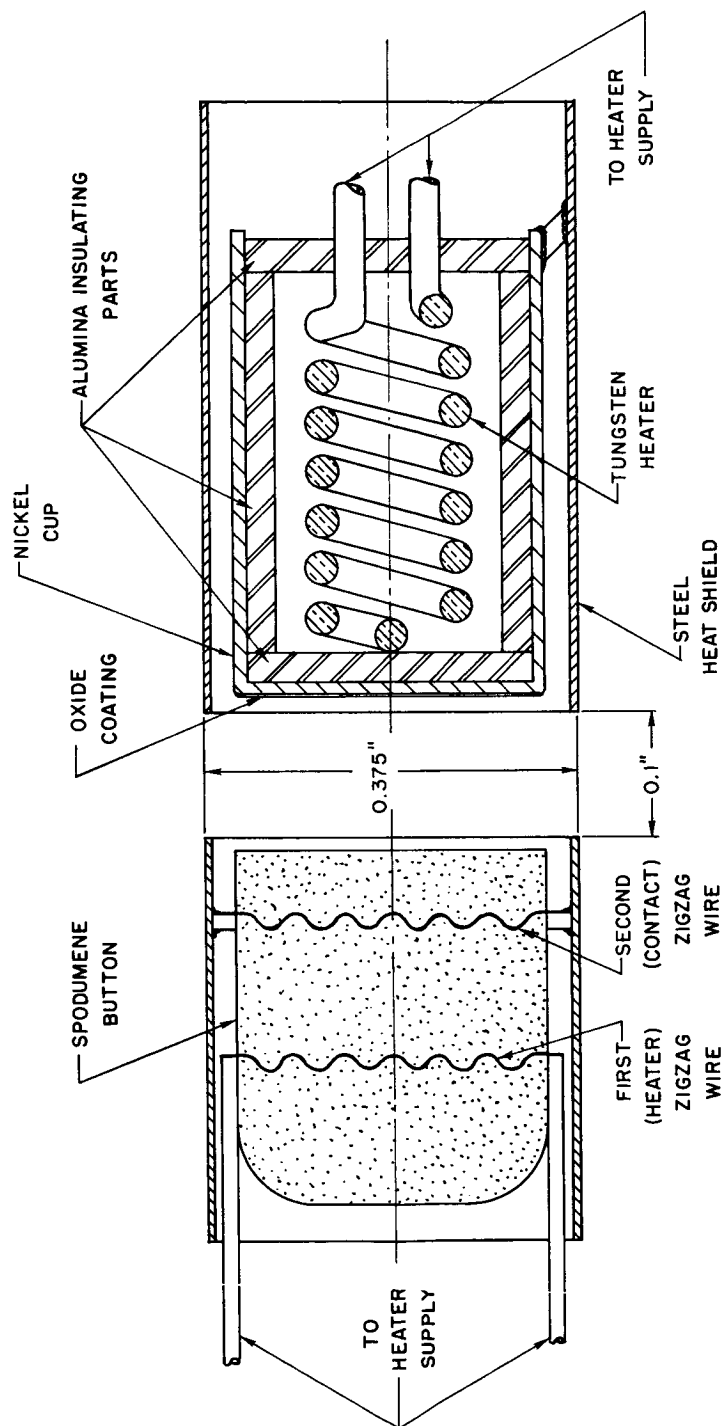
FIG. 22. CONSTRUCTION OF THE EXPERIMENTAL OPPOSITE-STREAM DIODE.
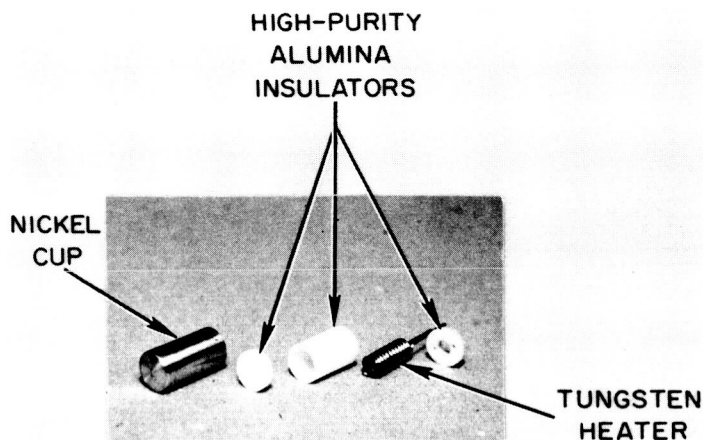
FIG. 23. HEATER ASSEMBLY FOR THE INDIRECTLY HEATED, OXIDE-COATED CATHODE.

applied across the emitters. Consequently, during those experiments which are reported here, the applied potential had to be kept below this value.

The ion emitter has to be shielded during the activation of the cathode because gases released from the surface of the electron emitter would deposit on the button and influence its electrical characteristics. Also, it is a good practice to draw a large electron current from the cathode during and immediately after activation, for this stabilizes the emission properties of the cathode. Both these functions can be executed by a metal disk that is placed in the diode space during activation. It is a slight technical problem to construct the shield in such a way that it can be removed from the diode space after activation, since the diode is placed in an evacuated bell jar during its operation. We used a 0.001-in.-thick circular disk with 1 in. diameter that could be rotated into the middle of the diode space by a thin rod (see photograph of the diode in Fig. 24). The crossbar at the end of the rod was made of magnetic material; and the disk could be rotated in and out of the diode space by a powerful magnet placed outside the bell jar. The magnet was removed, naturally, when the measurements were taken.
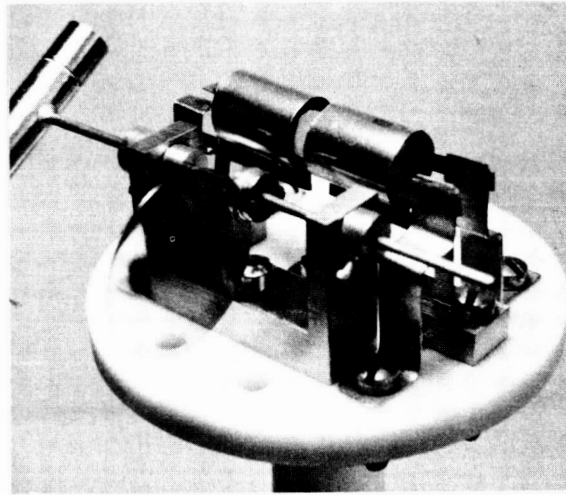
FIG. 24.   PHOTOGRAPH OF THE EXPERIMENTAL
OPPOSITE-STREAM PLASMA DIODE WITH THE
SEPARATING DISK REMOVED FROM THE DIODE
SPACE.   The electron emitter is at the
left, opposing the ion emitter.   Both
are surrounded with heat shields.

B.   THE EXPERIMENT AND ITS RESULTS

The diode (Fig. 24) was placed in the bell jar of a vacuum pump station.   Continuous pumping with a diffusion pump provided an indicated pressure of 10^{-7} mm Hg.   Though the pressure in the diode space was probably higher than at the point where the pressure gauge was placed, the difference was less than two orders of magnitude.   The mean free path of the particles at 10^{-5} mm Hg is still of the order of 10 cm, hence the separation distance of 0.25 cm insured collisionless operation.

The experiment began with the activation of the cathode.   The temperature of the nickel cup was raised slowly up to 1050 °C, while the separating disk was kept in the diode space.   The cup was at ground potential, and during activation 20 v was applied to the disk.   The temperature of the electron emitter was raised so slowly that the pressure in the bell jar could not rise above 5 x 10^{-6} mm Hg.   After holding the temperature of the emitter for 10 min at 1050 °C, it was

lowered to 900 °C. The temperature of the electron emitter was held at this value for the later part of the experiment. Before data were taken, the potential of the disk was set to a value that yielded 20 ma electron current. The activation of the cathode was completed by continuously drawing this current from the emitter for several hours.

When the voltage-current characteristics of the opposite-stream diode were measured, it was necessary to use pulsed measurements in order to eliminate a potential difference between the second zigzag wire and the face of the ion emitter button. Under dc conditions, this potential difference was drifting slowly in time which made it impossible to obtain consistent data. The probable cause of the drifting of this potential difference is the depletion of lithium in the spodumene button. This subject is currently under investigation at Stanford.

Pulses with 10-μsec duration eliminated this difficulty. The transient effects in the diode could be neglected for these measurements, for the average transit time of the ions was only a small fraction of a microsecond. The voltage range of these pulses extended from 0 to 15 v. The current pulses were measured across a 1-ohm resistor by an oscilloscope.

1. Determination of the Effective Area of the Diode

Our purpose is to show that the basic solution is present in the experimental opposite-stream diode by comparing the current in the diode with its theoretically calculated values. The dc parameters of the diode are determined as follows. The separation distance, the temperature of the emitters, and the applied potential across the diode are measured; the saturation currents of the emitters are estimated. Since the electron and ion currents in the diode are much smaller than the saturation currents of their respective emitters, even a large error in the saturation current of either emitter would not influence the calculated dc current. The dc parameters above determine the theoretical current density in the diode for the basic solution. In order to convert current density to current, we need to know the cross-sectional area of the diode.

The oxide-coated surface of the nickel cup has an area of 0.37 cm^2. The effective area of the emitter is larger than this value, because electrons fill up the space between the cup and the heat shield. Since the cup is welded to the heat shield, and the difference in the work functions of the oxide coating and the heat shield biases the heat shield positive, electrons will flow to the heat shield from the emitter. When potential is applied across the diode, electrons leave their emitter not only from the oxide surface but also from the space between the emitter and the heat shield. The low current that flows in the diode is associated with a large space-charge cloud of electrons near the electron emitter, hence the space charge and this cloud around the nickel cup increase the effective area of the emitter. It follows from this argument that the effective area of the emitter is smaller than the area that is enclosed by the heat shield $\left(0.678 \ cm^2\right)$.

The effective area of the electron emitter could be determined from the calculated dc current density and the measured current that flows between the separating disk and the electron emitter. When the potential of the disk was 10.2 v, the electron current through this short electron diode was 2.43 ma. The contact potential was approximately 1 v (see next section for details about contact potentials), hence the true applied potential between the emitter and the disk was 10.2 - 1 = 9.2 v. The other dc parameters were:

Temperature of the electron emitter: T_e = 1170 $^\circ$K

Separation distance: d = 0.142 cm

Saturation current density (assumed): J_{se} = 0.1 amp/cm^2

The theoretical dc current density of an electron diode with these parameters is 4.76 ma/cm^2. (This figure was calculated by the computer program of the dc states.) Hence the effective area of the electron emitter was:

$$A_{eff} = \frac{2.43 \ ma}{4.76 \ ma/cm^2} = 0.51 \ cm^2$$

This figure was used not only for the area of the electron emitter, but also for the effective area of the experimental diode, since the two emitters were similarly constructed and we could assume that our diode approximated a one-dimensional model.

2. Determination of the Contact Potential

The contact potential in an experimental diode is the difference between the potential that is applied across the terminals of the device and the potential that actually acts on the charged particles in the diode space. This difference is caused by the dissimilar work functions and mass constants of different emitting materials, by thermo-electric effects and by contact potentials between metals and semi-conductor types of materials. Our theoretical data are calculated for the actual potential difference between the emitters, or between the electron emitter and the metal disk; therefore, for each measurement the applied potential had to be corrected by the value of the contact potential. We can express the exact relationship between the applied and true potential in the diode by the following expression:

$$V_2 = V_{appl} - V_{cont} \tag{78}$$

where V_2 is the true potential across the diode, V_{appl} is the potential applied across the terminals of the diode, and V_{cont} is the contact potential by definition.

The relationship $J_{diode} = f(V_2)$ was calculated by numerical integrating methods (see Chapter IV) for the basic solution. We assume that the experimental curve follows the same law, i.e.,

$$J_{exp} (V_{appl}) = f(V_{appl} - V_{cont}) \tag{79}$$

where V_{cont} is a constant. The value of V_{cont} is determined by fitting the experimental curve to the theoretical curve at the point $V_2 = 0$. The theoretical curve gives a current value for $V_2 = 0$, which is $J_{diode}(0)$. When the contact potential is applied across the terminals of the diode, the current across it is $J_{diode}(0)$, or

$$V_{cont} = V_{appl}$$

$$J_{exp}(0) \stackrel{\triangle}{=} J_{diode}(0)$$

3. The Corrected Experimental Data

a. Measurements of the Electron Current Only

We have shown already that the experimental curve for the electron diode was fitted to the theoretical curve at 9.2 v true potential across the diode. The two curves are fitted also at zero applied potential when the contact potential for the electron diode is determined. The theoretical short-circuited electron current between the oxide cathode and the separating disk was 110 μa. In order to obtain this current value, the separating disk had to be at 0.98 v with respect to the electron emitter. According to Eq. (80), the contact potential for the electron diode was 0.98 v.

Other points between 0 and 9 v were determined both by the experiment and by numerical computations. One of the solid lines on Fig. 25 is the theoretically predicted voltage-current characteristic of the electron current only. The experimentally measured points follow closely the theoretical curve, showing that our assumptions that the diode is collisionless and one-dimensional are well approximated in this voltage range.

b. Measurements on the Opposite-Stream Diode

In order to measure the voltage-current characteristics of the opposite-stream diode, the separating disk was removed from the diode space and the spodumene button was heated to 900 °C. Pulses of 10 μsec were used with 60-cycle repetition rate for the measurements. The shapes of the current and voltage pulses were identical and there was no delay time between them. This fact showed that the transients in the diode died out within a fraction of a microsecond.

The effective area of the opposite-stream diode was assumed to be the same as that of the electron emitter because of the similar constructions of the two emitters. On the basis of earlier measurements of the saturation current of the spodumene buttons (see Ref. 23), we

SEL-64-012
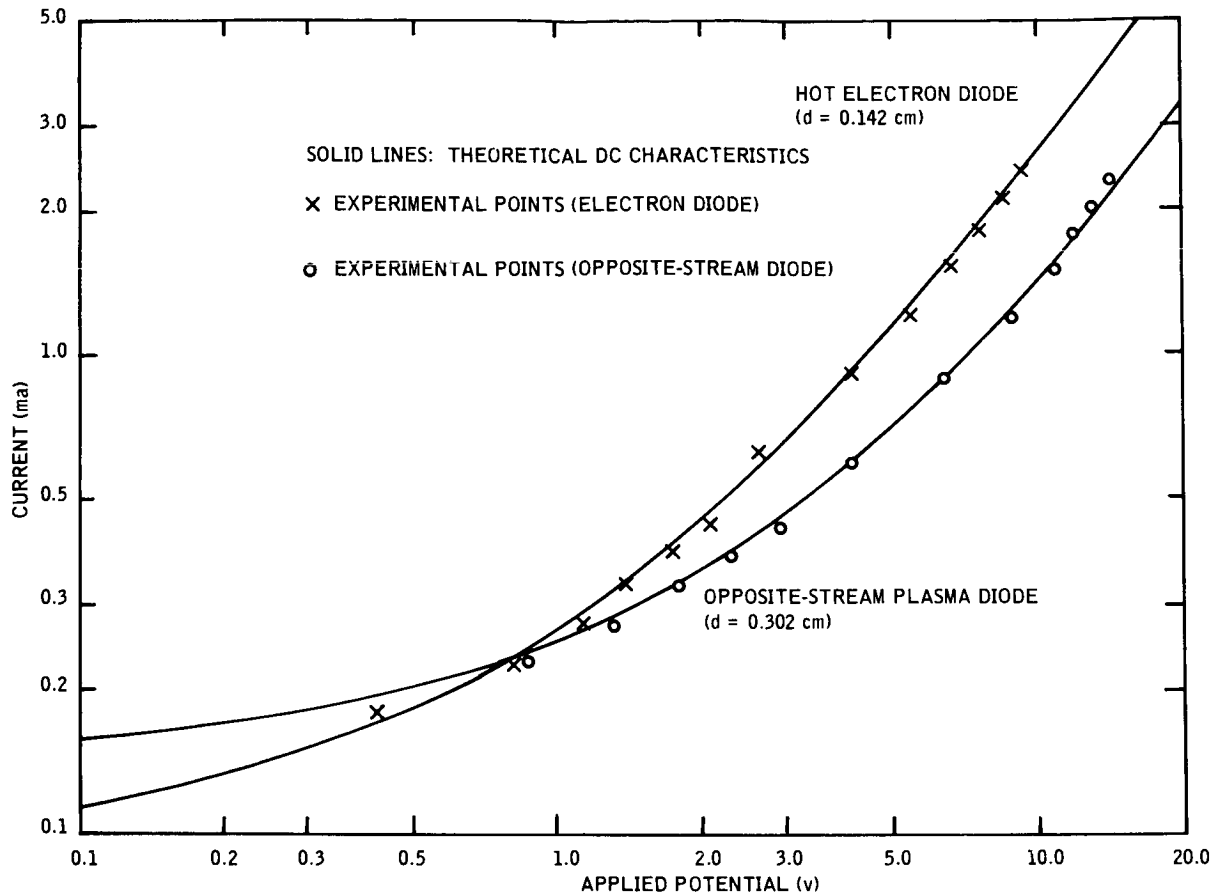
FIG. 25. THE EXPERIMENTAL DATA. (Solid lines are theoretical curves.)

assumed an ion saturation current density of 10 ma/cm^2. Hence the dc parameters of the diode were the following:

Temperature of electron emitter:	T_e	= 1170 °K
Temperature of the ion emitter:	T_i	= 1170 °K
Saturation current density of the electron emitter (assumed):	J_{se}	= 0.1 amp/cm^2
Saturation current density of the ion emitter (assumed):	J_{si}	= 10 ma/cm^2
Separation distance:	d	= 0.302 cm
Cross-sectional area of the diode:	A_{eff}	= 0.51 cm^2
Mass ratio:	m_e/m_i	= 7.93 x 10^{-5}

The voltage-current characteristics of the opposite-stream diode, with the above dc parameters, were computed by our dc theory. The resulting curve is shown as a solid line on Fig. 25.

The contact potential of this opposite-stream diode was determined again following the procedure outlined in Sec. B2 above. The theoretical short-circuited dc current for this diode was 159 μamp. In order to obtain this value 4.3 v had to be applied across the terminals of the diode, hence 4.3 v was the contact potential in this case.

The true potential across the diode was corrected (see Eq. (78)) again for each measurement, and the experimental points plotted on Fig. 25. Measurements were taken up to 18 v applied potential, i.e., 13.7 v corrected potential. The experimental data follow the theoretical curve remarkably well. Since the experimental curve is fitted to the theoretical curve only at the point of zero potential (this point is at $-\infty$ on the diagram), the results of these experiments prove unquestionably that the basic dc solution is present in the diode. No sign of instability, or increased current value was found. The close agreement between experiment and theory shows also that our experimental device was successfully approximated by our theoretical model.

VIII. CONCLUSIONS

We started the analysis of the opposite-stream plasma diode with an attempt to find all dc solutions that were consistent with our model. In order to prove the existence or nonexistence of different dc states in our diode, we had to find a rigorous mathematical treatment for this problem. We have found such a treatment by introducing symbolic functions into the solutions of our differential equation. In the process of solving our problem we found the three forms of the velocity distribution functions that could be applied to the general four-stream plasma diode. In future analyses these forms might help to find all possible dc states of the general case, though this work will require considerably more effort than we needed in applying our methods to the opposite-stream diode.

We have found all the possible dc states of the opposite-stream diode and have shown that a fundamental dc solution (the basic solution) always exists in our model. A numerical program was constructed that could accurately calculate the dc states of an arbitrary opposite-stream diode.

It was found that periodic types of potential functions could also exist as dc solutions to our opposite-stream diode. We presented diagrams from which the existence or nonexistence of these periodic solutions could be determined.

We found a clue to the question of stability of the dc states when we observed that the spatial derivative of the space-charge function became discontinuous for the periodic types of dc solutions. Up to the present time, authors have neglected to point out the importance of the derivative of the space charge in several papers that dealt with the dc states of various plasma diodes (see Refs. 6-10). The continuity or discontinuity in the derivative of the space-charge function is determined by dc analysis; therefore it should be required that this derivative be continuous whenever stable dc solutions are sought.

The stability of the dc states was checked by simulating the model of the opposite-stream diode on a computer. We have developed a computer program that is able to handle 10,000 sheets simultaneously. Because of the large number of sheets in the computer-simulated diode, this program

represented a good statistical model of a physical device and its equilibrium state agreed with the theoretically calculated basic dc state of the diode.

The computer model also showed that discontinuities in the derivative of the space-charge function made the periodic types of dc solutions highly unstable. This result confirmed the conjecture that this derivative plays an important role in the stability of dc states; it has to be continuous when the state is stable.

We have also constructed an experimental opposite-stream plasma diode, using a solid-state, thermionic, lithium-ion emitter (spodumene) and a barium oxide-coated electron emitter. Since the contact potential between the emitters was not known, the experimental data had to be matched to the theoretical curve at one point. We selected the value of zero applied potential for this point and obtained excellent agreement between experimental and theoretical data for other values of the applied potential. These measurements demonstrated that the basic dc solution was set up in the experimental diode and that our theoretical dc analysis, including the necessary stability considerations, had correctly predicted the behavior of the physical device.

There are great possibilities in applying the computer model to other types of one-dimensional plasmas, because it can be made suitable for a large variety of boundary conditions without essential changes or complications in the computer program. The data obtained by these computer "experiments" describe every physical aspect of the model. We extracted only those data which were relevant to our theory, but future applications of the computer program could include impedance measurements, wave propagation and other desired physical properties of one-dimensional plasmas.

APPENDIX A. DESCRIPTION OF THE COMPUTER PROGRAM
FOR THE DC STATES

In Sec. D of Chapter III, we outlined the procedure for calculating the dc characteristics of an opposite-stream diode from its known parameters. Since this procedure consists of numerical methods and logical operations, it is well suited for digital computers. We have used Burrough's algorithmic language to write a computer program which performs all the required functions of this procedure.

In the problem considered, the following seven parameters of the diode are given: J_{si}, J_{se}, T_i, T_e, V_2, d, and m_i/m_e. From these parameters we have to calculate V_{min}, V_{max}, which then determine the potential function in the diode completely. If V_{min} and V_{max} are known, any quantity related to this diode can be calculated.

It was shown in Chapter III that the solution of this problem breaks down into two steps:

1. Determining the applicable potential type for the problem, and

2. Setting the parameters of this potential form such that the total separation distance calculated from three integrals agrees with the given separation distance d.

1. The Normalization Procedure

It is convenient to use the normalization procedure of Chapter III to reduce the number of input parameters. If we assume that the current densities are given in amperes per centimeter squared, the temperatures in degrees Kelvin, the potential in volts, and the distance in centimeters, the constants of the problem can be calculated by the following expressions:

$$\left.\begin{array}{l} \alpha_e = \cfrac{1.0}{1.0 + \cfrac{J_{si}}{J_{se}} \sqrt{\cfrac{T_i m_i}{T_e m_e}}} \\[40pt] \alpha_i = 1.0 - \alpha_e \\[30pt] \beta_e = \cfrac{T_i}{T_i \alpha_e + T_e \alpha_i} \\[30pt] \beta_i = \beta_e \cfrac{T_e}{T_i} \\[30pt] \eta_2 = \cfrac{11600 V_2}{\beta_e T_e} \\[30pt] \xi_2 = \cfrac{d \sqrt{J_{se}}}{1.0878 \times 10^{-6} \, \beta_e \sqrt{T_e \alpha_e}} \end{array}\right\} \qquad (A.1)$$

2. Subroutines of the Program

In order to find the normalized transition lengths $\xi_{A_{max}}$ and $\xi_{D_{min}}$, we need to use two subroutines. These are the functions $G^-(x)$, $G^+(x)$ and the integral procedure.

a. The Functions $G^-(x)$, $G^+(x)$

The function $G^-(x)$ was defined by Eq. (22):

$$G^-(x) = \exp(x) \cdot (1.0 - \operatorname{erf} \sqrt{x}) + \frac{2\sqrt{x}}{\sqrt{\pi}} \qquad (A.2)$$

It is not possible to use the above expression for the numerical evaluation of $G^-(x)$ because cancellation occurs for x values larger than 2.0. We have used a power series to approximate $G^-(x)$ for $0 \leq x \leq 2.0$, and an asymptotic series for $x > 2.0$. We have matched the two series at $x = 2.0$ so that $G^-(x)$ is continuous at this point. The error of this approximation is smaller than 0.1 percent. The numerical values of the two series are listed in the text of the BALGOL program (see Appendix B).

The function $G^+(x)$ can be expressed by the functions $G^-(x)$ and exp (x) as follows:

$$G^+(x) = 2.0 \exp (x) - G^-(x) \qquad (A.3)$$

b. The Integral Procedure

We showed in Chapter III that the separation length of the diode can be calculated by three definite integrals [see Eq. (36)]. The integrands involve the $G^-(\eta)$ and $G^+(\eta)$ functions and the **three param-eters**, η_m, η_M and γ, which have to be determined before the **integration** can be carried out. For the potential types B, C, and D, **the value of** γ is fixed such that the integrands approach infinity when the **variable** approaches the limits of the integration.

Since the subroutine for calculating separation lengths is used many times in the program, the method of calculating definite integrals of the types shown must be efficient and accurate. Gauss's three-point quadrature formula is used for the integration procedure [Ref. 24].

In general, we have to evaluate an integral expression of the form:

$$\int_A^B f(x)\ dx \quad \text{when} \quad \begin{cases} f(x) \to \dfrac{\text{const}}{\sqrt{x - A}} & \text{as } x \to A \\[4mm] f(x) \to \dfrac{\text{const}}{\sqrt{B - x}} & \text{as } x \to B \end{cases} \qquad (A.4)$$

Gauss's three-point formula is

$$\int_A^B f(x) \, dx \cong (B - A) \left| c_1 \, f[Ax_1 + B(1.0 - x_1)] \right.$$

$$+ c_0 \, f[Ax_0 + B(1.0 - x_0)]$$

$$\left. + c_1 \, f(A(1.0 - x_1) + Bx_1] \right| \qquad (A.5)$$

When $f(x)$ is a smooth function,

$$c_1 = 0.27777778$$

$$c_0 = 0.44444444$$

$$x_1 = 0.88729833$$

$$x_0 = 0.5$$

Despite the fact that the points $x = A$, $x = B$ are avoided, the result is still accurate for smooth functions. In our case, we have to transform the variable of the integral to eliminate the singularities of $f(x)$ at the end points. As we shall show, this transformation will only change the values of c_1, c_0, x_1 and x_0.
We can use the transformation,

$$x = \frac{B + A}{2} + \frac{B - A}{2} \sin y \qquad (A.6)$$

Substituting Eq. (A.6) into the integral expression, we get

$$\int_A^B f(x) \, dx \cong \frac{B - A}{2} \int_{-\pi/2}^{\pi/2} \left[f\left(\frac{B + A}{2} + \frac{B - A}{2} \sin y\right) \cos y \right] dy \qquad (A.7)$$

We define $\phi(y)$ as

$$\phi(y) = f\left(\frac{B + A}{2} + \frac{B - A}{2} \sin y\right) \cos y \tag{A.8}$$

The function $\phi(y)$ is not singular at either end point; therfore we can use Gauss's formula for this function. This gives

$$\int_A^B f(x)\, dx = \frac{B - A}{2} \int_{-\pi/2}^{\pi/2} \phi(y)\, dy \cong \frac{B - A}{2} \pi \left\{ c_1 \phi\left[\frac{\pi}{2} x_1 - \frac{\pi}{2}(1.0 - x_1)\right] \right.$$

$$\left. + c_0 \phi\left[\frac{\pi}{2} x_0 - \frac{\pi}{2}(1.0 - x_0)\right] + c_1 \phi\left[\frac{\pi}{2}(1.0 - x_1) - \frac{\pi}{2} x_1\right] \right\} \tag{A.9}$$

Equation (A.9) can be simplified:

$$\int_A^B f(x)\, dx \cong \frac{B - A}{2} \pi \left\{ c_1 \phi\left[\pi x_1 - \frac{\pi}{2}\right] + c_0 \phi\left[\pi x_0 - \frac{\pi}{2}\right] + c_1 \phi\left[\frac{\pi}{2} - \pi x_1\right] \right\} \tag{A.10}$$

After substituting the values of c_1, c_0, x_1, x_0 into Eq. (A.10), we can find the required expression for the function $f(x)$ by using Eq. (A.8). The new formula will be

$$\int_A^B f(x)\, dx \cong (B - A)\ c_1' f[A x_1' + B(1.0 - x_1')]$$

$$+ c_0\ f[A x_0' + B(1.0 - x_0')] + c_1' f[A(1 - x_1') + B x_1'] \tag{A.11}$$

where

$$c_1' = 0.15128136$$

$$c_0' = 0.69743728$$

$$x_1' = 0.03101407$$

$$x_0' = 0.5$$

The integral expression in Eq. (36) is divided into three regions. Each of the three regions is divided into "N" equal intervals, and in every small interval we applied the derived three-point formula. The number of these small intervals depends upon the accuracy desired.[*] The sum of these partial integrals gives the total integral; or, if we wish, these partial integrals can be used to read out a tabulated form of the potential as a function of distance.

3. Determination of the Type of Potential Solution

We follow the procedure described in Sec. IIID to calculate the normalized transition lengths of a given diode. First we evaluate Eq. (38) which determines whether the diode is electron-rich, ion-rich, or neutral. Hence, depending on the value of the expression in Eq. (38), the transition lengths are ξ_{AB} and ξ_{BD} for the electron-rich case, ξ_{AC} and ξ_{CD} for the ion-rich case, and ξ_{AD} for the neutral case. To calculate any one of these transition lengths, we have to determine η_m, η_M and γ for the case in question and then evaluate the three integrals in Eq. (36). For the cases ξ_{AB}, ξ_{AC}, and ξ_{AD}, the calculation of η_m, η_M, and γ consists of evaluating the expressions given in Table 1 of Chapter III. Since only one of these three transition cases can be present in the given diode, we set the other two transition lengths equal to zero. Then, in general, $\xi_{A_{max}} = \xi_{AB} + \xi_{AC} + \xi_{AD}$.

---

[*]We used $N = 15$ and obtained results with four-digit accuracy.

For the determination of the transition lengths ξ_{BD} or ξ_{CD}, the three parameters η_m, η_M, and γ have to be calculated again. Table 1 indicates that we have to use an iteration procedure to find η_T from an equation of the form $\eta_T = f(\eta_T)$, i.e., Eqs. (41) and (42). We know that $\eta_T \geq \eta_2$, hence we can form the following sequence:

$$\eta_{T1} = f(\eta_2)$$

$$\eta_{T2} = f(\eta_{T1})$$

$$\cdot$$
$$\cdot$$ \hfill (A.12)
$$\cdot$$

$$\eta_{T(N+1)} = f[\eta_{T(N)}]$$

where the function $f(\eta_T)$ is given by Eq. (41) for the B-D transition case, and by Eq. (43) for the C-D transition case. The factor $\eta_{T(N+1)}$ is a solution if the error, i.e., the absolute value of the difference $\eta_{T(N+1)} - \eta_{T(N)}$, is less than a prescribed small positive number. In general, we set the error less than some percentage of the difference $\eta_{T(N+1)} - \eta_2$. In all the examples that we have calculated, this iteration procedure converged in five steps.

When η_T is known, the parameters η_m, η_M, and γ can be calculated, using the corresponding expressions given in Table 1. We evaluate Eq. (36) again and thus determine ξ_{BD} for the electron-rich diode and ξ_{CD} for the ion-rich diode. Setting that transition length equal to zero, which does not apply to the given diode, we calculate $\xi_{D_{min}}$ by the sum $\xi_{D_{min}} = \xi_{BD} + \xi_{CD} + \xi_{AD}$. After the values of $\xi_{A_{max}}$ and $\xi_{D_{min}}$ are known, the determination of the type of the potential function is possible. If $\xi_2 > \xi_{D_{min}}$, type D has to be used for the solution. If $\xi_2 < \xi_{A_{max}}$, the type A solution is applicable. Finally, if $\xi_{A_{max}} < \xi_2 < \xi_{D_{min}}$, type B or type C is the right potential form depending on whether the diode is electron-rich or ion-rich.

4. Determination of the Inside Parameters of the Solution

It was shown in Sec. IIID that once the type of potential function is known, there is a one-to-one correspondence between η_T or γ and the value of Eq. (36), which is the calculated separation distance of the diode. We have to use the method of successive approximations to find the right value of the independent parameter for a given separation distance ξ_2. For each potential type the problem is equivalent to finding the root $x = x_0$ for a given y_0 in the equation $y_0 = f(x_0)$, where $f(x)$ is a function which cannot be inverted. Even though the four types of potential solutions have different functional forms, we can choose the variables x, y in such a manner that the function $f(x)$ is monotonic, nonnegative, and starts at the origin. We have to consider three different cases in order to choose the variables x, y for the four types of the potential function.

a. Type A Solution

For a type A potential function, only γ can change, and $\eta_m = 0$, $\eta_M = \eta_2$. Table 2 shows that there is a lower limit on γ. If we call this limiting value γ_{min}, the variable x is defined by the expression

$$x \overset{\triangle}{=} \frac{1}{\gamma - \gamma_{min}} \tag{A.13}$$

When x approaches zero the separation length approaches zero also, since γ must approach infinity. Consequently, we can set the variable y equal to the calculated transition length.

b. Type B and Type C Solutions

The variable parameter is η_T for the type A and B solutions. The calculated separation distance is always larger than that of the transition case, $\xi_{A_{max}}$, which was calculated in the first part of the program. In addition, $\eta_T \geq \eta_2$; and η_T becomes equal to η_2 only at the transition point. If we denote the integral expression that calculates the separation length for type B or C solutions as $I_{B,C}(\eta_T)$,

our variable x becomes $x \triangleq \eta_T - \eta_2$ and y is given by

$$y = f_{B,C}(x) = I_{B,C}(\eta_T) - \xi_{A_{max}} .$$

c. Type D Solution

The procedure used in the type D solutions is similar to that used in each of the other three cases. For the type D solution, $\xi_2 \geq \xi_{D_{min}}$. The factor η_T is always larger than the η_T value that corresponds to the B-D or C-D transition case. We had to calculate this η_T in the first part of the program. If we call this value of η_T, $\eta_{T_{min}}$, then x is defined as $x \triangleq \eta_T - \eta_{T_{min}}$. The function $y = f_D(x)$ is defined by the expression $y \triangleq I_D(x) - \xi_{D_{min}}$, where $I_D(\eta_T)$ is the integral expression for the type D solution. Again we have to find the root x_0 for the equality $y_0 = f_D(x_0)$ where y_0 is given and $f_D(x)$ is a monotonically increasing function of x starting at the origin.

d. Finding x_0 for the Equation $y_0 = f(x_0)$

The monotonic function $y = f(x)$ and its value y_0 are given. To find the root x_0, we start with a trial value of x, called x_{try} and calculate the corresponding value of y, called y_{try}. If y_{try} does not differ from y_0 more than a prescribed percentage of y_0, we have obtained the solution. From the value of x_{try} we can calculate η_T and all the other inside parameters of the diode. However, we cannot expect to find the right x_{try} at the first trial, therefore we want to find a new trial point which is closer to the desired solution than the point obtained before. We have written a subroutine called "CORRECT" which supplies the new trial point in a systematic manner. After entering into CORRECT, we calculate the new y_{try} for the given x_{try} and test this y_{try} to see if it is sufficiently close to y_0. If the agreement is not close enough, we enter in CORRECT again, and follow this sequence until an acceptable solution is obtained.

Subroutine CORRECT consists of two methods which are commonly used for finding roots of equations. One method is linear interpolation or extrapolation, the other method is interval-halving. The linear-interpolating method can be described as follows.

Two points are obtained on the curve $y = f(x)$, and two cases are possible:

1. One point is at the origin and the other is below the root that has coordinates (x_1, y_1),

2. One point is above the root with coordinates (x_2, y_2) and the other is below the root with coordinates (x_1, y_1).

The conditions on the coordinates of these points are $y_1 < y_0 < y_2$, which implies that $x_1 < x_0 < x_2$. We can obtain these points in the subroutine from the current trial point which has coordinates x_{try}, y_{try}. If the trial point is below the root, i.e., $y_{try} < y_0$, we set $x_1 = x_{try}$, $y_1 = y_{try}$, and proceed with the determination of the new trial point. If the trial point is above the root, $y_{try} > y_0$, we set $x_2 = x_{try}$, $y_2 = y_{try}$, and calculate the new trial point from the values of x_1, y_1, x_2, and y_2. If during the iterating process we find no trial points above the root, we have values only for (x_1, y_1). In this case we extrapolate from the origin, and obtain the following expression for the new trial point:

$$x_{try} = y_0 \frac{x_1}{y_1} \tag{A.14}$$

If points are found above the root as well, we calculate the new trial point by the current values of (x_1, y_1) and (x_2, y_2) as follows:

$$x_{try} = x_1 + \frac{x_2 - x_1}{y_2 - y_1} (y_0 - y_1) \tag{A.15}$$

We have described the linear-interpolating method, which is convergent for any monotonic function. In our case, however, we found the convergence very slow. In many instances we were not able to obtain results with 0.1 percent accuracy less than 40 iteration steps. We found a very efficient way to speed up the convergence of this method considerably.

Before obtaining the points (x_1, y_1) or (x_2, y_2) from the current values of x_{try} and y_{try}, we store y_1 or y_2 respectively by setting its value equal to y_3. This means that if the trial point is above the root, we set $y_3 = y_2$ and then perform the substitutions

$x_2 = x_{try}$, $y_2 = y_{try}$. If the trial point is below the root, we set $y_3 = y_1$ first and proceed as before, setting $x_1 = x_{try}$ and $y_1 = y_{try}$. In the first case the expression $(y_3 - y_2)/(y_3 - y_0)$ is a measure of the speed of the convergence of the linear-interpolating method. When y_2--which is the last trial value--is near to the value of y_0, the linear interpolation is successful and the value of the above expression is near unity. When y_2 is near to y_3--which is the trial point of the succeeding step--the linear-interpolating method does not converge rapidly and the value of the above expression is near to zero. Consequently, when the value of $(y_3 - y_2)/(y_3 - y_0)$ is near unity, we want to proceed with linear interpolation; when its value is zero, we halve the interval to find the new trial value of x. The following expression performs both functions:

$$x_{try} = \left(\frac{x_1 + x_2}{2} \right)\left(1 - \frac{y_3 - y_2}{y_3 - y_0} \right) + \left[x_1 + \frac{x_2 - x_1}{y_2 - y_1}(y_0 - y_1) \right]\left(\frac{y_3 - y_2}{y_3 - y_0} \right)$$

(A.16)

After simplification Eq. (A.16) becomes

$$x_{try} = \frac{1}{2}\left[x_1 + x_2 + \frac{(y_3 - y_2)(2y_0 - y_1 - y_2)(x_2 - x_1)}{(y_3 - y_0)(y_2 - y_1)} \right]$$ (A.17)

In the second case the trial point is below the root. The roles of y_2 and y_1 are interchanged and the important factor is $(y_3 - y_1)/(y_3 - y_0)$. If we can use the interpolating formula (i.e., if the points above the root have already been obtained in the preceding steps), then the formula for the new x_{try} is similar to that of Eq. (A.17).

$$x_{try} = \frac{1}{2}\left[x_1 + x_2 + \frac{(y_3 - y_1)(2y_0 - y_1 - y_2)(x_2 - x_1)}{(y_3 - y_0)(y_2 - y_1)} \right]$$ (A.18)

If the extrapolation formula is used, we can speed up convergence by multiplying Eq. (A.14) with the factor $(y_3 - y_0)/(y_3 - y_1)$. This

factor becomes large if the extrapolating procedure does not converge rapidly, but it is unity if the convergence is good.

We have covered all the possible cases of this iterating procedure except the first two steps, in which a value to y_3 is not yet assigned. In this case we use the interpolating or the extrapolating procedure without the indicated correction for the first two steps.

The described procedure converged very rapidly in all the examples that were calculated. With the requirement of 0.1-percent accuracy, six iteration steps were sufficient in average.

APPENDIX B. BALGOL TEXT OF THE COMPUTER PROGRAM FOR THE DC STATES

The complete text of the described computer program in symbolic language is reproduced on pages 99 through 106. The program was written in BALGOL, which is the Stanford version of ALGOL 60.

```
COMMENT  ---MOST OF THE IDENTIFIERS USED IN THIS
    PROGRAM APPEAR AS SYMBOLS IN THE PAPER. FOR THEIR
    DEFINITION CONSULT THE REPORT .
    DEFINITION OF NEW VARIABLES  --
            ACURACY = THE PERCENTAGE ERROR ALLOWED IN THE
                CALCULATION OF  SEPARATION LENGTH.
            ACCY = 0.1.ACURACY .
            CSTE = ALPHAE.EXP( BETAE.ETAMIN )  .
            CSTI = ALPHAI.EXP( BETAI.( ETA2 - ETAMAX) )  .
            CURRENT = CURRENT/AREA FLOWING THROUGH THE DIODE .
            ERROR = PERCENTAGE ERROR COMITTED IN THE LAST
                        STEP OF THE ITERATION PROCESS  .
            MRATIO = MASS OF ELECTRONS/MASS OF IONS  .
            NO = NUMBER OF INTERVALS FOR INTEGRATION .
            POSMAX = THE DISTANCE BETWEEN THE ION EMITTER
                        AND THE POSITION OF MAXIMUM POTENTIAL  .
            POSMIN = THE DISTANCE BETWEEN THE ELECTRON
                        EMITTER AND THE POSITION OF
                        MINIMUM POTENTIAL .
            VMAX = THE MAXIMUM POTENTIAL IN THE DIODE .
            VMIN = THE MINIMUM POTENTIAL IN THE DIODE  .      $
PROCEDURE    GNEG( X )   $
    BEGIN
        EITHER IF X LEQ 0.0   $
            GNEG() = 1.0   $
        OR IF X LSS  2.0   $
            GNEG() = 1.0 + X.(1.0+X.(0.5+X.(0.16666667+X.(0.0416666
                        X.(0.0083333333+0.003473606.X)))) - SQRT(X).
                        (0.7522528+X.(0.30090112+X.(0.085971748+X.
                        (0.019104833+X.(0.003473606+0.0018228038.X))
        OR IF X LSS 500.0 $
            BEGIN
            Y  =  1.0/X   $
            GNEG() =   SQRT(X).(1.1283792+Y.(0.56418957-Y.(0.282094
                        Y.(0.42314218 - 0.42740262.Y))))  $

            END$
        OTHERWISE   $
            GNEG() =   1.1283792.SQRT(X)  $
        RETURN
    END    GNEG()   $
PROCEDURE    GPOS(X)  $
    BEGIN
        EITHER IF X LEQ 0.0  $
            GPOS() = 1.0  $
        OR IF X LEQ 10.0  $
            GPOS() = 2.0.EXP(X) - GNEG(X)  $
        OR IF X LEQ  80.0  $
            GPOS() = 2.0.EXP(X)  $
        OTHERWISE  $
            GPOS() = 1.0**38  $
```

```
        RETURN
        END GPOS() $
COMMENT --- THE FOLLOWING FUNCTIONS ARE THE INTEGRANDS
            FOR THE THREE REGIONS RESPECTIVELY .
                    ( SEE  EQUATIONS 36. AND 37. ) $
FUNCTION
    REGION1(ETA) = 1.0/SQRT( CSTI.GNEG(BETAI.(ETAMAX-ETA))
                        CSTE.GPOS(BETAE.(ETA-ETAMIN))+GAMMA) $
FUNCTION
    REGION2(ETA) = 1.0/SQRT( CSTI.GNEG(BETAI.(ETAMAX-ETA))
                        CSTE.GNEG(BETAE.(ETA-ETAMIN))+GAMMA) $
FUNCTION
    REGION3(ETA) = 1.0/SQRT( CSTI.GPOS(BETAI.(ETAMAX-ETA))
                        CSTE.GNEG(BETAE.(ETA-ETAMIN))+GAMMA) $
PROCEDURE     INT( N , A , B$$ F()  ) $
    BEGIN
    COMMENT --- THE INTEGRAL OF F(X) FROM A TO B IS DIVIDED
                INTO  N  EQUAL INTERVALS . THE CORRECTED
                GAUSS'S FORMULA IS USED FOR THE N
                INTERVALS $
        INTEGER  N , K $
        H = (B - A)/N $
        SUM = 0 $
        FOR K = (1 , 1 , N ) $
            SUM = SUM + 0.15128136.(F(A+H.(K-0.96898593)) +
                                F(A+H.(K-0.03101407))) +
                    .69743728.F(A+H.(K-0.5)) $
        INT() = H.SUM $
        RETURN
    END INT()  $
SUBROUTINE  CORRECT $
    BEGIN
        EITHER IF YTRY LSS YO $
            BEGIN
                Y3 = Y1 $
                Y1 = YTRY $
                X1 = XTRY $
                EITHER IF ( Y2 EQL 0.0 ) AND ( Y3 EQL 0.0 ) $
                    XTRY = X1.YO/Y1 $
                OR IF Y2 EQL 0.0 $
                    XTRY = ( X1.YO.(YO-Y3))/ ( Y1.(Y1-Y3)) $
                OTHERWISE $
                    XTRY = 0.5.(X1+X2+((X2-X1).(Y3-Y1).
                        (2.0.YO-Y1-Y2))/((Y3-YO).(Y2-Y1))) $
            END $
        OR IF YTRY GTR YO $
            BEGIN
                Y3 = Y2 $
                Y2 = YTRY $
                X2 = XTRY $
                EITHER IF Y3 EQL 0.0 $
                    XTRY = X1 +((YO-Y1).(X2-X1))/(Y2-Y1) $
```

```
                        OTHERWISE $
                           XTRY = 0.5.(X1+X2+((X2-X1).(Y3-Y2).
                                 (2.0.Y0-Y1-Y2))/((Y3-Y0).(Y2-Y1))) $
                  END $
              OTHERWISE $
                  RETURN $
      RETURN
      END CORRECT $
          COMMENT --- THE CONTROL DATA .
                     NO = NUMBER OF SUBDIVISIONS IN THE INTEGRAL
                          PROCEDURE .
                     ACURACY = MAXIMUM PERCENTAGE ERROR IN THE
                             CALCULATED SEPARATION LENGTH WHEN
                             COMPARED TO THE GIVEN LENGTH, XI2.
                     ACCY = MAXIMUM ERROR FOR THE ITERATING
                             STEPS WHICH DETERMINE ETATMIN $
      INTEGER   NO $
         READ ($$ CONTROL ) $
         INPUT CONTROL( NO , ACURACY ) $
            ACCY = 0.1.ACURACY $
      START..
         READ   ($$ DATA) $
            INPUT DATA( JSE,JSI,TE,TI,V2,D,MRATIO ) $
         WRITE ($$ INOUT,FMOUT ) $
            OUTPUT INOUT(JSE,JSI,TE,TI,V2,D,MRATIO ) $
            FORMAT FMOUT(B20,*THE PARAMETERS OF THE DIODE *,W2,
                B7,*JSE*,B11,*JSI*,B12,*TE*,B12,*TI*,B12,*V2*,
                B13,*D*,B11,*ME/MI*,W2, 7F14.5,W2 )   $
      NORMALIZE..
         COMMENT --- THE NORMALIZED PARAMETERS OF THE
                     DIODE ARE CALCULATED $
         ALPHAE = JSE/( JSE + JSI.SQRT(TI/(TE.MRATIO))) $
         ALPHAI = 1.0 - ALPHAE $
         BETAE = TI/(TI.ALPHAE + TE.ALPHAI)   $
         BETAI = BETAE.TE/TI $
         ETA2 = 11605.0.V2/( BETAE.TE )   $
         XI2 = 9.19286**5.D.SQRT(JSE.SQRT(TE)+JSI.SQRT(TI/
                     MRATIO))/( BETAE.TE)   $
      TRANSITION..
         COMMENT ---  EQU. 46 AND 47 ARE CALCULATED FIRST $
         QE = ALPHAE.( GNEG(BETAE.ETA2) - 1.0 ) $
         QI = ALPHAI.( GNEG(BETAI.ETA2) - 1.0 ) $
            IF ETA2 EQL 0.0 $
               BEGIN
                 COMMENT --- TAKE THE LIMIT $
                    QE = ALPHAE.BETAE $
                    QI = ALPHAI.BETAI $
               END $
         EITHER IF QE GTR QI $
            BEGIN
               COMMENT --- THE DIODE IS ELECTRON-RICH $
               XIAC = XIAD = XICD = 0.0 $
```

```
     GAMMAMIN = - ALPHAE - ALPHAI.GNEG( BETAI.ETA2 ) $
     GAMMA = GAMMAMIN $
         IF ETA2 EQL 0.0 $
             GAMMA = 0.0 $
     ETAMIN = 0.0 $
     ETAMAX = ETA2 $
     CSTE = ALPHAE $
     CSTI = ALPHAI $
   XIAB = INT( NO , 0.0 , ETA2 $$ REGION2() ) $
     EITHER IF ALPHAI EQL 0.0 $
     BEGIN
         XIBD = 1.1.XI2 $
         ETATMIN = ETA2 $
     END $
     OTHERWISE $
     BEGIN
     ETAT = ETA2 $
         IF ( BETAE.ETAT LSS 1.0**-7 )
             OR ( BETAI.ETAT LSS 1.0**-7 ) $
         ETAT = 1.0**-6/BETAE + 1.0**-6/BETAI $
     ETATRY = ETAT + 2.0.ACCY.(ETAT - ETA2) $
     UNTIL ABS(ETATRY - ETAT) LSS ACCY.(ETAT - ETA2) $
         BEGIN
           COMMENT --- SOLVING FOR ETAT BY ITERATION $
             ETATRY = ETAT $
             ETAT = ETA2 + LOG((ALPHAE.( GNEG( BETAE.
                 ETATRY) - 1.0))/(ALPHAI.( GNEG(
                 BETAI.ETATRY ) - 1.0 )))/BETAE $
         END $
     ETATMIN = ETAT $
     ETAMAX = ETA2 $
     ETAMIN = ETA2 - ETAT $
     CSTE = ALPHAE.EXP(BETAE.ETAMIN) $
     GAMMA = - MIN( (CSTE + CSTI.GNEG( BETAI.ETAT)) ,
                    (CSTE.GNEG(BETAE.ETAT) + CSTI )) $
   XIMIN = - INT( NO , 0.0 , ETAMIN $$ REGION1() ) $
   XIBD = XIMIN + INT(NO,ETAMIN,ETA2 $$ REGION2() ) $
    END $
    END $
OR IF QI GTR QE $
    BEGIN
      COMMENT --- THE DIODE IS ION-RICH $
      XIAB = XIBD = XIAD = 0.0 $
      GAMMAMIN = - ALPHAE.GNEG( BETAE.ETA2) - ALPHAI $
      GAMMA = GAMMAMIN $
          IF ETA2 EQL 0.0 $
              GAMMA = 0.0 $
      ETAMIN = 0.0 $
      ETAMAX = ETA2 $
      CSTE = ALPHAE $
      CSTI = ALPHAI $
   XIAC = INT( NO , 0.0 , ETA2 $$ REGION2() ) $
```

```
        EITHER IF ALPHAE EQL 0.0 $
        BEGIN
            XICD = 1.1.XI2 $
            ETATMIN = ETA2 $
        END $
        OTHERWISE $
        BEGIN
        ETAT = ETA2 $
            IF ( BETAE.ETAT LSS 1.0**-7 )
                OR ( BETAI.ETAT LSS 1.0**-7 ) $
            ETAT = 1.0**-6/BETAE + 1.0**-6/BETAI $
        ETATRY = ETAT + 2.0.ACCY.(ETAT - ETA2) $
        UNTIL ABS(ETATRY - ETAT) LSS ACCY.(ETAT - ETA2) $
            BEGIN
              COMMENT --- SOLVING FOR ETAT BY ITERATION $
                ETATRY = ETAT $
                ETAT = ETA2 + LOG((ALPHAI.( GNEG( BETAI.
                    ETATRY) - 1.0))/( ALPHAE.( GNEG(
                    BETAE.ETATRY ) - 1.0 )))/BETAI $
            END $
        ETATMIN = ETAT $
        ETAMAX = ETAT $
        ETAMIN = 0.0 $
        CSTI = ALPHAI.EXP( BETAI.( ETA2 - ETAMAX )) $
        GAMMA = - MIN( (CSTE + CSTI.GNEG( BETAI.ETAT)) ,
                      (CSTE.GNEG(BETAE.ETAT) + CSTI )) $
    XIMAX = - INT( NO,ETAMAX,ETA2 $$ REGION3() ) $
    XICD = XIMAX + INT( NO,0.0,ETAMAX $$ REGION2() ) $
     END $
    END $
OTHERWISE $
    BEGIN
      COMMENT --- THE DIODE IS NEUTRAL $
      XIAB = XIBD = XIAC = XICD = 0.0 $
      GAMMAMIN = - ALPHAE - ALPHAI.GNEG( BETAI.ETA2 ) $
      GAMMA = GAMMAMIN $
          IF ETA2 EQL 0.0 $
            GAMMA = 0.0 $
      ETAMIN = 0.0 $
      ETAMAX = ETA2 $
      ETATMIN = ETA2 $
      CSTE = ALPHAE $
      CSTI = ALPHAI $
    XIAD = INT( NO,0.0,ETA2 $$ REGION2() ) $
    END $
    WRITE ($$ OUTTRANS , FTRANS ) $
    OUTPUT   OUTTRANS ( XIAB,XIAC,XIBD,XICD,XIAD,XI2) $
    FORMAT
        FTRANS( B10,*THE NORMALIZED TRANSITION LENGTHS*,
            W4,B8 ,*XIAB*,B11,*XIAC*,B11,*XIBD*,B11,
            *XICD*,B11,*XIAD*,W4,5F15.5,W2,
```

```
                  B10,*THE NORMALIZED SEPARATION LENGTH*,
                  * XI2 = *, F20.5 ,W2 , W2 )  $
COMPARE..
     COMMENT --- THE NEXT STEP IS THE DETERMINATION OF THE
                 TYPE OF THE POTENTIAL SOLUTION $
   XIAMAX = XIAB + XIAC + XIAD $
   XIDMIN = XIBD + XICD + XIAD $
   EITHER IF XI2 LEQ XIAMAX $
       BEGIN
          WRITE ($$ LINEA ) $
          FORMAT  LINEA(B20,*THE SOLUTION IS TYPE A*,W2 ) $
          GO TO   TYPEA $
       END $
   OR IF XI2 GEQ XIDMIN $
       BEGIN
          WRITE ($$ LINED ) $
          FORMAT  LINED(B20,*THE SOLUTION IS TYPE D *,W2) $
          GO TO   TYPED $
       END $
   OR IF XICD EQL 0.0 $
       BEGIN
          WRITE ($$ LINEB ) $
          FORMAT  LINEB(B20,*THE SOLUTION IS TYPE B*,W2) $
          GO TO TYPEB $
       END $
   OTHERWISE $
       BEGIN
          WRITE ($$ LINEC ) $
          FORMAT  LINEC(B20,*THE SOLUTION IS TYPE C*,W2) $
          GO TO TYPEC $
       END $
COMMENT --- THE CALCULATION OF THE INSIDE PARAMETERS
            FOLLOWS. THE LABELS CORRESPOND TO THE FOUR
            TYPES OF POTENTIAL FUNCTIONS . TO TEST THE
            ITERATING PROCEDURE , THE RESULTS OF THE
            ITERATING STEPS ARE LISTED $
   FORMAT   ITHEAD  (B10,*DURING THE ITERATING PROCEDURE*,
                 * THE FOLLOWING STEPS WERE TAKEN*,W2)$
   OUTPUT   ITEROUT ( YTRY , YO ) $
   FORMAT    FMITER( B30,*THE TRIAL VALUE*,B10,
                 * THE SOLUTION *,W ,B30,F13.5,B12,
                 F13.5,W ) $
TYPEA..
   ETAMIN = 0.0 $
   ETAMAX = ETA2 $
   XIMIN = 0.0 $
   XIMAX = 0.0 $
   CSTE = ALPHAE $
   CSTI = ALPHAI $
   YO = XI2 $
   XTRY = (XI2*2 )/( (XI2 - XIAMAX)*2.SQRT(ETA2) ) $
   X1 = X2 = Y1 = Y2 = Y3 = 0.0   $
   ERROR = 1.1.ACURACY.XI2 $
```

```
                WRITE( $$ ITHEAD) $
        UNTIL ERROR LEQ ACURACY.XI2 $
            BEGIN
                GAMMA = 1.0/XTRY + GAMMAMIN $
                YTRY = INT( NO,0.0,ETA2 $$ REGION2() ) $
                ERROR = ABS( YTRY - XI2 ) $
                WRITE ( $$ ITEROUT,FMITER ) $
            ENTER CORRECT $
            END $
        GO TO FINAL $
TYPEB..
    ETAMAX = ETA2 $
    CSTI = ALPHAI $
    XIMAX = 0.0 $
    YO = XI2 - XIAMAX $
    XTRY = ETATMIN - ETA2 $
        IF XTRY EQL 0.0 $
            XTRY = LOG( 1.1 + XI2 ) / 0.5.BETAE $
    X1 = X2 = Y1 = Y2 = Y3 = 0.0  $
    ERROR = 1.1.ACURACY.XI2 $
            WRITE( $$ ITHEAD) $
    UNTIL ERROR LEQ ACURACY.XI2 $
        BEGIN
            ETAMIN = - XTRY $
            CSTE = ALPHAE.EXP( BETAE.ETAMIN ) $
            GAMMA = - CSTE - CSTI.GNEG(BETAI.(ETA2-ETAMIN)) $
            XIMIN = -INT( NO,0.0,ETAMIN $$ REGION1() ) $
            YTRY = XIMIN - XIAMAX  +
                        INT(NO,ETAMIN,ETA2 $$ REGION2() )   $
            ERROR =  ABS( YTRY + XIAMAX - XI2 ) $
            WRITE ( $$ ITEROUT,FMITER ) $
        ENTER CORRECT $
        END $
    GO TO FINAL $
TYPEC..
    ETAMIN = 0.0 $
    CSTE = ALPHAE $
    XIMIN = 0.0 $
    YO = XI2 - XIAMAX $
    XTRY = ETATMIN - ETA2 $
        IF XTRY EQL 0.0 $
            XTRY = LOG( 1.1 + XI2 ) / 0.5.BETAI $
    X1 = X2 = Y1 = Y2 = Y3 = 0.0   $
    ERROR = 1.1.ACURACY.XI2 $
            WRITE( $$ ITHEAD) $
    UNTIL ERROR LEQ ACURACY.XI2 $
        BEGIN
            ETAMAX = XTRY + ETA2 $
            CSTI = ALPHAI.EXP( -BETAI.XTRY ) $
            GAMMA = - CSTI - CSTE.GNEG( BETAE.ETAMAX ) $
            XIMAX = -INT( NO,ETAMAX,ETA2 $$ REGION3() ) $
```

```
                YTRY = XIMAX - XIAMAX +
                        INT(NO,0.0,ETAMAX $$ REGION2() ) $
            ERROR = ABS( YTRY + XIAMAX - XI2 ) $
            WRITE ( $$ ITEROUT,FMITER ) $
        ENTER CORRECT $
        END $
    GO TO FINAL $
TYPED..
    YO = XI2 - XIDMIN $
    XTRY = LOG( 1.1 + YO ) $
    X1 = X2 = Y1 = Y2 = Y3 = 0.0   $
    ERROR = 1.1.ACURACY.XI2 $
            WRITE( $$ ITHEAD) $
    UNTIL ERROR LEQ ACURACY.XI2 $
        BEGIN
            ETAT = ETATMIN + XTRY $
            ETAMAX = ( BETAE.ETAT+BETAI.ETA2-LOG( (ALPHAE.(
                    GNEG(BETAE.ETAT)-1.0))/(ALPHAI.(GNEG(
                    BETAI.ETAT)-1.0)) ))/(BETAI + BETAE) $
            ETAMIN = ETAMAX - ETAT $
            CSTE = ALPHAE.EXP( BETAE.ETAMIN ) $
            CSTI = ALPHAI.EXP( BETAI.(ETA2 - ETAMAX) ) $
            GAMMA = - MIN((CSTE+CSTI.GNEG(BETAI.ETAT)),
                    (CSTE.GNEG(BETAE.ETAT)+CSTI) ) $
            XIMIN = -INT( NO,0.0,ETAMIN $$ REGION1() ) $
            XIMAX = -INT( NO,ETAMAX,ETA2 $$ REGION3() ) $
            YTRY = XIMIN + XIMAX - XIDMIN +
                INT( NO,ETAMIN,ETAMAX $$ REGION2() ) $
            ERROR = ABS( YTRY + XIDMIN - XI2 ) $
            WRITE ( $$ ITEROUT,FMITER ) $
        ENTER CORRECT $
        END $
    GO TO FINAL $
FINAL..
    COMMENT --- THE DESIRED OUTPUT DATA ARE CALCULATED .
            HERE WE CALCULATE THE POTENTIAL MINIMUM AND
            MAXIMUM , THEIR POSITION , AND THE CURRENT
            DENSITY IN THE DIODE $
    VMIN = ETAMIN.BETAE.TE/11605.0   $
    VMAX = ETAMAX.BETAE.TE/11605.0   $
    POSMIN = XIMIN.D/XI2 $
    POSMAX = XIMAX.D/XI2 $
    CURRENT = JSE.EXP( BETAE.ETAMIN ) +
                JSI.EXP( BETAI.( ETA2 - ETAMAX ) ) $
      WRITE ( $$ RESHEAD )   $
        FORMAT  RESHEAD ( W2,B20,*THE CALCULATED RESULTS*,
                    * ARE THE FOLLOWING*,W2 ) $
      WRITE ( $$ RESULT,FMRESULT )    $


      OUTPUT    RESULT(VMIN,POSMIN,VMAX,POSMAX,CURRENT) $
      FORMAT FMRESULT(B5,*POT.MINIMUM (VOLTS)      *,
        *X.MINIMUM (CM)    POT.MAXIMUM (VOLTS)      *,
        *X.MAXIMUM (CM)    J/DIODE (AMP/SQCM)* , W2 ,
        5F20.5 ,W1 ) $
    GO TO START $
FINISH $
```

7

APPENDIX C. FINDING THE TRANSITION LENGTH
OF ANY OPPOSITE-STREAM DIODE

The seven diagrams presented on pages 107 through 110 give the transition length $\xi_{D_{min}}$ as a function of the variables α, β, η_2. These variables and ξ_2 are determined from the parameters of the diode. From α, β, η_2, with the help of the following diagrams, the value of $\xi_{D_{min}}$ can be found. The largest odd-integer number, which is still less than the ratio $\xi_2/\xi_{D_{min}}$, is the maximum number of half-periods that a periodic solution can contain in the diode. If $\xi_2/\xi_{D_{min}} < 3$, no periodic solution is possible. For $\beta > 1.0$, the parameters $1.0/\beta$ and $1.0/\alpha$ are used in place of β and α in order to find $\xi_{D_{min}}$.
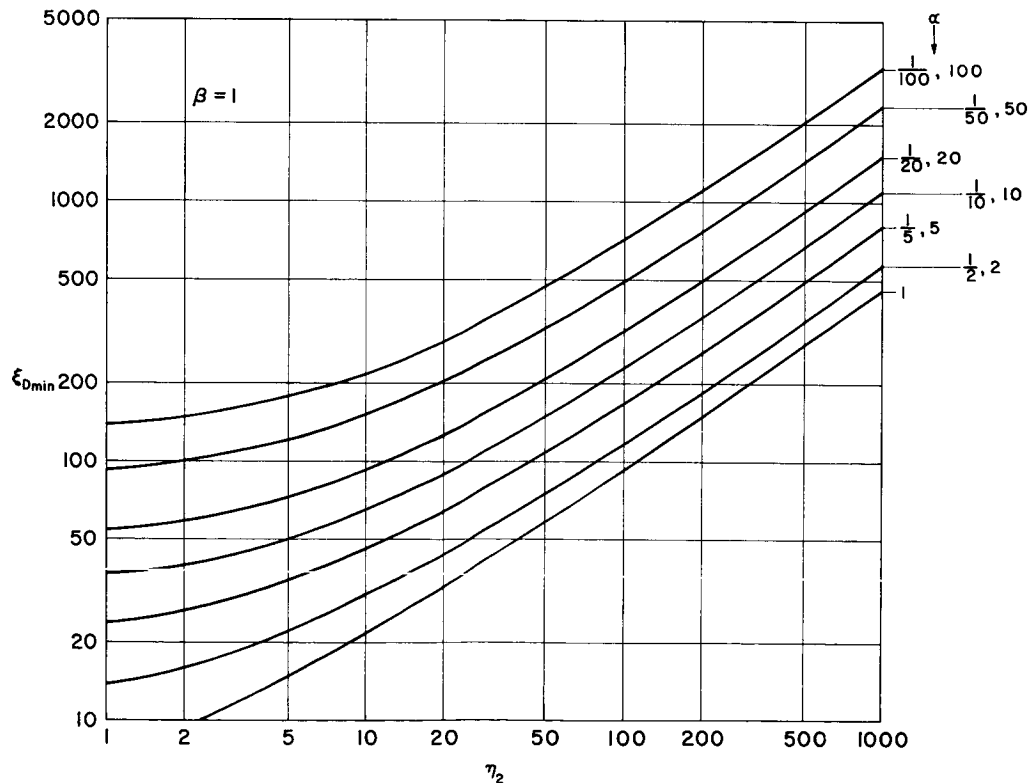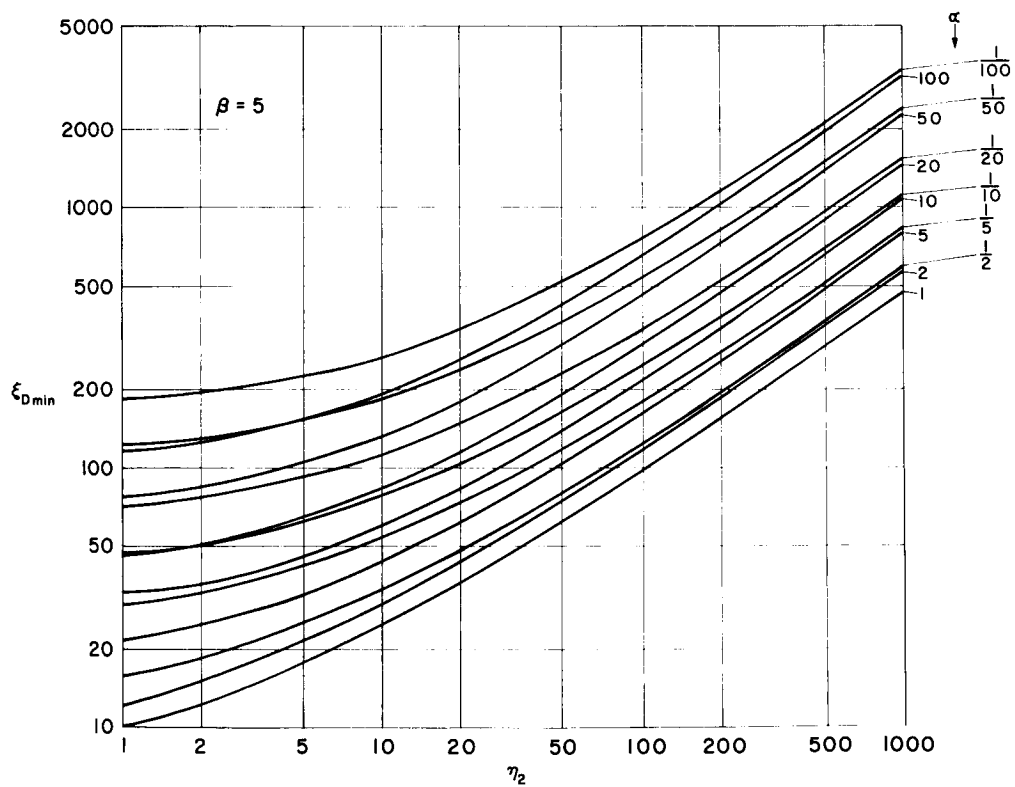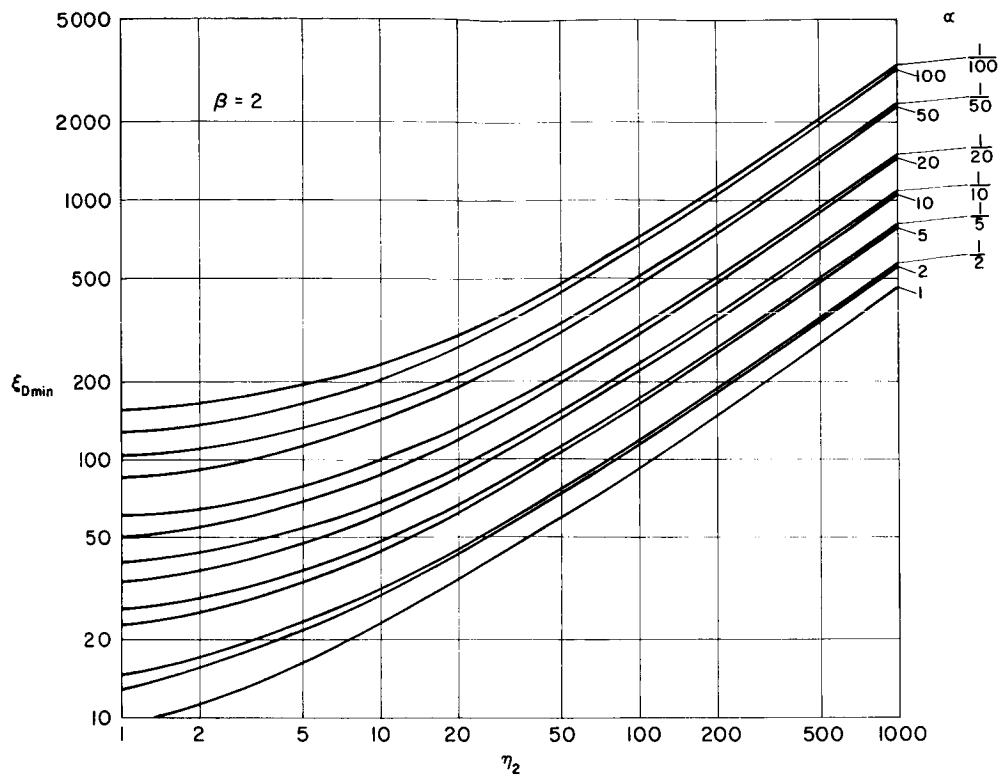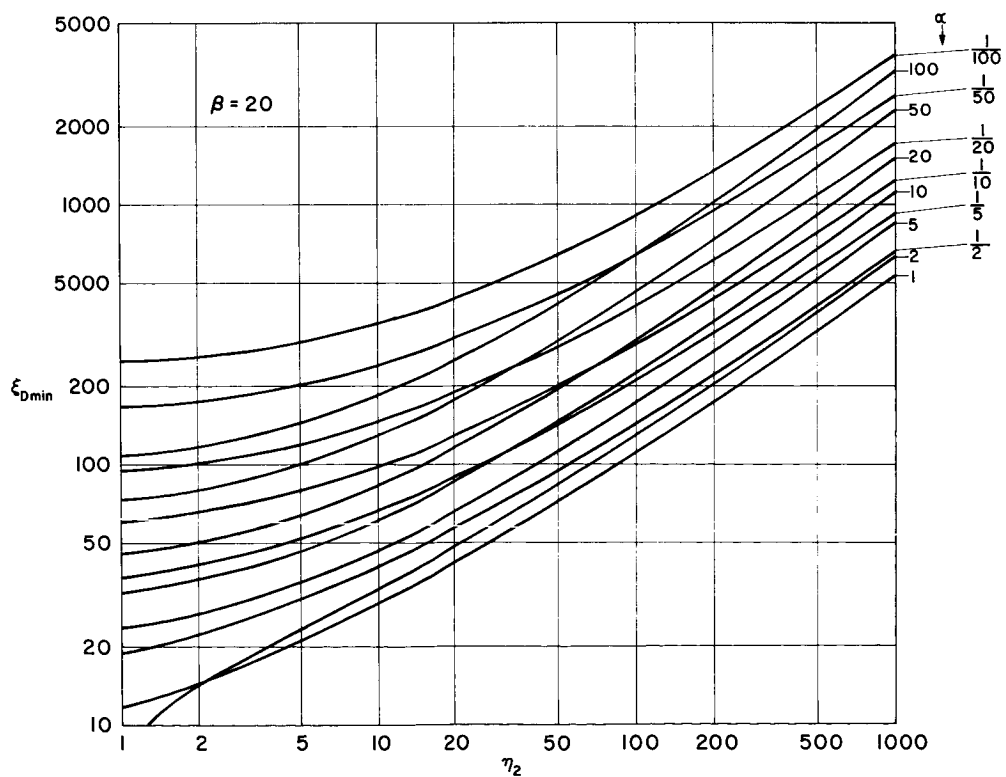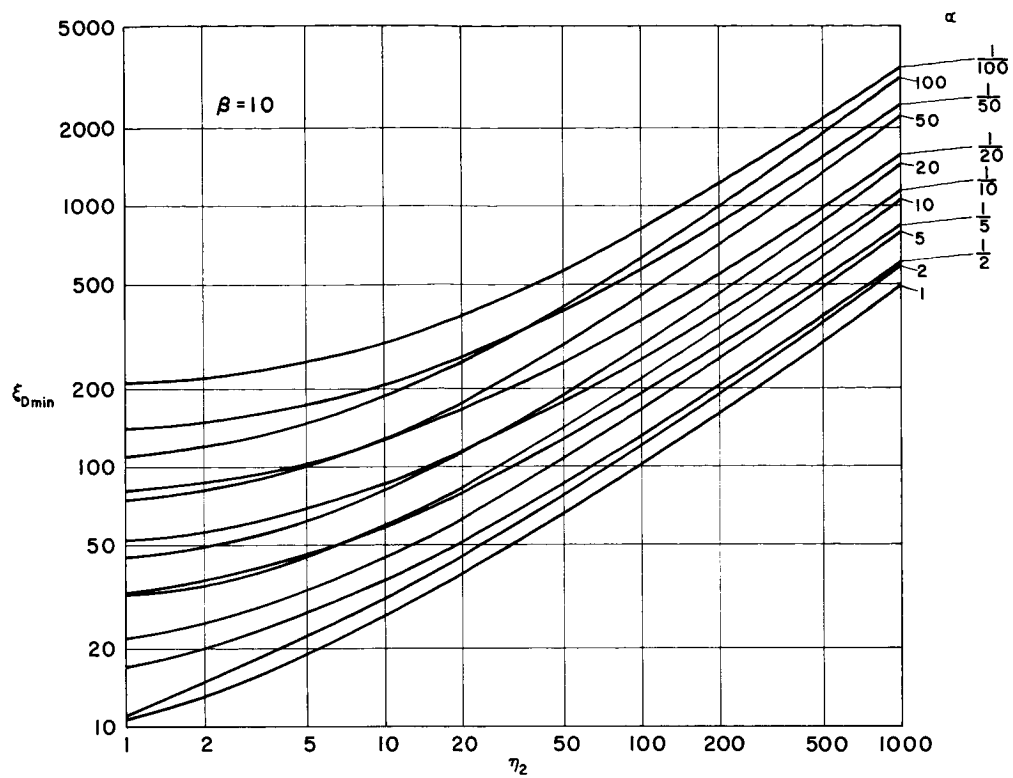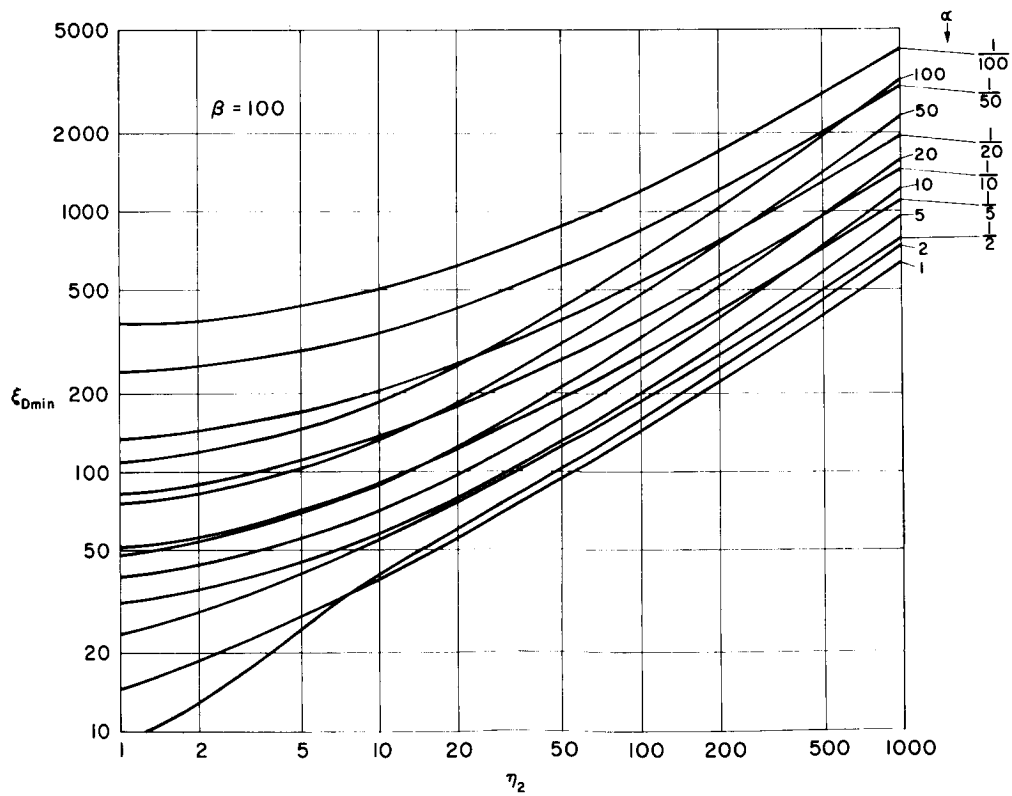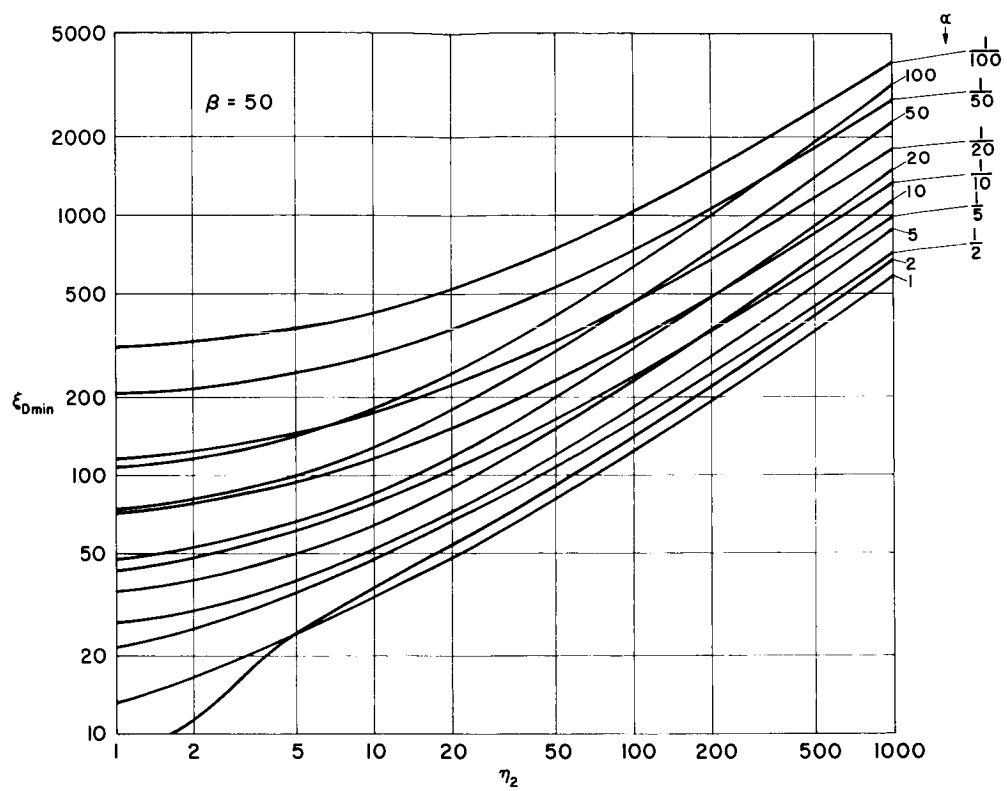
APPENDIX D. COMPUTER PROGRAM FOR THE SIMULATION OF THE OPPOSITE-
STREAM PLASMA DIODE

The basic principles in the simulation of the opposite-stream plasma diode by a computer were discussed in Chapter V. We are concerned here with incorporating these basic procedures into an accurate and fast computer program written specifically for the IBM 7090 computer. It is assumed that the reader is familiar with the facilities of this computer and with binary-integer arithmetic in general.

We used physical quantities in Chapter V to describe the computer model of a one-dimensional plasma. In order to deal with this problem on the computer it is necessary to normalize these quantities. The symbols in the following normalization procedure refer to the dc parameters of the diode defined in Chapter III and to the parameters of the computer program discussed in Chapter V.

1. The Normalization Procedure

For their easier identification, the variables and the constants of the computer program will be represented by capitalized words. Naturally, these quantities are dimensionless.

Position in the diode (POS) is measured from the electron emitter (left boundary plane), it is represented by an integer, and is normalized in such a manner that the position at the right boundary plane is 2^{34}. The relation between POS and the real position in the diode (x) is given by:

$$POS = 2^{34} \frac{x}{\xi_2 \bar{\lambda}} \tag{D.1}$$

With the characteristic temperature of the diode $\bar{T}$, a characteristic velocity $\bar{v}$ is defined by the following relation:

$$\bar{v} = \sqrt{\frac{2k\bar{T}}{m_e}} \tag{D.2}$$

where k is Boltzmann's constant and m_e is the mass of the electrons. Time is normalized by this velocity and the characteristic Debye length of the diode, $\bar{\lambda}$. The relation between the normalized time (TAU) and real time t is then:

$$TAU = \frac{\bar{v}}{\bar{\lambda}} t \qquad (D.3)$$

Normalized velocity in the computer (VEL) is defined by the first difference of position and of time, i.e., by $VEL = \frac{\triangle \, POS}{\triangle \, TAU}$. Substituting Eqs. (D.1) and (D.3) into this relation, we get the following equation between normalized and real velocities:

$$VEL = \frac{2^{34}}{\xi_2} \quad \frac{v}{\bar{v}} \qquad (D.4)$$

where v represents velocity in physical units.

We showed in Chapter V that the electron sheets are injected according to the distribution law

$$v_{0e} = \left(\frac{2kT_e}{m_e} \right)^{\frac{1}{2}} \sqrt{- \log R}$$

where R is a random variable uniformly distributed in the unit interval. Consequently, the normalized injected velocities of the electron sheets (VELOE) follow the distribution law:

$$VELOE = \frac{2^{34}}{\xi_2 \sqrt{\beta_e}} \sqrt{- \log R} \qquad (D.5)$$

The injected velocities of the ion sheets in normalized form (VELOI) are distributed similarly as

$$VELOI = \frac{2^{34}}{\xi_2 \sqrt{\beta_i}} \sqrt{\frac{m_e}{m_i}} \sqrt{- \log R} \qquad (D.6)$$

where R is again a random variable uniformly distributed in the unit interval.

The charge-to-mass ratio of an electron sheet is normalized to unity in our computer program. This means that the acceleration of the electron sheet (ACCE) is numerically equal to the negative of the electric field. The normalized value of the electric field will be represented by EFLD. In mks units the acceleration of an electron sheet (a_e) is given by the expression:

$$a_e = - \frac{e}{m_e} E \tag{D.7}$$

where e is the electronic charge, 1.6×10^{-19} coulombs and E is the electric field in mks units. Since acceleration is the first difference of velocity divided by the first difference of time in both the physical and the normalized systems, an expression between the normalized electric field and the real electric field (E) can be derived, yielding the expression

$$EFLD = \frac{2^{34} \bar{\lambda} e}{\xi_2 (\bar{v})^2 m_e} E \tag{D.8}$$

The electric field that is due to the externally applied potential (V_2) is E_2 and is given by Eq. (66). This quantity can be expressed in the normalized form (EFLD2) in terms of η_2 as follows

$$EFLD2 = - \frac{2^{33}}{\xi_2^2} \eta_2 \tag{D.9}$$

The contribution to the electric field of the sheets in the diode (E_1) can be expressed in normalized form if it is known how much change occurs in the normalized electric field when a sheet is crossed. The change in the actual field $(\triangle E)$ is

$$\triangle E = \frac{\sigma}{\epsilon_0} \tag{D.10}$$

where σ is equal to the coulombs-per-area surface charge that a sheet represents. This factor, σ, is a function of the number of electron

sheets injected per second. This electron-sheet injection rate is a parameter of the computer diode and it is more convenient to represent it by the number of electron sheets that are injected during a unit normalized time. We call this parameter Γ_e, or GMME. The saturation current density of the electron emitter (J_{se}) is equal to the product of σ and the number of electron sheets injected per second. Changing the time scale to normalized time and using Eq. (D.10) to express σ, we obtain J_{se} in the following form:

$$J_{se} = \frac{\bar{v}}{\bar{\lambda}} \epsilon_0 \, \triangle E \; (\text{GMME}) \tag{D.11}$$

In Eq. (15), J_{se} is given by a different expression. After introduction of the characteristic constants of the diode $(\bar{N}, \bar{T})$ into this expression, it becomes:

$$J_{se} = \frac{\bar{N} \, e}{\alpha_e \sqrt{\beta_e}} \sqrt{\frac{k\bar{T}}{2\pi \, m_e}} \tag{D.12}$$

The right-hand sides of Eqs. (D.12) and (D.11) are equated and $\triangle E$ is expressed as a function of the dc parameters of the diode and of GMME. The parameter $\triangle E$ is the change in the electric field that we were looking for. This change can be expressed in a normalized form (DEFD) by using Eq. (D.8). The resulting expression is

$$\text{DEFD} = \frac{2^{32}}{\sqrt{\pi} \; \alpha_e \sqrt{\beta_e} \; \text{GMME}} \tag{D.13}$$

Since the ion sheets are carrying the same amount of surface charge as the electron sheets (with a different sign, naturally), the injection rate of the ion sheets depends on the injection rate of the electron sheets through the dc parameters of the diode. If we call the number of injected ion sheets per unit normalized time GMMI, it is given by the relation:

$$\text{GMMI} = \text{GMME} \; \frac{\alpha_i \sqrt{\beta_i} \; m_e}{\alpha_e \sqrt{\beta_e} \; m_i} \tag{D.14}$$

We have expressed all the constants that are necessary for the calculation of the characteristics of the computer diode in terms of the normalized dc parameters of the diode. The size of the time step $\Delta\tau$, or DTAU, was not included amoung these constants because it is an independent parameter of the computer model and does not influence the constants. The constants and parameters of the diode are collected in Table 3 for reference.

2. Variables of the Computer Program

Strictly speaking, the variables of the computer program are only the positions and the previous change of positions of the sheets. All other quantities in the diode are determined from these variables. It is convenient, however, to select still other quantities in the program and consider them also as variables partly because of their physical significance (potential, current, etc.) and partly because of their roles in computing the characteristics of the diode. Most of these variables are collected into arrays. These arrays will be identified by capitalized words, and lower case subscripts will show their particular elements.

The positions and the previous changes in the positions of the sheets are placed into two arrays $(POS_n, DPOS_n)$. The sign of POS_n shows whether the nth elements of POS_n and $DPOS_n$ arrays belong to an electron sheet $(POS_n < 0)$ or to an ion sheet $(POS_n > 0)$. Place is reserved in the computer's memory for 10,000 elements of both arrays.

It was shown in Chapter V that it is sufficient to record the values of the electric field only at prescribed points in the diode. These points are the midpoints of the segments which divide the diode space into 1024 equal intervals. In order to identify them, these segments are numbered starting--for reasons that will be clear later--with the number 0. Hence, the segment that is nearest to the electron emitter is signified by the number 0, the next segment to the right corresponds to number 1, and so forth. The last segment, i.e., the segment nearest to the ion emitter, receives the number 1023. The values of the electric field at the midpoints of these segments then can be collected into a field array $(EFLD_k)$ whose index number runs

TABLE 4. CONSTANTS AND PARAMETERS OF THE COMPUTER-SIMULATED DIODE

Normalized dc parameters of the diode	$\alpha,\ \beta,\ \xi_2,\ \eta_2,\ \left(\dfrac{m_e}{m_i}\right)$
Parameters of the computer model	DTAU, GMME
Resulting normalized constants of the computer diode: Length of the diode	2^{34}
Injection rate of ion sheets	$GMMI = \dfrac{\alpha_i\sqrt{\beta_i}}{\alpha_e\sqrt{\beta_e}}\sqrt{\dfrac{m_e}{m_i}}\ \ GMME$
Injection velocities of electron sheets	$VELOE = \dfrac{2^{34}}{\xi_2\sqrt{\beta_e}}\ \sqrt{-\log R}$
Injection velocities of ion sheets	$VELOI = \dfrac{2^{34}}{\xi_2\sqrt{\beta_i}}\ \sqrt{\dfrac{m_e}{m_i}}\ \sqrt{-\log R}$
Electric field due to applied potential	$EFLD2 = -\dfrac{2^{33}}{\xi_2{}^2}\ \eta_2$
Acceleration of an electron sheet	$ACCE = -\ EFLD$
Acceleration of an ion sheet	$ACCI = \dfrac{m_e}{m_i}\ EFLD$
Change of electric field across a sheet	$DEFD = \dfrac{2^{32}}{\sqrt{\pi}\ \alpha_e\ \sqrt{\beta_e}\ GMME\ \xi_2}$

from 0 to 1023. Actually, it is more convenient to keep a record of the changes in $DPOS_n$ of the sheets during a time step (these quantities are proportional to the field values). For the electron sheets, the field values are multiplied by $-(\Delta\tau)^2$; for the ion sheets the multiplying factor is $(m_e/m_i) \cdot (\Delta\tau)^2$. Two arrays with 1024 elements are needed to store the resulting quantities $(DDPE_k, DDPI_k)$. the subscripts of these two arrays take the integer values of $0,1,2,\ldots,1023$.

The potential as a function of distance is calculated from the field by integration. Since the field varies linearly in each segment, this integration becomes a simple summation—though this introduces a slight inconsistency since the values of the potential are given at the boundary and not at the midpoints of the segments. Consequently, the potential array (POT_k) has an index that is running from 0 to 1023 also, but the values of the potential refer to the right boundary points of the segments that the index numbers signify. The values of the potential are given in their dc normalized form, hence POT_{1023} is always equal to η_2.

There are a few single variables in the program, i.e., the current through the diode $(CURR)$, the total number of sheets in the diode $(NTOT)$, and the number of ion and electron sheets that leave the diode during a particular time step $(ILEFT, ELEFT)$ at the plane of the electron emitter.

Naturally, all the variables are functions of the normalized time, or what is more appropriate in the computer program, functions of the number of time steps $(TCOUNT)$ counted from some reference time. The methods of computing these variables are discussed in the following sections in the order that they appear on Fig. 12.

3. Moving the Sheets During a Time Step

It is assumed that we know the state of the diode at the end of the time step TCOUNT, i.e., the positions and the previous changes in the positions of the sheets are given, and the elements of $DDPE_k$ and $DDPI_k$ have also been determined according to the distribution of the sheets in the diode (see Sec. 5). We want to calculate the positions of the sheets at the end of the next time step and then increase TCOUNT by one.

If $POS_n(new) \leq -2^{34}$ or ≥ 0, it has left the diode space at the ion emitter or at the electron emitter respectively and the position of the sheet is set equal to zero. The value of ELEFT is set equal to the total number of electron sheets that leave the diode at the electron emitter during this time step.

4. Injecting New Sheets

The distribution laws for the injected velocities of the ion and electron sheets are given in Table 3. According to these expressions the square root of the natural logarithm of a number (R) has to be calculated for each injected sheet. This number R is given as a 35-bit binary number, hence it could have any one of the $2^{35}-1$ values that are between 0 and 2^{35}. Accordingly, there are $2^{35}-1$ possible velocity values one of which is assigned to an entering sheet. Since the computer model can handle only 10,000 sheets at a time, it is not necessary to keep such a large variety of velocity classes. The computer results are hardly affected if the number of possible initial velocities is limited to $2^{10} = 1024$, for example, in which case the possible velocity values can be calculated at the beginning of the computations and stored for future reference.

We used the latter method, for it saved us considerable computer time. The uniformly distributed random number R was calculated as before (see Chapter V). It was considered as an integer and was shifted right 25 places. The resulting integer, R', could have values of 0,1,2,...,1023. These values occurred in a random manner, and each was equally probable. The number R' was used, then, to indicate the element of an array in which the calculated velocity values were stored.

In the actual calculations we were not interested in the initial velocities of the injected sheets directly, but rather in the position and previous change in the position of each injected sheet. Equation (59) in Chapter V shows how to calculate these quantities from the initial velocity of the injected sheet and from the acceleration that acts on the sheet in the neighborhood of the emitter. It is convenient to calculate the initial changes in the positions of the sheets INDPE for the electrons and INDPI for the ions. These changes are given

For these calculations we take the positions of the sheets (POS_n) one by one and test each for sign.

If $POS_n > 0$, this element of the array represents an ion sheet. The value of the position, an integer number between 0 and 2^{34}, determines the segment to which this sheet belongs. The segment number is determined by shifting POS_n to the right with 24 places. The resulting integer (we call it KIND) can have values of $0,1,2,\ldots,1023$ and corresponds to the segment number of the sheet. Hence, $DDPI_{KIND}$ gives the change in the value of $DPOS_n$ for this time step. The new position and the change in the position of this sheet are

$$DPOS_n(new) = DPOS_n(old) + DDPI_{KIND}$$

$$(D.15)$$

$$POS_n(new) = POS_n(old) + DPOS_n(new)$$

where KIND is the integer number that results by shifting right $POS_n(old)$ 24 places. The new position of the ion sheet is tested to determine whether it is still located in the diode space. If $POS_n(new) \geq 2^{34}$, the sheet has left the diode at the ion emitter; if $POS_n(new) \leq 0$, it has passed the plane of the electron emitter. In both of these cases the position of the sheet is set equal to zero, hence it is ignored until the position of a new sheet is placed in this element of the array during the injection of new sheets. The value of ILEFT is set equal to the total number of ion sheets that leave the diode space at the electron emitter during this time step.

If $POS_n < 0$, corresponding calculations are made for an electron sheet. The index number KIND is determined from the absolute value of POS_n (which is the actual position of the electron sheet) by the same shifting operation as before. The new values of $DPOS_n$ and POS_n are calculated by the following expressions.

$$DPOS_n(new) = DPOS_n(old) + DDPE_{KIND}$$

$$(D.16)$$

$$POS_n(new) = POS_n(old) - DPOS_n(new)$$

simply as the product of the initial velocity of the sheet and the length of the time step (DTAU).

In order to simulate the half-Maxwellian velocity distribution of the injected sheets by 1024 values, we have divided the unit interval into 1024 equal segments and calculated the velocities that corresponded to the midpoints of these segments. These segments were numbered from 0 to 1023, hence the midpoints of the segments could be represented by the expression $(1/2048 + r/1024)$ where r was the segment number. The corresponding velocity values were multiplied by DTAU and then stored in two arrays $(INDPE_r, INDPI_r)$ whose indices also ran from 0 to 1023. The elements of these arrays were calculated by the following expressions:

$$INDPE_r = \frac{2^{34}\ DTAU}{\xi_2 \sqrt{\beta_e}} \left(\sqrt{- \log \left(\frac{1}{2048} + r \frac{1}{1024} \right)} \right)$$

$$INDPI_r = \sqrt{\frac{m_e}{m_i}} \sqrt{\frac{\beta_e}{\beta_i}}\ INDPE_r \hspace{2cm} (D.17)$$

$$for\ \ r = 0,1,2,\ldots,1023$$

Injecting a sheet in the diode started with the calculation of a number from the random sequence R. The new random number R' was calculated from R by the shifting operation described above and then used as the index number for one of the arrays in Eq. (D.17). The procedure was slightly different for ion and electron sheets.

If an electron sheet was injected, it started at the electron emitter (POS = 0) with positive velocity and with negative position. The expressions for the position and change of position of the injected electron sheet were then:

$$POS = - \left(\frac{1}{2}\ INDPE_{R'} + \frac{1}{6}\ DDPE_0 \right)$$

$$DPOS = INDPE_{R'} \hspace{4cm} (D.18)$$

since the term $a_0 (\Delta\tau)^2$ in Eq. (59) is given simply by the first element of the $DDPE_k$ array.

If an ion sheet was injected, it started at the ion emitter $(POS = 2^{34})$ with negative velocity and its position had to be counted from the ion emitter. Consequently, the following expressions were used for an injected ion sheet.

$$POS = 2^{34} - \left(\frac{1}{2} INDPI_{R'} + \frac{1}{6} DDPI_{1023} \right)$$

$$DPOS = - INDPI_{R'}$$

(D.19)

We can see from Eq. (D.18) and Eq. (D.19) that the effect of large retarding fields at the emitters could return the injected sheets to their respective emitters. In these cases the positions of these returned sheets were set equal to zero and they were ignored in the same manner as those which left the diode space during the moving of the sheets.

5. Calculating the Elements of the Arrays $DDPI_k$ and $DDPE_k$

The kth element of the arrays $DDPI_k$ and $DDPE_k$ are proportional to the value of the electric field at the midpoint of the kth segment in the diode. (The segment number k can have values of $0,1,2,\ldots,1023$). The electric field in the diode is determined from the combined effects of the sheets in the diode and of the applied potential (η_2). The potential η_2 contributes a constant value (EFLD2) to the total electric field, hence the same value is added to the field in each segment.

The contribution of the sheets to the total electric field (EFLD1) is determined from the positions of the sheets with the condition:

$$\int_{0}^{2^{34}} EFLD1(POS) \, d(POS) = 0$$

(D.20)

Since the values of the electric field $(EFLD1_k)$ are given at the midpoints of the segments and the field is a linear function of position in each segment (see Fig. 11b), the integral of Eq. (D.20) becomes a summation. This gives the condition:

$$\sum_{k=0}^{1023} EFLD1_k = 0 \qquad\qquad (D.21)$$

Let us suppose that we know the total change of the electric field across each segment $(TDEFD_k)$. Then the calculation of the values of EFLD1 at the midpoints of the segments $(EFLD1_k)$ can proceed in two steps.

First, we make the assumption that the field is zero at the plane of the electron emitter $(POS = 0)$. Since we know the change of the electric field across each segment, the values of the field at the midpoints can be calculated--although these values will not be equal to $EFLD1_k$. In order to use corresponding symbols to those used in Chapter V, we call this hypothetical field EFLD1', and call its values at the midpoints $EFLD1_k'$. The following expression gives the values of this field:

$$EFLD1_0' = \frac{1}{2} TDEFD_0 \qquad\qquad (D.22)$$

$$EFLD1_k' = \sum_{\ell=0}^{k-1} TDEFD_\ell + \frac{1}{2} TDEFD_k$$

It was shown in Chapter V that EFLD1' and EFLD1 differ only by a constant and that this constant is equal to the average value of the field EFLD1' over the diode space. Accordingly, the values of EFLD1 at the midpoints of the segments are as given by the following relation:

$$EFLD1_k = EFLD1_k' - \frac{1}{1024} \sum_{k=0}^{1023} EFLD1_k' \qquad\qquad (D.23)$$

Combining the effects of the sheets and of the applied potential gives the following relation for the total field in the diode:

$$EFLD_k = EFLD1_k + EFLD2_k \qquad (D.24)$$

We showed in Sec. D.2 how the values of $DDPI_k$ and $DDPE_k$ were related to the field. Substitution of these relations into Eq. (D.23) gives the values for the arrays:

$$DDPI_k = \frac{m_e}{m_i} \; EFLD_k \; (DTAU)^2$$

$$\qquad (D.23)$$

$$DDPE_k = - EFLD_k \; (DTAU)^2$$

Before showing how the values of $TDEFD_k$ are calculated from the positions of the sheets, let us mention the fact that during the above calculations we determined the value of $TEFLD1$ at the electron emitter. This term is important when we want to calculate the convective current density in the diode (see next section). During these calculations we determined the average value of $EFLD1'$ over the diode space. Since $EFLD1'$ is zero at the electron emitter, and the total field, $EFLD$, is equal to $EFLD1' + EFLD2$ minus the average value of $EFLD1'$ everywhere in the diode, the value of the total field at the electron emitter $EFLD(POS = 0)$ is given by

$$EFLD(POS = 0) = - \frac{1}{1024} \sum_{k=0}^{1023} ELFD1_k' + EFLD2 \qquad (D.24)$$

The total change in the electric field across the kth segment $(TDEFD_k)$ is caused by the sheets that are located in this segment. The change of electric field across one sheet is given in Table 3. This change is positive for an ion sheet and negative for an electron sheet. For calculating the values of $TDEFD_k$ the following procedure is used:

1. First the elements of TDEFD_k are set equal to zero for all values of k. Then we take the positions of the sheets (POS_n) one by one and test each for sign.

2. If $\text{POS}_n > 0$, an ion sheet is represented by this element of the POS_n array. The segment number that corresponds to this sheet is determined, as before, by shifting POS_n to the right by 24 places. The resulting integer, KIND, is the number of the segment in which this sheet is located. The amount DEFD is the change in the electric field across one sheet, hence we add to the current value of $\text{TDEFD}_{\text{KIND}}$ this amount.

3. If $\text{POS}_n < 0$, an electron sheet has to be considered. The index number is determined from the absolute value of POS_n (which is the actual position of the electron sheet) and then the amount DEFD is subtracted from the current value of $\text{TDEFD}_{\text{KIND}}$.

4. After all sheets have been considered, the accumulated change in the electric field across the kth segment is given by TDEFD_k.

We have described the major loop of the computer program. At every time step the sheets are moved, new sheets are injected, and the field is calculated in the diode. After the field has been calculated, variables of the program are printed out according to what output quantities are needed. These outputs are discussed in the next section.

6. <u>The Current in the Diode and Other Output Quantities</u>

Current in the diode is normalized to the saturation current. If the electric field is constant in time, the convection current in the diode (ICONV) for a particular time step (TCOUNT) is given by the following expression:

$$\text{ICONV} = \frac{\text{ELEFT} - \text{ILEFT} - \text{GMME}}{(\text{GMME} + \text{GMMI})\,\text{DTAU}} \qquad (\text{D}.25)$$

where GMME and GMMI are the electron and ion sheet injection rates respectively, and the numerator gives the equivalent number of positive sheets that crossed the plane of the electron emitter from left to right during the normalized time interval DTAU. If the electric field is changing in time, its contribution to the convection current has to be calculated also at the plane of the electron emitter [see Eq. (72)]. We have already shown that the value of EFLD1 is determined at the plane of the electron emitter (POS = 0) at each time step, hence the

contribution of the electric field to the convection current at time TCOUNT is proportional to the term:

$$\frac{EFLD1(POS = 0, TCOUNT) - EFLD1(POS = 0, TCOUNT - 1)}{DTAU}$$

The factor of proportionality can be calculated from the condition that the convection current is constant in space, and we arrive at the following expression for the normalized convection current:

$$ICONV(TCOUNT) = \frac{1}{DTAU\ (GMME + GMMI)} \left[ELEFT - ILEFT - GMME \right.$$

$$\left. + \frac{EFLD1(POS = 0, TCOUNT) - EFLD1(POS = 0, TCOUNT - 1)}{DEFD} \right]$$

where DEFD is the change in the normalized electric field that occurs when a sheet is crossed.

We have already shown the procedure for calculating the potential as a function of position in the diode. The extrema of the potential function can be found easily by looking for those places where the electric field becomes zero.

These were the output quantities that we considered important for our problem. Naturally, other quantities--such as the position of the sheets, their velocity distributions at any point in the diode, or the charge density along the diode--could also be extracted from the computer program. These quantities are readily available during the computer calculations and their discussion would be superfluous here.

REFERENCES

1. I. Langmuir, _Phys. Rev._, 33, 1929, pp. 954-960.

2. K. Müller-Lübeck, _Feitschrift für angewandte Physik_, 3, 1951, p. 409.

3. I. Langmuir and Karl P. Compton, _Revs. Mod. Phys._, 3, 1931, pp. 191-258.

4. P. H. J. A. Kleynen, Philips Research Report, 1, 1946, p. 81.

5. I. Langmuir, _Phys. Rev._, 33, 1929, pp. 976-981.

6. P. L. Auer, _J. Appl. Phys._, 31, 12, 1960, p. 2096.

7. R. G. McIntyre, _J. Appl. Phys._, 33, 8, 1962, p. 2485.

8. R. G. McIntyre, _Proc. IEEE_, 51, 5, 1963, p. 760.

9. P. L. Auer and H. Hurwitz, _J. Appl. Phys._, 30, 2, 1959, p. 161.

10. A. L. Eichenbaum and D. G. Hernquist, _J. Appl. Phys._, 32, 1, 1961, p. 16.

11. Bernard Friedman, _Principles and Techniques of Applied Mathematics_, John Wiley and Sons, Inc., New York, 1960, pp. 136-143.

12. D. R. Hartree and P. Nicolson, _C.V.D. Repts. Mag._ 12 and 23, Brittish Admiralty, London, 1943.

13. O. Buneman, _Phys. Rev._, 115, 3, 1959, p. 503.

14. J. Dawson, _The Physics of Fluids_, 5, 4, 1962, p. 445.

15. C. K. Birdsall and W. B. Bridges, _J. Appl. Phys._, 32, 12, 1961, p. 2611.

16. G. C. Twombly and G. E. Lauer, Tech. Rep. No. 2, Engineering Experiment Station, University of Coloradio, Boulder, Colo., 1960.

17. R. J. Lomax, _J. Electronics and Control_, 9, 1960, p. 127.

18. D. A. Dunn and I. T. Ho, "Computer Experiments on Ion-Beam Neutralization with Initially Cold Electrons," Rept. SEL-63-046 (TR No. 0309-1), Stanford Electronics Laboratories, Stanford, Calif., Apr 1963.

19. O. Buneman and G. P. Kooyers, "Computer Simulation of the Electron Mixing Process in Ion Propulsion," AIAA Electric Propulsion Conference, Colorado Springs, Colo., 11-13 Mar 1963.

20. P. K. Tien and J. Moshman, _J. Appl. Phys._, 27, 9, 1956, p. 1067.

21. Quarterly Research Review No. 4, Electron Devices Lab., Stanford Electronics Laboratories, Stanford, Calif., 1 Jan - 31 Mar 1963.

22. IBM Reference Manual C20-8011, _Random Number Generation and Testing_, International Business Machines Corp., White Plains, N.Y., 1959.

23. Quarterly Research Review No. 2, Electron Devices Lab., Stanford Electronics Laboratories, Stanford, Calif., 1 Jul - 30 Sep 1962. pp. I-22, I-28.

24. Kaj. L. Nielsen, _Methods in Numerical Analysis_, Macmillan Co., New York, 1957, pp. 127-130.